UNIVERSITY OF CALIFORNIA
RIVERSIDE

The Effects of Aerosols From the Salton Sea Basin on Pulmonary Health

A Dissertation submitted in partial satisfaction
of the requirements for the degree of

Doctor of Philosophy

in

Biomedical Sciences

by

Trevor Alexander Biddle

June 2023

Dissertation Committee:
Dr. David D. Lo, Chairperson
Dr. Erica Heinrich
Dr. Meera G. Nair

The Dissertation of Trevor Alexander Biddle is approved:

Committee Chairperson

University of California, Riverside

1

2

ACKNOWLEDGMENTS:

The text of this dissertation, in part, is a reprint of the material as it appears in Science of the Total Environment Volume 858, Part 3, 1 February 2023, 159882 and Science of the Total Environment Volume 792, 20 October 2021, 148450. The co-author David D. Lo listed in these publications directed and supervised the research which forms the basis for this dissertation. Qi Li, Mia R. Maltz, Purvi N. Tandel, and Jasmine Yu helped to produce figures. Rajrupa Chakraborty, Keziyah Yisrael, Talyssa M. Topacio, Diana Del Castillo, and Malia L. Shapiro helped with data collection. Daniel Gonzalez and Ryan Drover ran the environmental exposure chamber used in these studies. Hannah L. Freund and Mark P. Swenson collected and processed the dust and water used in these studies. Jon K. Botthoff designed the passive dust collectors used in these studies. Emma Aronson and David R. Cocker III helped to edit and review the manuscripts.

DEDICATION:

I would like to dedicate this dissertation to my amazing wife, Sarah, who supported me throughout my time in the program. Without her love and support, I would never have been able to finish all of the work that contributed to this dissertation while maintaining my health and happiness.

ABSTRACT OF THE DISSERTATION

The Effects of Aerosols From the Salton Sea Basin
on Pulmonary Health

by

Trevor Alexander Biddle

Doctor of Philosophy, Graduate Program in Biomedical Sciences
University of California, Riverside, June 2023
Dr. David D. Lo, Chairperson

The Salton Sea is a large inland lake located in California on the border between Riverside and Imperial Counties. The communities surrounding the Salton Sea have unusually high rates of asthma. In this dissertation, I explain how different aerosol sources play a role in pulmonary inflammation. We used a specially designed environmental exposure chamber that allows mice to be exposed to a controlled and consistent dose of aerosols for up to 7 days without having to open the chamber. Once mice were exposed, we collected bronchoalveolar lavage fluid and lung tissue and analyzed whole lung tissue gene expression, inflammatory cell infiltration, performed histological analysis, and determined changes in airway hyperreactivity. We found that aerosolized Salton Sea Water, selected to mimic the effects of aerosolized sea spray, resulted in a minor change in inflammatory gene regulation without overt inflammatory cell infiltration. This was in stark contrast to a T2-like response to the fungal allergen *Alternaria alternata* and *Alternaria tenuis.* To understand if

there was a link between these, we exposed mice to the water followed by *Alternaria sp.* We found that there was no sensitization from pre-exposure to the water, which suggests that the primary aerosol driving the pulmonary inflammation is not the sea spray from the Salton Sea. To investigate other avenues of potential pulmonary inflammation, we exposed mice to aerosolized dust extract collected from around the Salton Sea. This produced a neutrophilic response with substantial upregulation of genes related to innate immune response. This was greater at 48-hours than at 7-days, mimicking the kinetics of acute, innate inflammation. This closely matched the response to TLR2/4 agonists LTA and LPS, providing insight into a potential mechanism for dust-related pulmonary inflammation.

Table of Contents

Chapter 1: Introduction 1

The Salton Sea 1
Immunology and Inflammation 7
Dust 15
Chronic Respiratory Disease 23
Conclusion 32
References 34
Glossary of Terms 57

Chapter 2: Investigation into the pulmonary health effects of sea spray from a decaying inland sea: An *in vivo* study of aerosolized Salton Sea water exposure in mice 63

Abstract 63
Introduction 64
Materials and methods 67
Results 75
Discussion 85
Conclusions 88
References 91

Chapter 3: The Effect of Preexposure to Salton Sea Water on Asthma Development 109

Abstract 109
Introduction 110
Materials and Methods 112
Results 119
Discussion 122
References 124

Chapter 4: Aerosolized Aqueous Dust Extracts Collected Near a Drying Lake Trigger Acute Neutrophilic Pulmonary Inflammation Reminiscent of Microbial Innate Immune Ligands 134

Abstract 134
Introduction 136
Methods 139
RNA Extraction 147
Results 149
Discussion 154
Conclusions 157
References: 160

Chapter 5: Conclusion 180

References 184

List of Figures

Chapter 2: Investigation into the pulmonary health effects of sea spray from a decaying inland sea: An *in vivo* study of aerosolized Salton Sea water exposure in mice

Figure 2.1 - Quantification of *Alternaria*, Pacific Ocean, and Salton Sea aerosols 96
Figure 2.2 - Inflammatory cell recruitment due to *Alternaria* aerosols 98
Figure 2.3 - Inflammatory cell recruitment due to Salton Sea and Pacific Ocean aerosols 100
Figure 2.4 - Gene expression changes due to *Alternaria* aerosol 102
Figure 2.5 - Gene expression changes due to Salton Sea aerosol 103
Figure 2.6 - Comparisons between Alternaria, Salton Sea and Pacific Ocean exposures 104
Figure 2.S1 - Gating strategy for flow cytometry 106
Figure 2.S2 - Gene expression changes due to Pacific Ocean aerosols 108

Chapter 3: The Effect of Preexposure to Salton Sea Water on Asthma Development

Figure 3.1 - Inflammatory cell recruitment in bronchoalveolar lavage fluid of control air, *Alternaria* exposed, and Salton Sea Water pretreated mice 127
Figure 3.2 - Inflammatory cell recruitment in digested lung tissue of control air, *Alternaria* exposed, and Salton Sea Water pretreated mice 129
Figure 3.3 - Gene expression analysis comparing *Alternaria* exposed and Salton Sea Water pretreated groups 131
Figure 3.4 - Changes in airway hyperreactivity between the control air, *Alternaria* exposed, and Salton Sea Water pretreated mice 133

Chapter 4: Aerosolized Aqueous Dust Extracts Collected Near a Drying Lake Trigger Acute Neutrophilic Pulmonary Inflammation Reminiscent of Microbial Innate Immune Ligands

Figure 4.1 - Collection Sites and Changes in Exposed Playa Over Time 167
Figure 4.2 - Pulmonary inflammation triggered by Salton Sea (Wister) Dust extract and by Desert (Boyd Deep Canyon) Dust extract 168
Figure 4.3 - Changes from 48-hour to 7-day timepoints for Salton Sea (Wister) Dust extract, Alternaria, LTA, and LPS exposed mice 171
Figure 4.4 - Gene expression comparisons for 48 hour and 7-day timepoints 173
Figure 4.S1 - Dos Palmas and Sonny Bono Cell infiltration and gene expression 175
Figure 4.S2 - Response to Corvina Beach Playa 177

List of Tables

Chapter 4: Aerosolized Aqueous Dust Extracts Collected Near a Drying Lake Trigger Acute Neutrophilic Pulmonary Inflammation Reminiscent of Microbial Innate Immune Ligands

Table 4.1 - Site and sampling characteristics 179

Chapter 1: Introduction

The Salton Sea

The Salton Sea is the largest inland sea in California at 343 mi^2 and is located on the border between Riverside and Imperial counties. The Salton Sea Basin comprises both the Coachella Valley and Imperial Valleys, with the Eastern Coachella Valley (ECV) and Imperial Valley (IV) directly contacting the sea. While the current iteration of the Salton Sea formed due to a break in a canal from the Colorado River, which caused flooding for over two years before being fixed. Since then, the Salton Sea has been maintained primarily due to agricultural runoff from farming in the ECV and IV, which are major agricultural centers for California.

Even though the Salton Sea was a relatively recent phenomenon, the Salton Sea basin has intermittently been home to a saline lake called Lake Cahuilla, which had been an important staple for the native communities for thousands of years. The modern Salton Sea community consists of over 177,000 people, with major population centers at the northwest and southeastern points of the Salton Sea. This is a predominantly Latino community and is especially vulnerable due to the immigrant status of many of the individuals along with high levels of poverty. The median household income of $35,000 is a little over half the California average of $61,400 (Marshall, 2017), and the community has among the worst socioeconomic burdens in the state (CalEnviroScreen 4.0). This vulnerability translates into poor health outcomes, as detailed in the next section.

The Salton Sea provides an important ecological niche in the modern world. It serves as a major stopover point for the Pacific Flyway, a migratory path for over 1 billion birds yearly (Bradley and Yanega, 2018). The Salton Sea is or has been home to a diverse population of fish, though due to worsening ecological health, tilapia are among the only fish still capable of living within the sea due to their uniquely high salt tolerance (Lorenzi and Schlenk, 2014). Additionally, the sea is home to a diverse microbial community, particularly archaea which are more able to tolerate extreme conditions, with *Euryarchaeota* and *Crenarchaeota* being especially common (Swan et al, 2010). Among the bacterial populations, Proteobacteria and Bacteroidetes were the most common (Hawley et al., 2014).

Due to increasing levels of salinity and abundant pollution, the Salton Sea's ecological health is worsening. The Salton Sea does not receive enough water to maintain current levels and increasing temperatures due to climate change exacerbate this issue. As the Salton Sea evaporates, salinity levels continue to rise, with current levels eclipsing 70 ppt (Bureau of Reclamation, 2022). The extreme temperatures also result in poor mixing of the water during the summer, creating an anoxic layer that results in massive fish kills during autumn as this anoxic layer begins to mix with the oxygenated surface layer (Reese et al., 2008). This causes a cascading effect that ends up hurting the migratory bird population as they lack a consistent food source. The remaining

bird populations also tend to have periodic die-offs due to bioaccumulation of pollutants in their prey (Carmichael and Li, 2006).

The rapid drying of the Salton Sea was exacerbated by a recent diversion of water from agricultural sources to San Diego in 2018. As the lake is relatively shallow, even a small decline of 3 ft in elevation will expose over 11,000 acres of lakebed (Johnston et al., 2019). Current estimates predict an 11% increase in exposed lakebed, also known as playa, between 2018 and 2030 (Parajuli and Zender, 2019). Playa currently makes up an average ~9% of particulate matter under 10 μm in size (PM_{10}) at population centers on the eastern and western shores of the Salton Sea (Frie et al., 2017), with peaks near the sea of up to 47% on the beach itself (Frie et al., 2019). Playa emissions will become an increasing concern in the future as more playa is exposed, which will likely exacerbate community health issues as in other communities exposed to high levels of exposed playa, such as those near the Aral Sea (Doede and DeGuzman, 2020).

Community Health

With the ecosystem in disarray, it should come as no surprise that there are serious health issues in the communities surrounding the Salton Sea. Of particular concern is respiratory illness. In 2011 and 2012, Imperial County, located on the southern border of the Salton Sea, was plagued by some of the highest rates of emergency room (ER) visits for children due to asthma in the state of California (Doede and DeGuzman, 2020). These levels have remained

high and are still among the worst in the state (CalEnviroscreen 4.0). Childhood diagnosis for asthma is also quite high, at 20-22.4% (Farzan et al., 2019), with even higher levels of respiratory symptoms such as wheezing, allergies, bronchitis symptoms, and dry cough.

Not only are respiratory illnesses common, but locals also suffer from high rates of cardiovascular ER visits (Miao et al., 2022). These diseases are compounded by the extreme socioeconomic vulnerability of the population, which is within the 90th percentile statewide (Miao et al., 2022). This vulnerability manifests as poor access to preventative healthcare, particularly in rural regions where the closest hospitals are between ~50 and ~61 minute away (Juturu 2021). The need to spend long periods of time outside, where individuals are exposed to potentially toxic dust and fumes from the Salton Sea, also likely contributes to a variety of health concerns.

Exacerbating community health issues is poor working and living conditions. Community surveys indicate that workers are poorly trained, exposed to harsh conditions without adequate safety precautions, and have little recourse to improve their conditions. As many of these individuals are immigrant workers, they fear deportation, and are worried that speaking up will cost them their jobs (Cheney et al., 2022).

An additional factor in community health concerns is the increasing levels of dust in the region. Increasing levels of playa exposure are linked to worsening pulmonary health outcomes, with more ER visits during times with poor air mixing

over the Salton Sea (Doede et al., 2021) Current models indicate that for each one-foot drop in the Salton Sea, are linked to an additional 0.68 deaths per 100,000 people at the county level (Jones and Fleck, 2020). This is likely underestimating the concern for people living in proximity to the sea, as the model used county level information, while only the most eastern portion of Riverside County is frequently exposed to the Salton Sea.

Based on other drying lakes in arid regions, the drying Salton Sea is likely to increase dust levels to potentially catastrophic levels such as those seen in the Aral Sea in Centra Asia (Doede and DeGuzman, 2020) and Owens Lake in California (Johnston et al., 2019). If conditions reach those extremes, dust from the newly exposed playa could easily threaten individuals who live outside of the Salton Sea Basin.

Salton Sea Pollutants

While the exact components of the Salton Sea that could be leading to poor community health are not known, there are many candidate components. As a stressed ecosystem, the Salton Sea contains many potentially harmful microbial communities. As previously mentioned, there are large number of both gram-positive and gram-negative bacteria in the Salton Sea (Hawley et al., 2014). These could contribute to the ambient levels of endotoxin in the dust, which could have some adverse health effects, particularly in larger dust fractions, which are shown to cause pulmonary inflammation (D'Evelyn et al.,

2021; Burr et al., 2021). While this is unlikely to be the only toxic factor in the dust, it could be a contributing factor.

Other potential microbial toxins include cyanotoxins such as microcystin, which has been detected in the Salton Sea. As the Salton Sea has nutrient loading from agricultural runoff and year-round sunlight, it is primed for algal blooms. This leads to elevated levels of microcystins in the environment, though detected levels are generally less than those known to cause acute lethal toxicity (Carmichael and Li, 2006). The high levels of selenium in the sea also cause increased levels of microcystin production while the high salinity can cause increased release of microcystin due to damaging cyanobacteria such as *Microcystis aeruginosa* (Zhou et al., 2017).

Selenium alone is another potentially toxic pollutant. When selenium is in its ionic forms of selenate and selenite and its organo-selenide form of Se(-II), it can easily bioaccumulate and become toxic (Kausch and Pallud, 2013). Selenium levels in the sea and sediment are quite high (Saiki et al., 2012; Xu et al., 2016), and due to bioaccumulation often reach dangerous levels in higher organisms such as fish and birds (Ohlendorf and Marois, 1990; Riedel et al., 2002).

Levels of sulfide in the Salton Sea are also exceptionally high, with levels exceeding the toxicity threshold for tilapia (Reese et al., 2008). This translates to high levels of hydrogen sulfide in the air above the Salton Sea, over 5 times that of background levels and urban areas (Reese et al., 2008).

One of the greatest concerns for the area is the heavy use of pesticides. While some pesticides such as DDT have been banned for use in the United States, there are still detectable levels in the water, sediments, and organisms (Ohlendorf and Marois, 1990; Riedel et al., 2002; Sapozhnikova et al., 2004; Xu et al., 2016). Other pesticides such as pyrethroids are also detectable at concerning levels in the area (Phillips et al., 2007; Xu et al., 2016). Polychlorinated biphenyls, an industrial contaminate similar to organochlorine pesticides such as DDT, are also detectable in waters and organisms around the Salton Sea (Riedel et al., 2002; Sapozhnikova et al., 2004; Xu et al., 2016).

More work must be done to link specific pollutants with specific community health issues, but overall, there are many potentially dangerous pollutants in the area. As the sea dries and more playa is exposed, these pollutants will continue to be released into the air in the form of windblown dust. Thus, it is critical for more research to be done to link the pollution to the community health issues. This will allow for more targeted and detailed remediation and policy guidelines.

Immunology and Inflammation

Inflammation is the process by which infections and/or tissue damage is cleared, and homeostasis is restored (Kotas and Medzhitov, 2015). This is a complex process, involving many types of cells, cytokines (small proteins which facilitate cell-to-cell communication in immune responses), and other secreted factors.

Generally, inflammation starts either through infection or tissue damage. Pathogen-associated molecular pattern molecules (PAMPs) are components of microorganisms and viruses that are recognized by pattern recognition receptors (PRRs) found on the surface of many types of cells (Zindel and Kubes, 2020). When tissue is damaged, damage-associated molecular pattern molecules (DAMPs) are released, which are also recognized by PRRs (Murao et al., 2021). Interactions between PAMPs/DAMPs and PRRs trigger an inflammatory response, which is characterized by the recruitment of leukocytes and the release of various proinflammatory molecules (Mack, 2018).

Inflammation relies on the two primary branches of the immune system, the innate and adaptive responses. These are detailed in the following sections.

Innate Immunity:

Innate immunity is the first line of defense against pathogens. At its most basic, innate immunity can include both hematopoietic and nonhematopoietic cells. The primary purpose of nonhematopoietic cells, primarily skin and epithelial cells, in innate immunity is to serve as barriers to keep out pathogens (Kaur and Secord, 2019). However, epithelial cells can also have sensing functionality via expression of PRRs (Kaur and Secord, 2019).

Hematopoietic cells involved in innate immunity include mononuclear and polymorphonuclear cells (Beutler, 2004). The most important mononuclear cells involved in innate immunity is the macrophages/monocytes, while

polymorphonuclear cells include neutrophils, and eosinophils among other cell types (Beutler, 2004).

A critical part of innate immunity is PAMP/PRR interactions. PAMPs are necessary and conserved elements from pathogens, including components of microbial membranes and walls such as lipopolysaccharide (LPS), peptidoglycan (PGN), and lipoteichoic acid (LTA). Other common indicators of infection, including dsRNA, are also recognized by PRRs (Tang et al., 2012).

PRRs can be either membrane associated, or cytoplasmic. Examples of membrane associated PRRs include toll-like receptors (TLRs) and C-type lectin receptors (McKernan, 2020). TLRs are particularly important in recognizing pathogenic components, as the family contains 10 variations in humans that can recognize the aforementioned pathogenic molecules such as LPS, PGN, LTA, dsRNA, etc (Dolasia et al., 2017). TLRs can work through a MyD88-dependent or independent pathway. The MyD88-dependent pathway results in the translocation of NF-κB, an important inflammatory transcription factor, to the nucleus (Takeda and Akira, 2004). The MyD88-independent pathway results in a strong type-I interferon response (Takeda and Akira, 2004).

Cytoplasmic PRRs include nucleoside-binding and oligomerization domain like receptors (NLRs), retinoic acid-inducible gene-I-like receptors (RLRs), and absent-in-melanoma like receptors (ALRs) (McKernan, 2020). NLRs are a critical part of inflammasome formation, which is a component of cytokine production and caspase activity in inflammation (Kelley et al., 2019).

Once PAMP/PRR interactions occur, cytokines and chemokines (chemotactic cytokines) are released, directing the recruitment and activation of hematopoietic cells (Tang et al., 2012). Generally, neutrophils are the first cells recruited to the site of infection/damage (Liew and Kubes, 2019). These cells follow a gradient of chemoattractant molecules released by epithelial, endothelial, or other resident cells such as tissue macrophages (Kolaczkowska and Kubes, 2013). Once neutrophils reach the site of infection/damage, they enter the tissue through the leukocyte adhesion cascade. This involves the neutrophils slowing via interactions between selectin ligands on the neutrophil surface and E- and P-selectin on epithelial cells (Ley et al., 2007). The neutrophils then bind tightly via integrin interactions and enter the tissue (Ley et al., 2007). Once there, neutrophils clear pathogens and cellular debris, followed by release of growth factors to promote healing (Zindel and Kubes, 2020). After this, neutrophils either undergo apoptosis and are then cleared by macrophages via a process called efferocytosis, which results in macrophages polarizing towards an anti-inflammatory, tissue-repair state known as M2 (Yunna et al., 2020), or by leaving the tissue through reverse transmigration (Xu et al., 2022). These macrophages secrete various anti-inflammatory molecules, further promoting inflammation resolution and wound healing (Yunna et al., 2020).

Innate immunity also contains a humoral component. Circulating molecules such as mannose-binding protein, lipopolysaccharide binding-protein, and secreted CD14 can bind to microbes and microbial components to aid

recognition of PRRs by serving as ligands (Beutler, 2004). Other molecules, such as lysozyme, lactoferrin, and antimicrobial peptides, are capable of directly killing microbes (Riera et al., 2016). The complement cascade is another critical aspect of the humoral response, and leads to the activation of C3b, which binds to microbes to enhance opsonization, the generation of C5a, which is an inflammatory and chemotactic molecule, and the generation of a membrane attack complex, which creates a pore in microbes, killing them (Noris and Remuzzi, 2013).

Under normal conditions, inflammation is an acute process, resolving in a matter of hours to days (Aristizábal and González, 2013). However, under certain pathogenic conditions, inflammation can become a chronic condition (Zhao et al., 2016). This is a key factor in several major diseases such as atherosclerosis, COPD, and asthma (Leuti et al., 2020).

Adaptive Immunity:

While innate immunity relies upon recognition of conserved molecular patterns, adaptive immunity can recognize a functionally unlimited number of antigenic epitopes. However, this breadth of response takes time, with the usual timeline being 1-2 weeks to mount a response to a new antigen (Janeway et al., 2001). This response is primarily driven by T and B lymphocytes and relies on the development of receptors that are specific for the antigen.

The adaptive immune response relies on the innate immune response to develop. Two critical ways that the innate immune response drives adaptive immunity is through antigen presentation and secretion of cytokines. In order for T lymphocytes to recognize antigen, it must be presented in either major histocompatibility complex class I (MHC class I) or class II (MHC class II) (Rock et al., 2016). Almost every cell expresses MHC class I, which is used to present intracellular antigens, such as in the case of viral infection (van Endert, 2016). MHC class II is expression is more limited. Only certain cells, such as macrophages and dendritic cells, upregulate major histocompatibility complex class II (MHC class II) upon activation (Kashem et al., 2017). Other innate cells, such as innate lymphoid cells (ILCs) secrete regulatory cytokines upon activation and help direct the T and B lymphocyte response to the specific pathogen (Sonnenberg and Hepworth, 2019).

T lymphocytes develop in the thymus. These rely upon the T cell receptor (TCR) for their antigen recognition capabilities (Courtney et al., 2018). The TCR undergoes germline recombination prior to expression, resulting in combination of a variable (V) and a joining (J) segment, with the TCR sometimes also having a diversity (D) segment (Krangel et al., 1998). These segments are joined together randomly by recombinase-activating genes 1 and 2 (RAG1/2) (Neihues et al., 2010). Additional diversity is acquired by repairing DNA damaged by the joining process (Bonilla and Oettgen, 2010). Once the TCR is expressed they then undergo positive and negative selection. Positive selection requires low

avidity to self-MHC, while negative selection occurs when there is very high avidity to self-MHC or peptides (Klein et al., 2014). If T lymphocytes fail either selection, they undergo apoptosis and never leave the thymus (Klein et al., 2014). During this process, T lymphocytes also commit to a CD4+ or CD8+ lineage (Taniuchi, 2018)

Once they leave the thymus, T cells migrate to lymphoid tissues where they undergo maturation (Masopust and Schenkel, 2013). This involves TCR binding to MHC presented antigens in the presence of other co-stimulatory signals, such as cytokines and secondary receptor-ligand binding between the T lymphocytes and antigen presenting cell (Geurder and Flavell, 1995). CD4+ T lymphocytes recognize antigens in MHC class II, while CD8+ T lymphocytes recognize antigens in MHC class I (Bonilla and Oettgen, 2010). CD4+ T lymphocytes undergo maturation into one of several T helper (Th) subtypes, each of which is specialized in dealing with specific types of infections. These include Th1, Th2, Th9, and Th17 (Bonilla and Oettgen, 2010). The primary role of these cells is to secrete cytokines and direct the immune response (Zhu et al., 2010). CD8+ T lymphocytes rely on cell-cell interactions to control infection. When CD8+ T lymphocytes bind MHC class I, they trigger apoptosis in the MHC class I expression cell (Gulzar and Copeland, 2004). This is important in controlling viral infections and diseases such as cancer (Philip and Schietinger, 2022).

B lymphocytes arise in the bone marrow and develop their B cell receptor (BCR) in a manner analogous to TCR development. The BCR is comprised of heavy and light chains (Pieper et al., 2013). Every heavy chain has a V, D, and J segment, along with a constant region (C), while the light chain has a V, J, and C region (Pieper et al., 2013). There are 9 heavy chain constant regions, corresponding to the 9 types of immunoglobulins (IgM, IgD, IgG1-4, IgA1-2, and IgE), while there are 2 types of light chain constant regions (κ and λ) (Bonilla and Oettgen, 2010). When B cells leave the bone marrow, they express IgM and IgD (Pieper et al., 2013).

B lymphocytes are primarily activated through a T-cell dependent manner (Bonilla and Oettgen, 2010). B lymphocytes are responsible for antibody production, which can aid in opsonization and inactivation of antigens. B lymphocytes bind and internalize antigens ligated to their BCR (Tanaka et al., 2020). These are then presented on MHC class II and can interact with a T lymphocyte via their TCR (Tanaka et al., 2020). When this occurs in the presence of a CD40/CD40L interaction, the B cell is activated (Karnell et al., 2019). These activated B cells may immediately become plasma cells and secrete low affinity IgM or enter a follicle to establish a germinal center (Bonilla and Oettgen, 2010). While in a germinal center, the B cells can undergo class-switching, which involves changing the constant region to one more suited for the specific infection, and somatic hypermutation (SHM) (Mesin et al., 2016). SHM relies upon the accumulation of point mutations in the variable regions of the

heavy and light chains (Mesin et al., 2016). B cells with mutations that result in better binding to the antigen undergo greater expansion, and through this process antibodies with higher affinity for the antigens propagate (Victora and Nussenzweig, 2022).

T and B lymphocytes can become memory cells, which allow for rapid expansion of antigen specific T and B lymphocytes in secondary exposure to pathogens (Cancro and Tomayko, 2021). This provides a more targeted and effective immune response than innate immunity alone.

Dust

Respirable dust comes in several different forms. These are generally broken up by size fraction, with typical categories being PM_{10}, $PM_{2.5}$, and $PM_{0.1}$. These stand for particulate matter under 10μm in aerosol diameter, under 2.5 μm in aerosol diameter, and under 0.1μm in aerosol diameter respectively. While PM_{10} can be used to describe $PM_{2.5}$, it is usually used to describe particulate matter smaller than 10μm but greater than 2.5μm. The same concept can be applied for $PM_{2.5}$, but this will depend on the paper in question. These size categories are also often referred to as coarse (PM_{10}), fine ($PM_{2.5}$), or ultrafine ($PM_{0.1}$). These different PM sizes are thought to penetrate the airways differently, with PM_{10} usually being filtered out in the nasal passages (Mo, 2019), $PM_{2.5}$ penetrating to the bronchioles and alveoli, and $PM_{0.1}$ directly reaching the bloodstream (Nelin et al., 2011. Thus, the size of the respiratory particles likely

matters with regards to inflammatory potency. However, this is not the only factor that matters, as the identity of the particulate matter dramatically changes the pulmonary inflammatory phenotype, as covered in the next section.

Effects of Desert Dust on Pulmonary Health

The composition of particulate matter can vary wildly depending on the location, such as cities typically having particulate matter heavy in small organics generated by combustion compared to other locations. As the studies done in this paper were done using aerosols from a desert location, this section will focus specifically on the role that desert dusts play in pulmonary inflammation and human health, rather than particulate matter from all sources.

One of the best studied types of desert dust is Asian Sand Dust (ASD). This dust originates in the deserts in the northwestern portions of China and Mongolia before being carried eastward to regions such as Japan, Taiwan, and South Korea (Hasunuma et al., 2021). This particulate matter passes through the large cities along the Chinese coastline, potentially gaining toxic pollutants from the cities in addition to the toxins from the original desert source. These include microbial components such as b-glucan, lipopolysaccharide (LPS), and other TLR agonists (Fussel and Kelly 2021). These dusts cover the range from 0.5-10μm, with a peak of around 4 μm (Kanatani et al., 2010), meaning that they can penetrate deep into the airways. Levels of dust during ASD events can be 2 or more times the normal levels (Yang et al., 2005).

There is strong epidemiological and laboratory-based research documenting the effects of ASD on a population and mechanistic level. These dusts have been correlated with increased hospital admission due to respiratory illness on the day of and following dust days (Kanatani et al., 2010; Watanabe et al., 2011). These effects can be further broken down on population subsets, with pregnant women have increased risk of asthma-symptoms (such as weezing, nose and eye irritations, coughing) on dust days (Kanatani et al., 2016). Depending on the study, these have been associated with hourly concentration of NO2 (Watanabe et al., 2012), and pollen levels (Watanabe et al., 2011), but these studies have been limited in scope. Some studies have suggested that these symptoms may be most prominent during time with low pollen, with the dust serving as an adjuvant and enhancing the effect of low pollen doses (Ogi et al., 2014). The strongest correlations are between ASD and asthma-like symptoms rather than a decrease in respiratory measurements such as peak expiratory flow (PEF) (Watanabe et al., 2015). However, children may be more vulnerable, as there is evidence that ASD can decrease in %maxPEF in children with and without asthma, though this is attenuated by standard inhaler treatment (Hasunuma et al., 2021)

Studies using intranasal administration of ASD indicate that ASD can trigger significant recruitment of inflammatory cell, particularly neutrophils to the airways (He et al., 2016). This is accompanied by secretion of inflammatory cytokines such as IL-6, -12, TNF-α, MIP-1α, and MCP-1. This effect appears to

be due to TLR signaling, as MyD88^{ko} mice had dramatically reduced inflammation. Individual TLR2^{ko} and TLR4^{ko} models had attenuated responses, with TLR4^{ko} having a more dramatic effect than TLR2^{ko}. Interestingly, research indicates that the inflammatory effect is likely due to pollutants entrained on the dust, as ASD that was heated at 360 °C for 24 hours (H-ASD) had diminished effectiveness (He et al., 2016). The inflammatory phenotype was restored when administering H-ASD with either an organic extract from ASD (Ren et al., 2014), ultrapure LPS, or peptidoglycan (PGN) (Sadakane et al., 2022). The combination of H-ASD and these pollutant/TLR agonists had a stronger response than either alone (Ren et al., 2014; He et al., 2019). These inflammatory cytokine secretions are also consistent in macrophage, human bronchial epithelial, and human epidermal keratinocyte cell lines, possibly indicating broad reactivity for ASD (Shin et al., 2013; He et al., 2016; Choi et al., 2019).

Notably, these results did not seem to suggest that ASD alone can trigger asthma development. Several studies address this concern and offer a plausible link between allergies and ASD. When mice are given a mixture ASD and ovalbumin (OVA) intranasally, they develop an allergic reaction to OVA (Fussell and Kelley 2021). The most extreme synergistic effect requires both entrained pollutants and ASD. Studies using an H-ASD + OVA + dust pollutant/TLR agonist have high levels of eosinophil recruitment and allergy associated cytokines, along with OVA specific IgE and IgG production (Ren et al., 2014a; Ren et al., 2014b; He et al., 2019; Ren et al., 2019; Sadakane et al., 2022). This synergistic

effect may require oxidative stress, as addition of NAC, an oxidative stress scavenger, eliminated this response (He et al., 2019). Co-exposure to a more common real-world allergen, house-dust mite (HDM), also triggered a synergistic response (Ichinose et al., 2006). Together these studies suggest that ASD may serve as an adjuvant that enhances allergic development.

While not as well studied as ASD, several other regions of desert dust have been linked to poor pulmonary health. The Sahara and Sahel regions of North Africa are another large source of desert dust. This dust primarily effects Europe and Turkey, but it can also be transported across the Atlantic Ocean and has been linked to asthma exacerbations in the Caribbean (Akpinar-Elci et al., 2015). Studies in Europe and Anatolia indicate that day's high in desert dust from North Africa leads to increase levels of ER visits due to pulmonary diseases such as asthma, COPD, and respiratory infections (Samoli et al., 2011; Yitshak et al., 2015; Soy et al., 2016; Trianti et al., 2017; Lorentzou et al., 2019), as well as worsening of ischemic heart disease (Dominguez-Rodriguez et al., 2020). This effect correlates with PM_{10} levels, with particularly high levels of PM_{10} during severe dust storm days triggering an increase in ER visits that last several days. As dust storms and high levels of indoor PM_{10} occur at the same time, it is likely that individuals living in the region are constantly being exposed to potential pulmonary inflammatory agents (Sahin et al., 2022).

The interplay between indoor and outdoor aeroallergens may be important to understanding the ways that desert dust relates to asthma. Studies from the

Middle East indicate that the dust in the region has mild toxicity (Wilfong et al., 2011; Fussell and Kelley, 2021). Despite this, rates of asthma and allergies have been increasing since at least the 1980's (Strannegård and Strannegård, 1987; Strannegård and Strannegård, 1990). This has been linked to importation of non-native pollinating plants and the proliferation of household cooling systems such as air conditioning increasing levels of allergens, all of which commonly show up in skin prick tests (Dowaisan et al., 2000; Ezeamuzie et al., 2000; Bener et al., 2002; Hijazi et al., 2002; Sattar et al., 2003; AlKhater et al., 2017). Of particular note are mold allergens, which are associated with asthma among children (Ezeamuzie et al., 2000). While older studies did not find a link between dust storms and ER visits due to respiratory illnesses (Strannegård and Strannegård, 1987; Strannegård and Strannegård, 1990), newer studies indicate increased admissions on dust storm days (Thalib and Al-Taiar, 2012). The exact reason for this discrepancy has not been explored and may be due to new techniques to measure dust levels and better record keeping or due to increased levels of allergens carried on the dust due to aforementioned importation of plants and adoption of cooling systems.

While other regions are less well-studied, there have been some documented effects of desert dust from other sources. Desert dust collected from desert regions in India were found to induce a decline in forced expiratory volume in 1 second (FEV_1) in humans. The worst declines were when patients inhaled smaller, more adhesive PM (Gupta et al., 2012). Asthma in Utah was linked to

arid desert regions, particularly those with a history of mining activity and poor socioeconomic parameters (Vowles et al., 2020). Much like in the Middle East, there is likely a connection between the desert environment and exposure to indoor allergens, with individuals in homes with an evaporative cooler having much higher levels of fungal allergens (Lemons et al., 2017). In the Sonoran Desert region, pollens and indoor allergens dominated in skin prick test results (Buckley and Carr, 2017). Afghanistan dust was found to work in concert with HDM to increase airway hyperreactivity in mice, even when sensitization to HDM occurred a week after exposure to the Afghanistan dust (Berman et al., 2021).

When put together, these studies indicate a role for desert dusts to exacerbate asthma symptoms during dust storm events, along with a role in sensitization when combined with indoor and outdoor allergens such as molds, dust mites, and pollen. While the Salton Sea Basin in particular has yet to be studied in detail, the ability of desert dusts from around the world to cause pulmonary distress indicates that it could be a critical component of the poor respiratory health in the region. Despite the similarities in overall response between different point sources of desert dust, each had a unique toxicity. Thus, it is critical to study the unique characteristics of dust in the Salton Sea Basin and how it specifically triggers pulmonary inflammation. The Coachella valley is already the dustiest region in the Mojave and Colorado Deserts and will only get worse as the Salton Sea dries. Other dried arid lakes in California have led to massive dust storms, with Owens Lake and Mono Lake storms reaching highs of

40,620 and 65,112 μg/m^3 for PM_{10} (Goudie, 2014). With the potential for massive dust storms on the horizon, and knowledge of how dust storms in other regions can exacerbate and even lead to asthma, understanding the characteristics of particulate matter near the Salton Sea is of the utmost importance.

Dust Generation from Playa

When reviewing dust from the Salton Sea Basin, it is important to understand the unique characteristics of dust generation from playa in a desert environment. While deserts can generate dust from non-playa sources, the vast majority of desert surfaces are not susceptible to wind erosion, and thus dust generation. The exact amount depends on several factors, primarily whether the land is cultivated, as that can increase the amount of surface susceptible to wind erosion.

Playa is uniquely suited to generate dust compared to other desert sources. Firstly, arid lakes and playa can serve as sinks for dust, as fine silts are either carried to the lakes by input streams and rivers, or through settling in the lakes and playa (Gill, 1996). These fine silts are more easily aerosolized compared to larger, coarse particles. Second, playa is particularly susceptible to salt weathering. During this process, salt breaks apart the playa surface and helps release any trapped fine silt- or clay-size particles (Gillette, 1979). This is perhaps the most important mechanism in dust generation from playa, particularly in arid lakes such as Owens Lake (Cahill et al., 1994; Cahill et al.,

1996). Finally, playa tends to be a flat, friable surface, which increases the rate of wind erosion (Blackwelder 1931). Unlike cultivation of arid regions leading to an increase in desert dusts, this is not an anthropogenic process. However, this process can and has been sped up by diverting water sources and increasing temperatures due to climate change.

Chronic Respiratory Disease

Chronic respiratory disease is one of the largest burdens on human health globally. Every year, an estimated 4 million people die due to respiratory diseases such as asthma, chronic obstructive pulmonary disorder (COPD) and a myriad of other chronic respiratory diseases such as interstitial lung disease and sarcoidosis (WHO). This is particularly prevalent among children and is one of the more common causes of death in children under the age of 5 (Burney et al., 2017). Additionally, chronic respiratory disease is a massive burden on the healthcare system, costing hundreds of billions yearly in treatment and workhours lost (European Respiratory Society, 2018).

As recently as 2017, approximately 554.9 million people, or 7.1% of the global population, had some form of chronic respiratory disease. By far the most common are asthma and COPD, which make up approximately 50% and 55% of individuals with chronic respiratory diseases (GBD Chronic Respiratory Disease Collaborators, 2020). Asthma is more common among children, with it being skewed towards males in children under 10 and towards females in the 10+ age

range. COPD is more common among older individuals, with a slightly higher rate in men. It is also more deadly than asthma on the global scale (GBD Chronic Respiratory Disease Collaborator, 2020). As these are the two major chronic respiratory diseases, asthma and COPD will be the focus of the following sections.

Asthma

Traditionally, asthma has been defined as an atopic disease driven by Th2 cells, eosinophils, and allergen specific IgE production (Kuruvilla et al., 2019). However, this definition has been called into question over the past decade as more has been discovered about the presentation of asthma. Now, asthma is recognized as a heterogeneous disease with many possible causes, all of which present as increased airway hyperreactivity (Gans and Gavrilova, 2020).

Currently, asthma is divided into two broad categories, type-2-high (T2-high) and type-2-low (T2-low) (Fitzpatrick et al., 2020). Traditional atopic asthma falls into the T2-high category and is the most well understood of the multitude of ways asthma presents. T2-low asthma is less well understood and is broken down into neutrophilic and paucigranulocytic subtypes, which are characterized by high neutrophil counts in sputum or no elevation in either neutrophil or eosinophil levels in sputum respectively (Sze et al., 2020). Generally, T2-high asthma presents earlier, with symptoms often emerging in childhood or young adulthood, while T2-low asthma presents later, often when the patient is solidly in

adulthood (Hudey et al., 2020). T2-low asthma also tends to be corticosteroid resistant, and thus has limited treatment options (Ricciardolo et al., 2021).

As previously mentioned, T2-high asthma is better understood and has a well-defined pathway. When under allergen challenge, epithelial cells produce several key alarmins, which prime the immune system towards a T2 response. These include thymic stromal lymphopoietin (TSLP), and interleukins (IL) -25 and -33 (Kubo, 2017). This process likely depends on damage to the tight junction between epithelial cells, as asthmatics usually have the loss of E-cadherin and claudin-18, which are key components in the tight junction (Yang et al., 2019). Several allergens have direct protease-cleaving abilities, and can directly cleave these tight junction proteins, which may aid in their ability to induce allergic reactions (Chevigné and Jacquet, 2018).

Once released, these alarmins begin to activate several downstream processes that promote an allergic response. IL-33 binds to receptor ST-2, which is highly expressed on Group 2 Innate Lymphoid Cells (ILC2s) (Salimi et al., 2013). Once activated, ILC2s undergo expansion and begin to produce high levels of T2 cytokines IL-5 and -13 (Maggi et al., 2021). This is a critical component of early, acute allergic response, particularly in protease-containing allergens (Gold et al., 2014). IL-5 drives eosinophil production in the bone marrow (Menzies et al., 2003) and acts as a potent eosinophil recruiter (Kandikattu et al., 2019) while IL-13 promotes goblet cell hyperplasia and mucus hypersecretion (Pelaia et al., 2022).

TSLP binds to and activates dendritic cells, which present antigen to naïve T cells and promotes differentiation into CD4+ Th2 T cells (Soumelis et al., 2002). Additionally, TSLP plays a role in basophil recruitment to sites of allergic inflammation (Lv et al., 2018).

Th2 cells produce cytokines such as IL-4, -5, -9, and -13 (Romagnani, 2000). IL-4 is a key regulatory cytokine that drives B cell class switching to IgE+ B cells (Kashiwada et al., 2010) and promotes their further development into immunoglobulin E+ (IgE+) plasma B cells, which are the primary secretors of allergen specific IgE (Saito et al., 2008). IL-9 promotes mast cell (MC) hyperplasia (Tete et al., 2012).

Eosinophils are the critical cell type associated with T2-high asthma. Clinical determination of T2-high asthma relies on detecting high levels of eosinophil in the sputum of patients (Coverstone et al., 2020). These cells are recruited to the site of inflammation primarily by eotaxin and IL-5 (Nussbaum et al., 2013). Once eosinophils reach the site of inflammation, they are activated by the multitude of T2 cytokines such as IL-4, IL-5, and IL-13 and begin to secrete a variety of inflammatory molecules (Ravin and Loy, 2016). These have a variety of downstream effects, including activation of bronchial fibroblasts (Dolgachev et al., 2008), increased airway smooth muscle contractility (Janulaityte et al., 2021), increased bronchoconstriction (Dimova-Yaneva and Helms, 2003), and increased ILC2 activation (Badrani et al., 2021).

Mast cells (MC) and basophils have similar functions in T2-high asthma, as they are both cells that secrete histamines and lipid mediators in response to IgE binding and crosslinking FcεR1 on their surfaces (Holgate, 2014). However, there are several key differences between the cell types. MCs are tissue-based cells, while basophils are bloodborne (Marone et al., 2005). MCs appear to be critical for IgE driven airway hyperreactivity (Sawaguchi et al., 2012), while basophils appear to be necessary for protease allergen-mediate acute lung inflammation (Motomura et al., 2014). When these cells are activated, they degranulate and release a variety of inflammatory mediators, among which are histamines and prostaglandin D2 (PGD2) (Kabashima et al., 2018). These are potent vasoactive substances that can induce anaphylactic reactions in patients (Nguyen et al., 2021).

As previously mentioned, T2-low is not as well understood as T2-high asthma. Despite this, T2-low asthma may account for almost half of asthma cases and over 60% of severe asthma cases (Kuruvilla et al., 2019).

For the T2-low neutrophilic asthma, there have been some studies linking the response to both Th1 and Th17. Th1 cells are known secretors of IFN-γ (Zygmunt et al., 2018). In approximately 50% of patients with severe asthma, IFN-γ production is dysregulated, and this correlates with airway resistance and corticosteroid refractoriness (Raundhal et al., 2015). This has been confirmed in animal models of severe asthma, which have high levels of IFN-γ production and

low secretory leukocyte protease inhibitor (SLPI), which may be the primary driver of the airway hyperreactivity (Raundhal et al., 2015).

Neutrophilic Th17 asthma depends on the secretion of IL-17A, -17F, and -22 by Th17 cells (Sugaya, 2020). High levels of IL-17A and IL-17F have been found in patients with neutrophilic asthma (Ramakrishnan et al., 2019). IL-17A and -22 contribute to airway remodeling via increased smooth muscle cell proliferation (Chang et al., 2012) and collagen deposition (Sisto et al., 2019). IL-17A and -17F promote the secretion of neutrophil chemokines CXCL1 and CXCL8 (IL-8) from airway epithelial cells (Cao et al, 2011). Additionally, IL-17 triggers IL-6 secretion (Ning et al., 2005), which is correlated with worse lung function (Peters et al., 2020).

The direct role that neutrophils may play in neutrophilic asthma is currently unknown. There is some research that suggests that neutrophil extracellular traps (NETs) may play a role, as patients with severe asthma have higher levels of airway neutrophil-derived sputum extracellular DNA levels (Lachowicz-Scroggins et al., 2019). Neutrophils also mediate persistent inflammation, which could play a role in damaging the airways (Sze et al., 2020).

Paucigranulocytic asthma is currently thought to be due to dysregulation of neural mediators and sphingolipids (Hudey et al., 2020). Airway hyperreactivity relies upon airway smooth muscle contraction. Asthmatics tend to have greater cholinergic nerve density in bronchial biopsies (Dragunas et al., 2020). While this may play a role in other forms of asthma, it has been shown that administration

of nerve growth factor (NGF) alone was capable of inducing airway hyperreactivity to a similar degree as allergen sensitization without promoting airway inflammation (Braun et al., 2001).

Sphingolipids are mediators that play a role in a wide range of cellular functions including roles in cell growth, cell death, inflammation, and immune response (Gomez-Larrauri et al., 2020). Studies with mice that overexpress ORMDL3, which inhibits sphingolipid synthesis, have increased airway hyperreactivity and airway remodeling without airway inflammation, indicating that dysregulation of this pathway may be sufficient to cause paucigranulocytic asthma (Millet et al., 2014). This is corroborated by the finding that T2-low asthmatic children tend to have lower serum sphingolipid levels compared to T2-high and non-asthmatic children (Ono et al., 2020).

As can be seen, asthma is a truly heterogeneous disease with mechanisms that need further elucidation. While T2-high asthma is relatively well understood, T2-low asthma is poorly defined and lacks effective treatments. To advance the field of asthma research, it is important to keep an open mind on potential mechanisms and examine the potential for both T2-high and T2-low responses.

Chronic Obstructive Pulmonary Disorder (COPD)

Chronic obstructive pulmonary disorder is a disease characterized by fixed airflow obstruction as measure by spirometry, with a forced expiratory volume in

1 second (FEV_1)/forced vital capacity (FVC) ratio of <70% (Barnes PJ, 2019). This disease often presents with small airway disease with peribronchiolar fibrosis and emphysema with alveolar destruction (Fazleen and Wilkinson, 2020). Smoking is the most important environmental factor for development of COPD (Christenson et al., 2022). Mechanistically, COPD is thought to be driven by oxidative stress, imbalance in protease/anti-protease levels, and chronic inflammation (Guo et al., 2022).

Oxidative stress markers are elevated in patients with COPD (Stanojkovic et al., 2011). Pollutants such as cigarette smoke (CS) or biomass burning can supply exogenous sources of oxidative stress, aiding in COPD progression (Faux et al., 2009). Increased oxidative burden directly ties into several other facets of COPD. In addition to exogenous sources of oxidative stress, activated neutrophils and macrophages produce and secrete reactive oxygen species (ROS) such as superoxide anions and H_2O_2 (Dominic et al., 2022). These ROS have a multitude of damaging effects in the lung. The xanthine/xanthine oxidase system increases epithelial mucus secretion (Hiraishi et al., 1991). ROS can directly damage the lung tissue, leading to secretion of alarmins that can enhance inflammation (Ryter et al., 2007). Additionally, ROS can directly enhance inflammation through activation of redox-sensitive transcription factors such as NF-κB, AP-1, ERK, JNK, and p38MAPK (Barnes PJ, 2020). ROS can lead to lipid peroxidation and protein carbonylation, which can create neoantigens and enhance CD8+ T cell-driven cytotoxicity and lung tissue

damage (Kirkham et al., 2011). α1-antitrypsin, a key antiprotease, can be directly inactivated by ROS (Siddiqui et al., 2016). It can also increase expression of proteases such as MMP-9 (Bernard et al., 2008). Oxidative stress also reduces the activity and expression of histone deacetylase-2 (HDAC2) (Osoata et al., 2009). HDAC2 is required for inflammatory gene suppression by corticosteroids (Barnes, 2010), and this interaction may explain the insensitivity of COPD to corticosteroids (Barnes, 2009). The TGF-β signaling pathway, which is involved in airway remodeling, is also activated by oxidative stress (Liu and Gaston Pravia, 2010). This pathway also has an inhibitory effect on Nrf2, which is a transcription factor involved with antioxidant gene expression, exacerbating oxidative stress (Wang et al., 2020).

Protease/anti-protease imbalance is thought to lead to emphysema in COPD (Abboud and Vimalanathan, 2008). The primary producers of proteases in the lungs of COPD patients are activated neutrophils and macrophages (Wang et al., 2018). The two major categories that are implicated in COPD are serine proteases and metalloproteinases (MMPs) (Tetley et al., 2002). MMPs, such as MMP-9, promote vascular remodeling and proliferation of smooth muscle and endothelial cells (Grzela et al., 2016). Neutrophil elastase (NE), a major serine protease in neutrophils, can degrade structural components of the extracellular matrix (ECM) (Voynow and Shinbashi, 2021). NE can additionally enhance fibroblast proliferation and mucus secretion (Voynow and Shinbashi, 2021), playing a role in airway remodeling. The combined effects of MMPs and serine

proteases degrade the extracellular matrix, releasing alarmins and enhancing inflammation (Burgess and Harmsen, 2022).

Chronic neutrophilic inflammation is a hallmark of COPD (Liang et al., 2020). NF-κB signaling is enhanced in COPD patients, along with TNF-α, IL-1β, and IL-6 (Wang et al., 2020). These inflammatory cytokines and their signaling pathways trigger neutrophil and macrophage recruitment and retainment in the lung tissue (Pettersen and Adler, 2002). Once recruited and activated, neutrophils and macrophages are major producers of proteinases and ROS (Wang et al., 2020). These cells additionally produce inflammatory cytokines and chemokines such as IL-8, IL-1β, which further recruit inflammatory cells and enhance the inflammatory cascade (Wang et al., 2018).

Even with the current mechanistic understanding of COPD, much remains to be elucidated. As COPD is primarily a late-onset disease (Raherison and Girodet, 2009), there is a need to understand early signs of COPD. Thus, it is important to keep the pathogenesis of COPD in mind when examining an unknown trigger of pulmonary inflammation, as the phenotype observed may relate to COPD development in the future.

Conclusion

As the communities surrounding the Salton Sea are experiencing a pulmonary health crisis, it is critical to begin to answer questions about the potential triggers and mechanisms. Desert dusts around the world play a role in

causing and exacerbating chronic pulmonary diseases such as asthma. As pulmonary diseases such as asthma and COPD can be displayed in a multitude of ways, it is important to keep an open mind in the potential pathogenic mechanisms of aerosols around the Salton Sea. The work outlined in this dissertation begins to answer the ways that these aerosols may relate to chronic pulmonary disease, keeping in mind the heterogeneous ways that these chronic pulmonary diseases may present.

References

Abboud RT, Vimalanathan S. Pathogenesis of COPD. Part I. The role of protease-antiprotease imbalance in emphysema. Int J Tuberc Lung Dis. 2008 Apr;12(4):361-7. PMID: 18371259.

Akpinar-Elci M, Martin FE, Behr JG, Diaz R. Saharan dust, climate variability, and asthma in Grenada, the Caribbean. Int J Biometeorol. 2015 Nov;59(11):1667-71. doi: 10.1007/s00484-015-0973-2. Epub 2015 Feb 24. PMID: 25707919.

AlKhater SA. Sensitization to Common Aeroallergens in Asthmatic Children in the Eastern Region of Saudi Arabia. Saudi J Med Med Sci. 2017 May-Aug;5(2):136-141. doi: 10.4103/1658-631X.204876. Epub 2017 Apr 20. PMID: 30787771; PMCID: PMC6298380.

Aristizábal B, González Á. Innate immune system. In: Anaya JM, Shoenfeld Y, Rojas-Villarraga A, et al., editors. Autoimmunity: From Bench to Bedside [Internet]. Bogota (Colombia): El Rosario University Press; 2013 Jul 18. Chapter 2. Available from: https://www.ncbi.nlm.nih.gov/books/NBK459455/

Badrani JH, Doherty TA. Cellular interactions in aspirin-exacerbated respiratory disease. Curr Opin Allergy Clin Immunol. 2021 Feb 1;21(1):65-70. doi: 10.1097/ACI.0000000000000712. PMID: 33306487; PMCID: PMC7769923.

Barnes PJ. Inflammatory endotypes in COPD. Allergy. 2019 Jul;74(7):1249-1256. doi: 10.1111/all.13760. Epub 2019 Mar 31. PMID: 30834543.

Barnes PJ. Inhaled Corticosteroids. Pharmaceuticals (Basel). 2010 Mar 8;3(3):514-540. doi: 10.3390/ph3030514. PMID: 27713266; PMCID: PMC4033967.

Barnes PJ. Oxidative stress-based therapeutics in COPD. Redox Biol. 2020 Jun;33:101544. doi: 10.1016/j.redox.2020.101544. Epub 2020 Apr 20. PMID: 32336666; PMCID: PMC7251237.

Barnes PJ. Role of HDAC2 in the pathophysiology of COPD. Annu Rev Physiol. 2009;71:451-64. doi: 10.1146/annurev.physiol.010908.163257. PMID: 18817512.

Bener A, Safa W, Abdulhalik S, Lestringant GG. An analysis of skin prick test reactions in asthmatics in a hot climate and desert environment. Allerg Immunol (Paris). 2002 Oct;34(8):281-6. PMID: 12449666.

Berman R, Min E, Huang J, Kopf K, Downey GP, Riemondy K, Smith HA, Rose CS, Seibold MA, Chu HW, Day BJ. Single-Cell RNA Sequencing Reveals a Unique Monocyte Population in Bronchoalveolar Lavage Cells of Mice Challenged With Afghanistan Particulate Matter and Allergen. Toxicol Sci. 2021 Aug 3;182(2):297-309. doi: 10.1093/toxsci/kfab065. PMID: 34051097; PMCID: PMC8331170.

Bernard Y, Melchior C, Tschirhart E, Bueb JL. Co-cultures of human coronary smooth muscle cells and dimethyl sulfoxide-differentiated HL60 cells upregulate ProMMP9 activity and promote mobility-modulation by reactive oxygen species. Inflammation. 2008 Oct;31(5):287-98. doi: 10.1007/s10753-008-9077-z. PMID: 18665441.

Beutler B. Innate immunity: an overview. Mol Immunol. 2004 Feb;40(12):845-59. doi: 10.1016/j.molimm.2003.10.005. PMID: 14698223.

Blackwelder, E., 1931. The lowering of playas by deflation. Am. J. Sci., 21: 140-144

Bonilla FA, Oettgen HC. Adaptive immunity. J Allergy Clin Immunol. 2010 Feb;125(2 Suppl 2):S33-40. doi: 10.1016/j.jaci.2009.09.017. Epub 2010 Jan 12. PMID: 20061006.

Bradley TJ, Yanega GM. Salton Sea: Ecosystem in transition. Science. 2018 Feb 16;359(6377):754. doi: 10.1126/science.aar6088.

Braun A, Quarcoo D, Schulte-Herbrüggen O, Lommatzsch M, Hoyle G, Renz H. Nerve growth factor induces airway hyperresponsiveness in mice. Int Arch Allergy Immunol. 2001 Jan-Mar;124(1-3):205-7. doi: 10.1159/000053711. PMID: 11306969.

Buckley RD, Carr TF. Association of aeroallergen sensitization and atopic disease in the Sonoran Desert. Allergy Asthma Proc. 2017 Sep 1;38(5):370-375. doi: 10.2500/aap.2017.38.4077. PMID: 28814357.

Bureau of Reclamation. *Annual Report on the Salton Sea*. (Online). February 2022. Available: https://saltonsea.ca.gov/wp-content/uploads/2022/02/2022-Annual-Report_English_Feb-24-2022_Final.pdf. Referenced: March 10, 2023

Burgess JK, Harmsen MC. Chronic lung diseases: entangled in extracellular matrix. Eur Respir Rev. 2022 Mar 9;31(163):210202. doi: 10.1183/16000617.0202-2021. PMID: 35264410; PMCID: PMC9488575.

Burney P, Perez-Padilla R, Marks G, et al. Chronic Lower Respiratory Tract Diseases. In: Prabhakaran D, Anand S, Gaziano TA, et al., editors. Cardiovascular, Respiratory, and Related Disorders. 3rd edition. Washington (DC): The International Bank for Reconstruction and Development / The World Bank; 2017 Nov 17. Chapter 15. Available from: https://www.ncbi.nlm.nih.gov/books/NBK525159/ doi: 10.1596/978-1-4648-0518-9_ch15

Burr AC, Velazquez JV, Ulu A, Kamath R, Kim SY, Bilg AK, Najera A, Sultan I, Botthoff JK, Aronson E, Nair MG, Nordgren TM. Lung Inflammatory Response to Environmental Dust Exposure in Mice Suggests a Link to Regional Respiratory Disease Risk. J Inflamm Res. 2021 Aug 21;14:4035-4052. doi: 10.2147/JIR.S320096. PMID: 34456580; PMCID: PMC8387588.

Cahill, T.A., Gill, T.E., Reid, J.S., Gearhart, E.A. and Gillette, D.A., 1996. Saltating particles, playa crusts and dust aerosols from Owens (Dry) Lake, California. Earth Surface Processes Landforms, in press.

Cahill, T.A., Gillette, D.A., Gill, T.E., Gearhart, E.A., Reid, J.S. and Yau, M.L., 1994. Generation, Characterization and Transport of Owens (Dry) Lake Dusts. Final Report to the California Air Resources Board, Contract No. A-132-105.

California Environmental Protection Agency, Office of Environmental Health Hazard Assessment, 2021, October 20. CalEnviroScreen 4.0. Retrieved from. https://oehha.ca.gov/calenviroscreen/report/calenviroscreen-40

Cancro MP, Tomayko MM. Memory B cells and plasma cells: The differentiative continuum of humoral immunity. Immunol Rev. 2021 Sep;303(1):72-82. doi: 10.1111/imr.13016. Epub 2021 Aug 15. PMID: 34396546.

Cao J, Ren G, Gong Y, Dong S, Yin Y, Zhang L. Bronchial epithelial cells release IL-6, CXCL1 and CXCL8 upon mast cell interaction. Cytokine. 2011 Dec;56(3):823-31. doi: 10.1016/j.cyto.2011.09.016. Epub 2011 Oct 24. PMID: 22030312.

Carmichael WW, Li R. Cyanobacteria toxins in the Salton Sea. Saline Syst. 2006 Apr 19;2:5. doi: 10.1186/1746-1448-2-5. PMID: 16623944; PMCID: PMC1472689.

Chang Y, Al-Alwan L, Risse PA, Halayko AJ, Martin JG, Baglole CJ, Eidelman DH, Hamid Q. Th17-associated cytokines promote human airway smooth muscle cell proliferation. FASEB J. 2012 Dec;26(12):5152-60. doi: 10.1096/fj.12-208033. Epub 2012 Aug 16. PMID: 22898922.

Cheney AM, Barrera T, Rodriguez K, Jaramillo López AM. The Intersection of Workplace and Environmental Exposure on Health in Latinx Farm Working Communities in Rural Inland Southern California. Int J Environ Res Public Health. 2022 Oct 10;19(19):12940. doi: 10.3390/ijerph191912940. PMID: 36232240; PMCID: PMC9566176.

Chevigné A, Jacquet A. Emerging roles of the protease allergen Der p 1 in house dust mite-induced airway inflammation. J Allergy Clin Immunol. 2018 Aug;142(2):398-400. doi: 10.1016/j.jaci.2018.05.027. Epub 2018 Jun 12. PMID: 29906529.

Choi H, Shin DW, Kim W, Doh SJ, Lee SH, Noh M. Asian dust storm particles induce a broad toxicological transcriptional program in human epidermal keratinocytes. Toxicol Lett. 2011 Jan 15;200(1-2):92-9. doi: 10.1016/j.toxlet.2010.10.019. Epub 2010 Nov 4. PMID: 21056094.

Christenson SA, Smith BM, Bafadhel M, Putcha N. Chronic obstructive pulmonary disease. Lancet. 2022 Jun 11;399(10342):2227-2242. doi: 10.1016/S0140-6736(22)00470-6. Epub 2022 May 6. PMID: 35533707.

Courtney AH, Lo WL, Weiss A. TCR Signaling: Mechanisms of Initiation and Propagation. Trends Biochem Sci. 2018 Feb;43(2):108-123. doi: 10.1016/j.tibs.2017.11.008. Epub 2017 Dec 18. PMID: 29269020; PMCID: PMC5801066.

Coverstone AM, Seibold MA, Peters MC. Diagnosis and Management of T2-High Asthma. J Allergy Clin Immunol Pract. 2020 Feb;8(2):442-450. doi: 10.1016/j.jaip.2019.11.020. PMID: 32037108.

D'Evelyn SM, Vogel C, Bein KJ, Lara B, Laing EA, Abarca RA, Zhang Q, Li L, Li J, Nguyen TB, Pinkerton KE. Differential inflammatory potential of particulate matter (PM) size fractions from Imperial Valley, CA. Atmos Environ (1994). 2021 Jan 1;244:117992. doi: 10.1016/j.atmosenv.2020.117992. Epub 2020 Oct 14. PMID: 33184556; PMCID: PMC7654835.

Dimova-Yaneva DN, Helms PJ. The role of leukotrienes and eosinophil cationic protein in acute respiratory syncytial virus bronchiolitis. Folia Med (Plovdiv). 2003;45(3):5-11. PMID: 15366660.

Doede AL, Davis R, DeGuzman PB. Use of trajectory models to track air pollution from source to exposure: A methodological approach for identifying communities at risk. Public Health Nurs. 2021 Mar;38(2):212-222. doi: 10.1111/phn.12859. Epub 2021 Jan 7. PMID: 33410552.

Doede AL, DeGuzman PB. The Disappearing Lake: A Historical Analysis of Drought and the Salton Sea in the Context of the GeoHealth Framework. Geohealth. 2020 Sep 23;4(9):e2020GH000271. doi: 10.1029/2020GH000271. PMID: 32999947; PMCID: PMC7509641.

Dolasia K, Bisht MK, Pradhan G, Udgata A, Mukhopadhyay S. TLRs/NLRs: Shaping the landscape of host immunity. Int Rev Immunol. 2018 Jan 2;37(1):3-19. doi: 10.1080/08830185.2017.1397656. Epub 2017 Dec 1. PMID: 29193992.

Dolgachev V, Berlin AA, Lukacs NW. Eosinophil activation of fibroblasts from chronic allergen-induced disease utilizes stem cell factor for phenotypic changes. Am J Pathol. 2008 Jan;172(1):68-76. doi: 10.2353/ajpath.2008.070082. Epub 2007 Dec 21. PMID: 18156208; PMCID: PMC2189616.

Dominguez-Rodriguez A, Rodríguez S, Baez-Ferrer N, Abreu-Gonzalez P, Abreu-Gonzalez J, Avanzas P, Carnero M, Moris C, López-Darias J, Hernández-Vaquero D. Impact of Saharan dust exposure on airway inflammation in patients with ischemic heart disease. Transl Res. 2020 Oct;224:16-25. doi: 10.1016/j.trsl.2020.05.011. Epub 2020 Jun 3. PMID: 32504824.

Dominic A, Le NT, Takahashi M. Loop Between NLRP3 Inflammasome and Reactive Oxygen Species. Antioxid Redox Signal. 2022 Apr;36(10-12):784-796. doi: 10.1089/ars.2020.8257. Epub 2022 Jan 17. PMID: 34538111.

Dowaisan A, Al-Ali S, Khan M, Hijazi Z, Thomson MS, Ezeamuzie CI. Sensitization to aeroallergens among patients with allergic rhinitis in a desert environment. Ann Allergy Asthma Immunol. 2000 Apr;84(4):433-8. doi: 10.1016/s1081-1206(10)62277-6. PMID: 10795652.

Dragunas G, Woest ME, Nijboer S, Bos ST, van Asselt J, de Groot AP, Vohlídalová E, Vermeulen CJ, Ditz B, Vonk JM, Koppelman GH, van den Berge M, Ten Hacken NHT, Timens W, Munhoz CD, Prakash YS, Gosens R, Kistemaker LEM. Cholinergic neuroplasticity in asthma driven by TrkB signaling. FASEB J. 2020 Jun;34(6):7703-7717. doi: 10.1096/fj.202000170R. Epub 2020 Apr 11. PMID: 32277855; PMCID: PMC7302963.

European Respiratory Society, E. "The economic burden of lung disease." European lung white book (2018).

Ezeamuzie CI, Al-Ali S, Khan M, Hijazi Z, Dowaisan A, Thomson MS, Georgi J. IgE-mediated sensitization to mould allergens among patients with allergic respiratory diseases in a desert environment. Int Arch Allergy Immunol. 2000 Apr;121(4):300-7. doi: 10.1159/000024343. PMID: 10828720.

Ezeamuzie CI, Thomson MS, Al-Ali S, Dowaisan A, Khan M, Hijazi Z. Asthma in the desert: spectrum of the sensitizing aeroallergens. Allergy. 2000 Feb;55(2):157-62. doi: 10.1034/j.1398-9995.2000.00375.x. PMID: 10726730.

Farzan, S. F., Razafy, M., Eckel, S. P., Olmedo, L., Bejarano, E., & Johnston, J. E. (2019). Assessment of respiratory health symptoms and asthma in children near a drying saline lake. International Journal of Environmental Research and Public Health, 16(20). https://doi.org/10.3390/ijerph16203828

Faux SP, Tai T, Thorne D, Xu Y, Breheny D, Gaca M. The role of oxidative stress in the biological responses of lung epithelial cells to cigarette smoke. Biomarkers. 2009 Jul;14 Suppl 1:90-6. doi: 10.1080/13547500902965047. PMID: 19604067.

Fazleen A, Wilkinson T. Early COPD: current evidence for diagnosis and management. Ther Adv Respir Dis. 2020 Jan-Dec;14:1753466620942128. doi: 10.1177/1753466620942128. PMID: 32664818; PMCID: PMC7394029.

Fitzpatrick AM, Chipps BE, Holguin F, Woodruff PG. T2-"Low" Asthma: Overview and Management Strategies. J Allergy Clin Immunol Pract. 2020 Feb;8(2):452-463. doi: 10.1016/j.jaip.2019.11.006. PMID: 32037109.

Frie AL, Dingle JH, Ying SC, Bahreini R. The Effect of a Receding Saline Lake (The Salton Sea) on Airborne Particulate Matter Composition. Environ Sci Technol. 2017 Aug 1;51(15):8283-8292. doi: 10.1021/acs.est.7b01773. Epub 2017 Jul 21. PMID: 28697595.

Frie AL, Garrison AC, Schaefer MV, Bates SM, Botthoff J, Maltz M, Ying SC, Lyons T, Allen MF, Aronson E, Bahreini R. Dust Sources in the Salton Sea Basin: A Clear Case of an Anthropogenically Impacted Dust Budget. Environ Sci Technol. 2019 Aug 20;53(16):9378-9388. doi: 10.1021/acs.est.9b02137. Epub 2019 Aug 6. PMID: 31339712.

Fussell JC, Kelly FJ. Mechanisms underlying the health effects of desert sand dust. Environ Int. 2021 Dec;157:106790. doi: 10.1016/j.envint.2021.106790. Epub 2021 Jul 29. PMID: 34333291; PMCID: PMC8484861.

Gans MD, Gavrilova T. Understanding the immunology of asthma: Pathophysiology, biomarkers, and treatments for asthma endotypes. Paediatr Respir Rev. 2020 Nov;36:118-127. doi: 10.1016/j.prrv.2019.08.002. Epub 2019 Oct 9. PMID: 31678040.

GBD Chronic Respiratory Disease Collaborators. Prevalence and attributable health burden of chronic respiratory diseases, 1990-2017: a systematic analysis for the Global Burden of Disease Study 2017. Lancet Respir

Med. 2020 Jun;8(6):585-596. doi: 10.1016/S2213-2600(20)30105-3. PMID: 32526187; PMCID: PMC7284317.

Gillette, D.A., 1979. Environmental factors affecting dust emission by wind erosion. In: C. Morales (Editor), Saharan Dust(SCOPE 14). Wiley, Chichester, pp. 71-91.

Gold MJ, Antignano F, Halim TY, Hirota JA, Blanchet MR, Zaph C, Takei F, McNagny KM. Group 2 innate lymphoid cells facilitate sensitization to local, but not systemic, TH2-inducing allergen exposures. J Allergy Clin Immunol. 2014 Apr;133(4):1142-8. doi: 10.1016/j.jaci.2014.02.033. PMID: 24679471.

Gomez-Larrauri A, Presa N, Dominguez-Herrera A, Ouro A, Trueba M, Gomez-Muñoz A. Role of bioactive sphingolipids in physiology and pathology. Essays Biochem. 2020 Sep 23;64(3):579-589. doi: 10.1042/EBC20190091. PMID: 32579188.

Goudie AS. Desert dust and human health disorders. Environ Int. 2014 Feb;63:101-13. doi: 10.1016/j.envint.2013.10.011. Epub 2013 Nov 26. PMID: 24275707.

Griffiths HR. Is the generation of neo-antigenic determinants by free radicals central to the development of autoimmune rheumatoid disease? Autoimmun Rev. 2008 Jul;7(7):544-9. doi: 10.1016/j.autrev.2008.04.013. Epub 2008 May 5. PMID: 18625443.

Grzela K, Litwiniuk M, Zagorska W, Grzela T. Airway Remodeling in Chronic Obstructive Pulmonary Disease and Asthma: the Role of Matrix Metalloproteinase-9. Arch Immunol Ther Exp (Warsz). 2016 Feb;64(1):47-55. doi: 10.1007/s00005-015-0345-y. Epub 2015 Jun 28. PMID: 26123447; PMCID: PMC4713715.

Guerder S, Flavell RA. T-cell activation. Two for T. Curr Biol. 1995 Aug 1;5(8):866-8. doi: 10.1016/s0960-9822(95)00175-8. PMID: 7583143.

Gulzar N, Copeland KF. CD8+ T-cells: function and response to HIV infection. Curr HIV Res. 2004 Jan;2(1):23-37. doi: 10.2174/1570162043485077. PMID: 15053338.

Guo P, Li R, Piao TH, Wang CL, Wu XL, Cai HY. Pathological Mechanism and Targeted Drugs of COPD. Int J Chron Obstruct Pulmon Dis. 2022 Jul 12;17:1565-1575. doi: 10.2147/COPD.S366126. PMID: 35855746; PMCID: PMC9288175.

Gupta P, Singh S, Kumar S, Choudhary M, Singh V. Effect of dust aerosol in patients with asthma. J Asthma. 2012 Mar;49(2):134-8. doi: 10.3109/02770903.2011.645180. Epub 2012 Jan 3. PMID: 22211448.

Hasunuma H, Takeuchi A, Ono R, Amimoto Y, Hwang YH, Uno I, Shimizu A, Nishiwaki Y, Hashizume M, Askew DJ, Odajima H. Effect of Asian dust on respiratory symptoms among children with and without asthma, and their sensitivity. Sci Total Environ. 2021 Jan 20;753:141585. doi: 10.1016/j.scitotenv.2020.141585. Epub 2020 Aug 18. PMID: 32890882.

Hawley ER, Schackwitz W, Hess M. Metagenomic sequencing of two salton sea microbiomes. Genome Announc. 2014 Jan 23;2(1):e01208-13. doi: 10.1128/genomeA.01208-13. PMID: 24459270; PMCID: PMC3900902.

He M, Ichinose T, Song Y, Yoshida Y, Bekki K, Arashidani K, Yoshida S, Nishikawa M, Takano H, Shibamoto T, Sun G. Desert dust induces TLR signaling to trigger Th2-dominant lung allergic inflammation via a MyD88-dependent signaling pathway. Toxicol Appl Pharmacol. 2016 Apr 1;296:61-72. doi: 10.1016/j.taap.2016.02.011. Epub 2016 Feb 13. PMID: 26882889.

He M, Ichinose T, Yoshida S, Nishikawa M, Sun G, Shibamoto T. Role of iron and oxidative stress in the exacerbation of allergic inflammation in murine lungs caused by urban particulate matter <2.5 μm and desert dust. J Appl Toxicol. 2019 Jun;39(6):855-867. doi: 10.1002/jat.3773. Epub 2019 Jan 30. PMID: 30698282.

Hijazi Z, Ezeamuzie CI, Khan M, Dowaisan AR. Characteristics of asthmatic children in Kuwait. J Asthma. 2002 Oct;39(7):603-9. doi: 10.1081/jas-120014924. PMID: 12442949.

Hiraishi H, Terano A, Ota S, Mutoh H, Sugimoto T, Razandi M, Ivey KJ. Oxygen metabolites stimulate mucous glycoprotein secretion from cultured rat gastric mucous cells. Am J Physiol. 1991 Oct;261(4 Pt 1):G662-8. doi: 10.1152/ajpgi.1991.261.4.G662. PMID: 1928352.

Holgate ST. New strategies with anti-IgE in allergic diseases. World Allergy Organ J. 2014 Jul 29;7(1):17. doi: 10.1186/1939-4551-7-17. PMID: 25097719; PMCID: PMC4114087.

Hudey SN, Ledford DK, Cardet JC. Mechanisms of non-type 2 asthma. Curr Opin Immunol. 2020 Oct;66:123-128. doi: 10.1016/j.coi.2020.10.002. Epub 2020 Nov 4. PMID: 33160187; PMCID: PMC7852882.

Ichinose T, Sadakane K, Takano H, Yanagisawa R, Nishikawa M, Mori I, Kawazato H, Yasuda A, Hiyoshi K, Shibamoto T. Enhancement of mite allergen-

induced eosinophil infiltration in the murine airway and local cytokine/chemokine expression by Asian sand dust. J Toxicol Environ Health A. 2006 Aug;69(16):1571-85. doi: 10.1080/15287390500470833. PMID: 16854786.

Janeway CA Jr, Travers P, Walport M, et al. Immunobiology: The Immune System in Health and Disease. 5th edition. New York: Garland Science; 2001. Principles of innate and adaptive immunity. Available from: https://www.ncbi.nlm.nih.gov/books/NBK27090/

Janulaityte I, Januskevicius A, Kalinauskaite-Zukauske V, Palacionyte J, Malakauskas K. Asthmatic Eosinophils Promote Contractility and Migration of Airway Smooth Muscle Cells and Pulmonary Fibroblasts In Vitro. Cells. 2021 Jun 4;10(6):1389. doi: 10.3390/cells10061389. PMID: 34199925; PMCID: PMC8229663.

Johnston JE, Razafy M, Lugo H, Olmedo L, Farzan SF. The disappearing Salton Sea: A critical reflection on the emerging environmental threat of disappearing saline lakes and potential impacts on children's health. Sci Total Environ. 2019 May 1;663:804-817. doi: 10.1016/j.scitotenv.2019.01.365. Epub 2019 Jan 29. PMID: 30738261; PMCID: PMC7232737.

Jones BA, Fleck J. Shrinking lakes, air pollution, and human health: Evidence from California's Salton Sea. Sci Total Environ. 2020 Apr 10;712:136490. doi: 10.1016/j.scitotenv.2019.136490. Epub 2020 Jan 7. PMID: 31931219.

Juturu P. Assessing emergency healthcare accessibility in the Salton Sea region of Imperial County, California. PLoS One. 2021 Jun 30;16(6):e0253301. doi: 10.1371/journal.pone.0253301. PMID: 34191806; PMCID: PMC8244845.

Kabashima K, Nakashima C, Nonomura Y, Otsuka A, Cardamone C, Parente R, De Feo G, Triggiani M. Biomarkers for evaluation of mast cell and basophil activation. Immunol Rev. 2018 Mar;282(1):114-120. doi: 10.1111/imr.12639. PMID: 29431209.

Kanatani KT, Hamazaki K, Inadera H, Sugimoto N, Shimizu A, Noma H, Onishi K, Takahashi Y, Itazawa T, Egawa M, Sato K, Go T, Ito I, Kurozawa Y, Konishi I, Adachi Y, Nakayama T; Japan Environment & Children's Study Group. Effect of desert dust exposure on allergic symptoms: A natural experiment in Japan. Ann Allergy Asthma Immunol. 2016 May;116(5):425-430.e7. doi: 10.1016/j.anai.2016.02.002. Epub 2016 Mar 11. PMID: 26976782.

Kanatani KT, Ito I, Al-Delaimy WK, Adachi Y, Mathews WC, Ramsdell JW; Toyama Asian Desert Dust and Asthma Study Team. Desert dust exposure is associated with increased risk of asthma hospitalization in children. Am J Respir

Crit Care Med. 2010 Dec 15;182(12):1475-81. doi: 10.1164/rccm.201002-0296OC. Epub 2010 Jul 23. PMID: 20656941; PMCID: PMC3159090.

Kandikattu HK, Upparahalli Venkateshaiah S, Mishra A. Synergy of Interleukin (IL)-5 and IL-18 in eosinophil mediated pathogenesis of allergic diseases. Cytokine Growth Factor Rev. 2019 Jun;47:83-98. doi: 10.1016/j.cytogfr.2019.05.003. Epub 2019 May 10. PMID: 31126874; PMCID: PMC6781864.

Karnell JL, Rieder SA, Ettinger R, Kolbeck R. Targeting the CD40-CD40L pathway in autoimmune diseases: Humoral immunity and beyond. Adv Drug Deliv Rev. 2019 Feb 15;141:92-103. doi: 10.1016/j.addr.2018.12.005. Epub 2018 Dec 13. PMID: 30552917.

Kashem SW, Haniffa M, Kaplan DH. Antigen-Presenting Cells in the Skin. Annu Rev Immunol. 2017 Apr 26;35:469-499. doi: 10.1146/annurev-immunol-051116-052215. Epub 2017 Feb 6. PMID: 28226228.

Kashiwada M, Levy DM, McKeag L, Murray K, Schröder AJ, Canfield SM, Traver G, Rothman PB. IL-4-induced transcription factor NFIL3/E4BP4 controls IgE class switching. Proc Natl Acad Sci U S A. 2010 Jan 12;107(2):821-6. doi: 10.1073/pnas.0909235107. Epub 2009 Dec 22. PMID: 20080759; PMCID: PMC2818942.

Kaur BP, Secord E. Innate Immunity. Pediatr Clin North Am. 2019 Oct;66(5):905-911. doi: 10.1016/j.pcl.2019.06.011. PMID: 31466680.

Kausch MF, Pallud CE. Science, policy, and management of irrigation-induced selenium contamination in california. J Environ Qual. 2013 Nov;42(6):1605-14. doi: 10.2134/jeq2013.04.0154. PMID: 25602401.

Kelley N, Jeltema D, Duan Y, He Y. The NLRP3 Inflammasome: An Overview of Mechanisms of Activation and Regulation. Int J Mol Sci. 2019 Jul 6;20(13):3328. doi: 10.3390/ijms20133328. PMID: 31284572; PMCID: PMC6651423.

Kirkham PA, Caramori G, Casolari P, Papi AA, Edwards M, Shamji B, Triantaphyllopoulos K, Hussain F, Pinart M, Khan Y, Heinemann L, Stevens L, Yeadon M, Barnes PJ, Chung KF, Adcock IM. Oxidative stress-induced antibodies to carbonyl-modified protein correlate with severity of chronic obstructive pulmonary disease. Am J Respir Crit Care Med. 2011 Oct 1;184(7):796-802. doi: 10.1164/rccm.201010-1605OC. PMID: 21965015; PMCID: PMC3398415.

Klein L, Kyewski B, Allen PM, Hogquist KA. Positive and negative selection of the T cell repertoire: what thymocytes see (and don't see). Nat Rev Immunol. 2014 Jun;14(6):377-91. doi: 10.1038/nri3667. Epub 2014 May 16. PMID: 24830344; PMCID: PMC4757912.

Kolaczkowska E, Kubes P. Neutrophil recruitment and function in health and inflammation. Nat Rev Immunol. 2013 Mar;13(3):159-75. doi: 10.1038/nri3399. PMID: 23435331.

Kotas ME, Medzhitov R. Homeostasis, inflammation, and disease susceptibility. Cell. 2015 Feb 26;160(5):816-827. doi: 10.1016/j.cell.2015.02.010. PMID: 25723161; PMCID: PMC4369762.

Krangel MS, Hernandez-Munain C, Lauzurica P, McMurry M, Roberts JL, Zhong XP. Developmental regulation of V(D)J recombination at the TCR alpha/delta locus. Immunol Rev. 1998 Oct;165:131-47. doi: 10.1111/j.1600-065x.1998.tb01236.x. PMID: 9850858.

Kubo M. Innate and adaptive type 2 immunity in lung allergic inflammation. Immunol Rev. 2017 Jul;278(1):162-172. doi: 10.1111/imr.12557. PMID: 28658559.

Kuruvilla ME, Lee FE, Lee GB. Understanding Asthma Phenotypes, Endotypes, and Mechanisms of Disease. Clin Rev Allergy Immunol. 2019 Apr;56(2):219-233. doi: 10.1007/s12016-018-8712-1. PMID: 30206782; PMCID: PMC6411459.

Lachowicz-Scroggins ME, Dunican EM, Charbit AR, Raymond W, Looney MR, Peters MC, Gordon ED, Woodruff PG, Lefrançais E, Phillips BR, Mauger DT, Comhair SA, Erzurum SC, Johansson MW, Jarjour NN, Coverstone AM, Castro M, Hastie AT, Bleecker ER, Fajt ML, Wenzel SE, Israel E, Levy BD, Fahy JV. Extracellular DNA, Neutrophil Extracellular Traps, and Inflammasome Activation in Severe Asthma. Am J Respir Crit Care Med. 2019 May 1;199(9):1076-1085. doi: 10.1164/rccm.201810-1869OC. PMID: 30888839; PMCID: PMC6515873.

Lemons AR, Hogan MB, Gault RA, Holland K, Sobek E, Olsen-Wilson KA, Park Y, Park JH, Gu JK, Kashon ML, Green BJ. Microbial rRNA sequencing analysis of evaporative cooler indoor environments located in the Great Basin Desert region of the United States. Environ Sci Process Impacts. 2017 Feb 22;19(2):101-110. doi: 10.1039/c6em00413j. PMID: 28091681; PMCID: PMC5450635.

Leuti A, Fazio D, Fava M, Piccoli A, Oddi S, Maccarrone M. Bioactive lipids, inflammation and chronic diseases. Adv Drug Deliv Rev. 2020;159:133-169. doi: 10.1016/j.addr.2020.06.028. Epub 2020 Jul 3. PMID: 32628989.

Ley K, Laudanna C, Cybulsky MI, Nourshargh S. Getting to the site of inflammation: the leukocyte adhesion cascade updated. Nat Rev Immunol. 2007 Sep;7(9):678-89. doi: 10.1038/nri2156. PMID: 17717539.

Liang X, Liu T, Zhang Z, Yu Z. Airway Inflammation Biomarker for Precise Management of Neutrophil-Predominant COPD. Methods Mol Biol. 2020;2204:181-191. doi: 10.1007/978-1-0716-0904-0_16. PMID: 32710325.

Liew PX, Kubes P. The Neutrophil's Role During Health and Disease. Physiol Rev. 2019 Apr 1;99(2):1223-1248. doi: 10.1152/physrev.00012.2018. PMID: 30758246.

Liu RM, Gaston Pravia KA. Oxidative stress and glutathione in TGF-beta-mediated fibrogenesis. Free Radic Biol Med. 2010 Jan 1;48(1):1-15. doi: 10.1016/j.freeradbiomed.2009.09.026. Epub 2009 Oct 2. PMID: 19800967; PMCID: PMC2818240.

Lorentzou C, Kouvarakis G, Kozyrakis GV, Kampanis NA, Trahanatzi I, Fraidakis O, Tzanakis N, Kanakidou M, Agouridakis P, Notas G. Extreme desert dust storms and COPD morbidity on the island of Crete. Int J Chron Obstruct Pulmon Dis. 2019 Aug 6;14:1763-1768. doi: 10.2147/COPD.S208108. PMID: 31496675; PMCID: PMC6689762.

Lv J, Yu Q, Lv J, Di C, Lin X, Su W, Wu M, Xia Z. Airway epithelial TSLP production of TLR2 drives type 2 immunity in allergic airway inflammation. Eur J Immunol. 2018 Nov;48(11):1838-1850. doi: 10.1002/eji.201847663. Epub 2018 Oct 12. PMID: 30184256; PMCID: PMC6282509.

Mack M. Inflammation and fibrosis. Matrix Biol. 2018 Aug;68-69:106-121. doi: 10.1016/j.matbio.2017.11.010. Epub 2017 Nov 28. PMID: 29196207.

Maggi L, Mazzoni A, Capone M, Liotta F, Annunziato F, Cosmi L. The dual function of ILC2: From host protection to pathogenic players in type 2 asthma. Mol Aspects Med. 2021 Aug;80:100981. doi: 10.1016/j.mam.2021.100981. Epub 2021 Jun 27. PMID: 34193344.

Marone G, Triggiani M, de Paulis A. Mast cells and basophils: friends as well as foes in bronchial asthma? Trends Immunol. 2005 Jan;26(1):25-31. doi: 10.1016/j.it.2004.10.010. PMID: 15629406.

Marshall JR. Why Emergency Physicians Should Care About the Salton Sea. West J Emerg Med. 2017 Oct;18(6):1008-1009. doi: 10.5811/westjem.2017.8.36034. Epub 2017 Sep 21. PMID: 29085530; PMCID: PMC5654867.

Masopust D, Schenkel JM. The integration of T cell migration, differentiation and function. Nat Rev Immunol. 2013 May;13(5):309-20. doi: 10.1038/nri3442. Epub 2013 Apr 19. PMID: 23598650.

McKernan DP. Pattern recognition receptors as potential drug targets in inflammatory disorders. Adv Protein Chem Struct Biol. 2020;119:65-109. doi: 10.1016/bs.apcsb.2019.09.001. Epub 2019 Nov 26. PMID: 31997773.

Menzies-Gow A, Flood-Page P, Sehmi R, Burman J, Hamid Q, Robinson DS, Kay AB, Denburg J. Anti-IL-5 (mepolizumab) therapy induces bone marrow eosinophil maturational arrest and decreases eosinophil progenitors in the bronchial mucosa of atopic asthmatics. J Allergy Clin Immunol. 2003 Apr;111(4):714-9. doi: 10.1067/mai.2003.1382. PMID: 12704348.

Mesin L, Ersching J, Victora GD. Germinal Center B Cell Dynamics. Immunity. 2016 Sep 20;45(3):471-482. doi: 10.1016/j.immuni.2016.09.001. PMID: 27653600; PMCID: PMC5123673.

Miao Y, Porter WC, Schwabe K, LeComte-Hinely J. Evaluating health outcome metrics and their connections to air pollution and vulnerability in Southern California's Coachella Valley. Sci Total Environ. 2022 May 15;821:153255. doi: 10.1016/j.scitotenv.2022.153255. Epub 2022 Jan 20. PMID: 35066029.

Miller M, Rosenthal P, Beppu A, Mueller JL, Hoffman HM, Tam AB, Doherty TA, McGeough MD, Pena CA, Suzukawa M, Niwa M, Broide DH. ORMDL3 transgenic mice have increased airway remodeling and airway responsiveness characteristic of asthma. J Immunol. 2014 Apr 15;192(8):3475-87. doi: 10.4049/jimmunol.1303047. Epub 2014 Mar 12. PMID: 24623133; PMCID: PMC3981544.

Mo JH. Association of Particulate Matter With ENT Diseases. Clin Exp Otorhinolaryngol. 2019 Aug;12(3):237-238. doi: 10.21053/ceo.2019.00752. Epub 2019 Jul 8. PMID: 31295994; PMCID: PMC6635701.

Motomura Y, Morita H, Moro K, Nakae S, Artis D, Endo TA, Kuroki Y, Ohara O, Koyasu S, Kubo M. Basophil-derived interleukin-4 controls the function of natural helper cells, a member of ILC2s, in lung inflammation. Immunity. 2014 May 15;40(5):758-71. doi: 10.1016/j.immuni.2014.04.013. PMID: 24837103.

Murao A, Aziz M, Wang H, Brenner M, Wang P. Release mechanisms of major DAMPs. Apoptosis. 2021 Apr;26(3-4):152-162. doi: 10.1007/s10495-021-01663-3. Epub 2021 Mar 13. PMID: 33713214; PMCID: PMC8016797.

Nelin TD, Joseph AM, Gorr MW, Wold LE. Direct and indirect effects of particulate matter on the cardiovascular system. Toxicol Lett. 2012 Feb 5;208(3):293-9. doi: 10.1016/j.toxlet.2011.11.008. Epub 2011 Nov 18. PMID: 22119171; PMCID: PMC3248967.

Nguyen SMT, Rupprecht CP, Haque A, Pattanaik D, Yusin J, Krishnaswamy G. Mechanisms Governing Anaphylaxis: Inflammatory Cells, Mediators, Endothelial Gap Junctions and Beyond. Int J Mol Sci. 2021 Jul 21;22(15):7785. doi: 10.3390/ijms22157785. PMID: 34360549; PMCID: PMC8346007.

Niehues T, Perez-Becker R, Schuetz C. More than just SCID--the phenotypic range of combined immunodeficiencies associated with mutations in the recombinase activating genes (RAG) 1 and 2. Clin Immunol. 2010 May;135(2):183-92. doi: 10.1016/j.clim.2010.01.013. Epub 2010 Feb 20. PMID: 20172764.

Ning W, Choi AM, Li C. Carbon monoxide inhibits IL-17-induced IL-6 production through the MAPK pathway in human pulmonary epithelial cells. Am J Physiol Lung Cell Mol Physiol. 2005 Aug;289(2):L268-73. doi: 10.1152/ajplung.00168.2004. PMID: 16003000.

Noris M, Remuzzi G. Overview of complement activation and regulation. Semin Nephrol. 2013 Nov;33(6):479-92. doi: 10.1016/j.semnephrol.2013.08.001. PMID: 24161035; PMCID: PMC3820029.

Nussbaum JC, Van Dyken SJ, von Moltke J, Cheng LE, Mohapatra A, Molofsky AB, Thornton EE, Krummel MF, Chawla A, Liang HE, Locksley RM. Type 2 innate lymphoid cells control eosinophil homeostasis. Nature. 2013 Oct 10;502(7470):245-8. doi: 10.1038/nature12526. Epub 2013 Sep 15. PMID: 24037376; PMCID: PMC3795960.

Ogi K, Takabayashi T, Sakashita M, Susuki D, Yamada T, Manabe Y, Fujieda S. Effect of Asian sand dust on Japanese cedar pollinosis. Auris Nasus Larynx. 2014 Dec;41(6):518-22. doi: 10.1016/j.anl.2014.05.020. Epub 2014 Jun 11. PMID: 24928063.

Ohlendorf HM, Marois KC. Organochlorines and selenium in California night-heron and egret eggs. Environ Monit Assess. 1990 Jul;15(1):91-104. doi: 10.1007/BF00454751. PMID: 24243431.

Ono JG, Kim BI, Zhao Y, Christos PJ, Tesfaigzi Y, Worgall TS, Worgall S. Decreased sphingolipid synthesis in children with 17q21 asthma-risk genotypes. J Clin Invest. 2020 Feb 3;130(2):921-926. doi: 10.1172/JCI130860. PMID: 31929190; PMCID: PMC6994114.

Osoata GO, Yamamura S, Ito M, Vuppusetty C, Adcock IM, Barnes PJ, Ito K. Nitration of distinct tyrosine residues causes inactivation of histone deacetylase 2. Biochem Biophys Res Commun. 2009 Jul 3;384(3):366-71. doi: 10.1016/j.bbrc.2009.04.128. Epub 2009 May 3. PMID: 19410558.

Pelaia C, Heffler E, Crimi C, Maglio A, Vatrella A, Pelaia G, Canonica GW. Interleukins 4 and 13 in Asthma: Key Pathophysiologic Cytokines and Druggable Molecular Targets. Front Pharmacol. 2022 Mar 8;13:851940. doi: 10.3389/fphar.2022.851940. PMID: 35350765; PMCID: PMC8957960.

Peters MC, Mauger D, Ross KR, Phillips B, Gaston B, Cardet JC, Israel E, Levy BD, Phipatanakul W, Jarjour NN, Castro M, Wenzel SE, Hastie A, Moore W, Bleecker E, Fahy JV, Denlinger LC. Evidence for Exacerbation-Prone Asthma and Predictive Biomarkers of Exacerbation Frequency. Am J Respir Crit Care Med. 2020 Oct 1;202(7):973-982. doi: 10.1164/rccm.201909-1813OC. PMID: 32479111; PMCID: PMC7528796.

Pettersen CA, Adler KB. Airways inflammation and COPD: epithelial-neutrophil interactions. Chest. 2002 May;121(5 Suppl):142S-150S. doi: 10.1378/chest.121.5_suppl.142s. PMID: 12010843.

Philip M, Schietinger A. $CD8^+$ T cell differentiation and dysfunction in cancer. Nat Rev Immunol. 2022 Apr;22(4):209-223. doi: 10.1038/s41577-021-00574-3. Epub 2021 Jul 12. PMID: 34253904; PMCID: PMC9792152.

Phillips BM, Anderson BS, Hunt JW, Tjeerdema RS, Carpio-Obeso M, Connor V. Causes of water toxicity to Hyalella azteca in the New River, California, USA. Environ Toxicol Chem. 2007 May;26(5):1074-9. doi: 10.1897/06-432r.1. PMID: 17521157.

Pieper K, Grimbacher B, Eibel H. B-cell biology and development. J Allergy Clin Immunol. 2013 Apr;131(4):959-71. doi: 10.1016/j.jaci.2013.01.046. Epub 2013 Mar 5. PMID: 23465663.

Raherison C, Girodet PO. Epidemiology of COPD. Eur Respir Rev. 2009 Dec;18(114):213-21. doi: 10.1183/09059180.00003609. PMID: 20956146.

Ramakrishnan RK, Al Heialy S, Hamid Q. Role of IL-17 in asthma pathogenesis and its implications for the clinic. Expert Rev Respir Med. 2019

Nov;13(11):1057-1068. doi: 10.1080/17476348.2019.1666002. Epub 2019 Sep 17. PMID: 31498708.

Raundhal M, Morse C, Khare A, Oriss TB, Milosevic J, Trudeau J, Huff R, Pilewski J, Holguin F, Kolls J, Wenzel S, Ray P, Ray A. High IFN-γ and low SLPI mark severe asthma in mice and humans. J Clin Invest. 2015 Aug 3;125(8):3037-50. doi: 10.1172/JCI80911. Epub 2015 Jun 29. PMID: 26121748; PMCID: PMC4563754.

Ravin KA, Loy M. The Eosinophil in Infection. Clin Rev Allergy Immunol. 2016 Apr;50(2):214-27. doi: 10.1007/s12016-015-8525-4. PMID: 26690368.

Reese BK, Anderson MA, Amrhein C. Hydrogen sulfide production and volatilization in a polymictic eutrophic saline lake, Salton Sea, California. Sci Total Environ. 2008 Nov 15;406(1-2):205-18. doi: 10.1016/j.scitotenv.2008.07.021. Epub 2008 Aug 29. PMID: 18760446.

Ren Y, Ichinose T, He M, Arashidani K, Yoshida Y, Yoshida S, Nishikawa M, Takano H, Sun G, Shibamoto T. Aggravation of ovalbumin-induced murine asthma by co-exposure to desert-dust and organic chemicals: an animal model study. Environ Health. 2014 Oct 18;13:83. doi: 10.1186/1476-069X-13-83. PMID: 25326908; PMCID: PMC4216376.

Ren Y, Ichinose T, He M, Song Y, Yoshida Y, Yoshida S, Nishikawa M, Takano H, Sun G, Shibamoto T. Enhancement of OVA-induced murine lung eosinophilia by co-exposure to contamination levels of LPS in Asian sand dust and heated dust. Allergy Asthma Clin Immunol. 2014 Jun 9;10(1):30. doi: 10.1186/1710-1492-10-30. PMID: 24982682; PMCID: PMC4058696.

Ren Y, Ichinose T, He M, Youshida S, Nishikawa M, Sun G. Co-exposure to lipopolysaccharide and desert dust causes exacerbation of ovalbumin-induced allergic lung inflammation in mice via TLR4/MyD88-dependent and -independent pathways. Allergy Asthma Clin Immunol. 2019 Dec 18;15:82. doi: 10.1186/s13223-019-0396-4. PMID: 31889961; PMCID: PMC6921588.

Ricciardolo FLM, Carriero V, Bertolini F. Which Therapy for Non-Type(T)2/T2-Low Asthma. J Pers Med. 2021 Dec 23;12(1):10. doi: 10.3390/jpm12010010. PMID: 35055325; PMCID: PMC8779705.

Riedel R, Schlenk D, Frank D, Costa-Pierce B. Analyses of organic and inorganic contaminants in Salton Sea fish. Mar Pollut Bull. 2002 May;44(5):403-11. doi: 10.1016/s0025-326x(01)00254-5. PMID: 12146823.

Riera Romo M, Pérez-Martínez D, Castillo Ferrer C. Innate immunity in vertebrates: an overview. Immunology. 2016 Jun;148(2):125-39. doi: 10.1111/imm.12597. Epub 2016 Apr 5. PMID: 26878338; PMCID: PMC4863567.

Rock KL, Reits E, Neefjes J. Present Yourself! By MHC Class I and MHC Class II Molecules. Trends Immunol. 2016 Nov;37(11):724-737. doi: 10.1016/j.it.2016.08.010. Epub 2016 Sep 7. PMID: 27614798; PMCID: PMC5159193.

Romagnani S. T-cell subsets (Th1 versus Th2). Ann Allergy Asthma Immunol. 2000 Jul;85(1):9-18; quiz 18, 21. doi: 10.1016/S1081-1206(10)62426-X. PMID: 10923599.

Ryter SW, Kim HP, Hoetzel A, Park JW, Nakahira K, Wang X, Choi AM. Mechanisms of cell death in oxidative stress. Antioxid Redox Signal. 2007 Jan;9(1):49-89. doi: 10.1089/ars.2007.9.49. PMID: 17115887.

Sadakane K, Ichinose T, Maki T, Nishikawa M. Co-exposure of peptidoglycan and heat-inactivated Asian sand dust exacerbates ovalbumin-induced allergic airway inflammation in mice. Inhal Toxicol. 2022;34(9-10):231-243. doi: 10.1080/08958378.2022.2086650. Epub 2022 Jun 13. PMID: 35698289.

Sahin C, Rastgeldi Dogan T, Yildiz M, Sofuoglu SC. Indoor environmental quality in naturally ventilated schools of a dusty region: Excess health risks and effect of heating and desert dust transport. Indoor Air. 2022 Jul;32(7):e13068. doi: 10.1111/ina.13068. PMID: 35904387.

Saiki MK, Martin BA, May TW. Selenium in aquatic biota inhabiting agricultural drains in the Salton Sea Basin, California. Environ Monit Assess. 2012 Sep;184(9):5623-40. doi: 10.1007/s10661-011-2367-1. Epub 2011 Sep 14. PMID: 21915593.

Saito T, Kitayama D, Sakamoto A, Tsuruoka N, Arima M, Hatano M, Miyazaki M, Tokuhisa T. Effective collaboration between IL-4 and IL-21 on B cell activation. Immunobiology. 2008;213(7):545-55. doi: 10.1016/j.imbio.2008.01.006. Epub 2008 Feb 20. PMID: 18656702.

Salimi M, Barlow JL, Saunders SP, Xue L, Gutowska-Owsiak D, Wang X, Huang LC, Johnson D, Scanlon ST, McKenzie AN, Fallon PG, Ogg GS. A role for IL-25 and IL-33-driven type-2 innate lymphoid cells in atopic dermatitis. J Exp Med. 2013 Dec 16;210(13):2939-50. doi: 10.1084/jem.20130351. Epub 2013 Dec 9. PMID: 24323357; PMCID: PMC3865470.

Samoli E, Nastos PT, Paliatsos AG, Katsouyanni K, Priftis KN. Acute effects of air pollution on pediatric asthma exacerbation: evidence of association and effect modification. Environ Res. 2011 Apr;111(3):418-24. doi: 10.1016/j.envres.2011.01.014. PMID: 21296347.

Sapozhnikova Y, Bawardi O, Schlenk D. Pesticides and PCBs in sediments and fish from the Salton Sea, California, USA. Chemosphere. 2004 May;55(6):797-809. doi: 10.1016/j.chemosphere.2003.12.009. PMID: 15041284.

Sattar HA, Mobayed H, al-Mohammed AA, Ibrahim AS, Jufairi AA, Balamurugan P, Mary VP, Bener A. The pattern of indoor and outdoor respiratory allergens in asthmatic adult patients in a humid and desert newly developed country. Eur Ann Allergy Clin Immunol. 2003 Oct;35(8):300-5. PMID: 14653049.

Sawaguchi M, Tanaka S, Nakatani Y, Harada Y, Mukai K, Matsunaga Y, Ishiwata K, Oboki K, Kambayashi T, Watanabe N, Karasuyama H, Nakae S, Inoue H, Kubo M. Role of mast cells and basophils in IgE responses and in allergic airway hyperresponsiveness. J Immunol. 2012 Feb 15;188(4):1809-18. doi: 10.4049/jimmunol.1101746. Epub 2012 Jan 16. PMID: 22250079.

Shin SH, Ye MK, Hwang YJ, Kim ST. The effect of Asian sand dust-activated respiratory epithelial cells on activation and migration of eosinophils. Inhal Toxicol. 2013 Sep;25(11):633-9. doi: 10.3109/08958378.2013.826755. PMID: 24044679.

Siddiqui T, Zia MK, Ali SS, Rehman AA, Ahsan H, Khan FH. Reactive oxygen species and anti-proteinases. Arch Physiol Biochem. 2016;122(1):1-7. doi: 10.3109/13813455.2015.1115525. Epub 2015 Dec 23. PMID: 26699123.

Sisto M, Lorusso L, Tamma R, Ingravallo G, Ribatti D, Lisi S. Interleukin-17 and -22 synergy linking inflammation and EMT-dependent fibrosis in Sjögren's syndrome. Clin Exp Immunol. 2019 Nov;198(2):261-272. doi: 10.1111/cei.13337. Epub 2019 Jun 5. PMID: 31165469; PMCID: PMC6797899.

Sonnenberg GF, Hepworth MR. Functional interactions between innate lymphoid cells and adaptive immunity. Nat Rev Immunol. 2019 Oct;19(10):599-613. doi: 10.1038/s41577-019-0194-8. Epub 2019 Jul 26. PMID: 31350531; PMCID: PMC6982279.

Soumelis V, Reche PA, Kanzler H, Yuan W, Edward G, Homey B, Gilliet M, Ho S, Antonenko S, Lauerma A, Smith K, Gorman D, Zurawski S, Abrams J, Menon S, McClanahan T, de Waal-Malefyt Rd R, Bazan F, Kastelein RA, Liu YJ. Human epithelial cells trigger dendritic cell mediated allergic inflammation by producing TSLP. Nat Immunol. 2002 Jul;3(7):673-80. doi: 10.1038/ni805. Epub 2002 Jun 10. PMID: 12055625.

Soy FK, Yazıcı H, Kulduk E, Dündar R, Gülen ŞT, Doğan S, Can İH. The effects of dust storms on quality of life of allergic patients with or without asthma. Kulak Burun Bogaz Ihtis Derg. 2016;26(1):19-27. doi: 10.5606/kbbihtisas.2016.56254. PMID: 26794331.

Stanojkovic I, Kotur-Stevuljevic J, Milenkovic B, Spasic S, Vujic T, Stefanovic A, Llic A, Ivanisevic J. Pulmonary function, oxidative stress and inflammatory markers in severe COPD exacerbation. Respir Med. 2011 Oct;105 Suppl 1:S31-7. doi: 10.1016/S0954-6111(11)70008-7. PMID: 22015083.

Strannegård IL, Strannegård O. Asthma and serum IgE levels in children in a desert country. Int Arch Allergy Appl Immunol. 1987;82(3-4):553-4. doi: 10.1159/000234278. PMID: 3570524.

Strannegård IL, Strannegård O. Childhood bronchial asthma in a desert country. Allergy. 1990 Jul;45(5):327-33. doi: 10.1111/j.1398-9995.1990.tb00507.x. PMID: 2378437.

Sugaya M. The Role of Th17-Related Cytokines in Atopic Dermatitis. Int J Mol Sci. 2020 Feb 15;21(4):1314. doi: 10.3390/ijms21041314. PMID: 32075269; PMCID: PMC7072946.

Swan BK, Ehrhardt CJ, Reifel KM, Moreno LI, Valentine DL. Archaeal and bacterial communities respond differently to environmental gradients in anoxic sediments of a California hypersaline lake, the Salton Sea. Appl Environ Microbiol. 2010 Feb;76(3):757-68. doi: 10.1128/AEM.02409-09. Epub 2009 Nov 30. PMID: 19948847; PMCID: PMC2812989.

Sze E, Bhalla A, Nair P. Mechanisms and therapeutic strategies for non-T2 asthma. Allergy. 2020 Feb;75(2):311-325. doi: 10.1111/all.13985. Epub 2019 Aug 14. PMID: 31309578.

Takeda K, Akira S. TLR signaling pathways. Semin Immunol. 2004 Feb;16(1):3-9. doi: 10.1016/j.smim.2003.10.003. PMID: 14751757.

Tanaka S, Baba Y. B Cell Receptor Signaling. Adv Exp Med Biol. 2020;1254:23-36. doi: 10.1007/978-981-15-3532-1_2. PMID: 32323266.4

Tang D, Kang R, Coyne CB, Zeh HJ, Lotze MT. PAMPs and DAMPs: signal 0s that spur autophagy and immunity. Immunol Rev. 2012 Sep;249(1):158-75. doi: 10.1111/j.1600-065X.2012.01146.x. PMID: 22889221; PMCID: PMC3662247.

Taniuchi I. CD4 Helper and CD8 Cytotoxic T Cell Differentiation. Annu Rev Immunol. 2018 Apr 26;36:579-601. doi: 10.1146/annurev-immunol-042617-053411. PMID: 29677476.

Tete S, Saggini A, Maccauro G, Rosati M, Conti F, Cianchetti E, Tripodi D, Toniato E, Fulcheri M, Salini V, Caraffa A, Antinolfi P, Frydas S, Pandolfi F, Conti P, Potalivo G, Nicoletti M, Theoharides TC. Interleukin-9 and mast cells. J Biol Regul Homeost Agents. 2012 Jul-Sep;26(3):319-26. PMID: 23034251.

Tetley TD. Macrophages and the pathogenesis of COPD. Chest. 2002 May;121(5 Suppl):156S-159S. doi: 10.1378/chest.121.5_suppl.156s. PMID: 12010845.

Thalib L, Al-Taiar A. Dust storms and the risk of asthma admissions to hospitals in Kuwait. Sci Total Environ. 2012 Sep 1;433:347-51. doi: 10.1016/j.scitotenv.2012.06.082. Epub 2012 Jul 20. PMID: 22819885.

Thomas E. Gill. Eolian sediments generated by anthropogenic disturbance of playas: human impacts on the geomorphic system and geomorphic impacts on the human system. Geomorphology. 1996 Sep;17(1-3): 207-228. Doi: 10.1016/0169-555X(95)00104-D.

Trianti SM, Samoli E, Rodopoulou S, Katsouyanni K, Papiris SA, Karakatsani A. Desert dust outbreaks and respiratory morbidity in Athens, Greece. Environ Health. 2017 Jul 1;16(1):72. doi: 10.1186/s12940-017-0281-x. PMID: 28666479; PMCID: PMC5493869.

van Endert P. Intracellular recycling and cross-presentation by MHC class I molecules. Immunol Rev. 2016 Jul;272(1):80-96. doi: 10.1111/imr.12424. PMID: 27319344.

Varenka Lorenzi & Daniel Schlenk (2014) Impacts of Combined Salinity and Temperature Extremes on Different Strains and Species of Tilapia Inhabiting the Watershed of the Salton Sea, North American Journal of Aquaculture, 76:3, 211-221, DOI: 10.1080/15222055.2014.893471

Victora GD, Nussenzweig MC. Germinal Centers. Annu Rev Immunol. 2022 Apr 26;40:413-442. doi: 10.1146/annurev-immunol-120419-022408. Epub 2022 Feb 3. PMID: 35113731.

Vowles M, Kerry R, Ingram B, Mason L. Investigation of the Environmental and Socio-Economic Characteristics of Counties with a High Asthma Burden to Focus Asthma Action in Utah. Int J Environ Res Public Health. 2020 Jul 21;17(14):5251. doi: 10.3390/ijerph17145251. PMID: 32708146; PMCID: PMC7400464.

Voynow JA, Shinbashi M. Neutrophil Elastase and Chronic Lung Disease. Biomolecules. 2021 Jul 21;11(8):1065. doi: 10.3390/biom11081065. PMID: 34439732; PMCID: PMC8394930.

Wang C, Zhou J, Wang J, Li S, Fukunaga A, Yodoi J, Tian H. Progress in the mechanism and targeted drug therapy for COPD. Signal Transduct Target Ther. 2020 Oct 27;5(1):248. doi: 10.1038/s41392-020-00345-x. PMID: 33110061; PMCID: PMC7588592.

Wang Y, Xu J, Meng Y, Adcock IM, Yao X. Role of inflammatory cells in airway remodeling in COPD. Int J Chron Obstruct Pulmon Dis. 2018 Oct 12;13:3341-3348. doi: 10.2147/COPD.S176122. PMID: 30349237; PMCID: PMC6190811.

Watanabe M, Igishi T, Burioka N, Yamasaki A, Kurai J, Takeuchi H, Sako T, Yoshida A, Yoneda K, Fukuoka Y, Nakamoto M, Hasegawa Y, Chikumi H, Matsumoto S, Minato S, Horasaki K, Shimizu E. Pollen augments the influence of desert dust on symptoms of adult asthma patients. Allergol Int. 2011 Dec;60(4):517-24. doi: 10.2332/allergolint.10-OA-0298. PMID: 22113159.

Watanabe M, Noma H, Kurai J, Shimizu A, Sano H, Kato K, Mikami M, Ueda Y, Tatsukawa T, Ohga H, Yamasaki A, Igishi T, Kitano H, Shimizu E. Association of Sand Dust Particles with Pulmonary Function and Respiratory Symptoms in Adult Patients with Asthma in Western Japan Using Light Detection and Ranging: A Panel Study. Int J Environ Res Public Health. 2015 Oct 16;12(10):13038-52. doi: 10.3390/ijerph121013038. PMID: 26501307; PMCID: PMC4627015.

Watanabe M, Noma H, Kurai J, Shimizu A, Sano H, Kato K, Mikami M, Ueda Y, Tatsukawa T, Ohga H, Yamasaki A, Igishi T, Kitano H, Shimizu E. Association of Sand Dust Particles with Pulmonary Function and Respiratory Symptoms in Adult Patients with Asthma in Western Japan Using Light Detection and Ranging: A Panel Study. Int J Environ Res Public Health. 2015 Oct 16;12(10):13038-52. doi: 10.3390/ijerph121013038. PMID: 26501307; PMCID: PMC4627015.

Wilfong ER, Lyles M, Rietcheck RL, Arfsten DP, Boeckman HJ, Johnson EW, Doyle TL, Chapman GD. The acute and long-term effects of Middle East sand particles on the rat airway following a single intratracheal instillation. J Toxicol Environ Health A. 2011;74(20):1351-65. doi: 10.1080/15287394.2010.516239. PMID: 21899408.

Xu EG, Bui C, Lamerdin C, Schlenk D. Spatial and temporal assessment of environmental contaminants in water, sediments and fish of the Salton Sea and its two primary tributaries, California, USA, from 2002 to 2012. Sci Total

Environ. 2016 Jul 15;559:130-140. doi: 10.1016/j.scitotenv.2016.03.144. Epub 2016 Apr 6. PMID: 27058132.

Xu Q, Zhao W, Yan M, Mei H. Neutrophil reverse migration. J Inflamm (Lond). 2022 Nov 24;19(1):22. doi: 10.1186/s12950-022-00320-z. PMID: 36424665; PMCID: PMC9686117.

Yang CY, Tsai SS, Chang CC, Ho SC. Effects of Asian dust storm events on daily admissions for asthma in Taipei, Taiwan. Inhal Toxicol. 2005 Dec 15;17(14):817-21. doi: 10.1080/08958370500241254. PMID: 16282159.

Yang R, Tan M, Xu J, Zhao X. Investigating the regulatory role of ORMDL3 in airway barrier dysfunction using in vivo and in vitro models. Int J Mol Med. 2019 Aug;44(2):535-548. doi: 10.3892/ijmm.2019.4233. Epub 2019 Jun 6. PMID: 31173170; PMCID: PMC6605285.

Yitshak-Sade M, Novack V, Katra I, Gorodischer R, Tal A, Novack L. Non-anthropogenic dust exposure and asthma medication purchase in children. Eur Respir J. 2015 Mar;45(3):652-60. doi: 10.1183/09031936.00078614. Epub 2014 Oct 16. PMID: 25323244.

Yunna C, Mengru H, Lei W, Weidong C. Macrophage M1/M2 polarization. Eur J Pharmacol. 2020 Jun 15;877:173090. doi: 10.1016/j.ejphar.2020.173090. Epub 2020 Mar 29. PMID: 32234529.

Zhao R, Liang H, Clarke E, Jackson C, Xue M. Inflammation in Chronic Wounds. Int J Mol Sci. 2016 Dec 11;17(12):2085. doi: 10.3390/ijms17122085. PMID: 27973441; PMCID: PMC5187885.

Zhou C, Huang JC, Liu F, He S, Zhou W. Effects of selenite on Microcystis aeruginosa: Growth, microcystin production and its relationship to toxicity under hypersalinity and copper sulfate stresses. Environ Pollut. 2017 Apr;223:535-544. doi: 10.1016/j.envpol.2017.01.056. Epub 2017 Jan 24. PMID: 28129951.

Zhu J, Yamane H, Paul WE. Differentiation of effector CD4 T cell populations (*). Annu Rev Immunol. 2010;28:445-89. doi: 10.1146/annurev-immunol-030409-101212. PMID: 20192806; PMCID: PMC3502616.

Zindel J, Kubes P. DAMPs, PAMPs, and LAMPs in Immunity and Sterile Inflammation. Annu Rev Pathol. 2020 Jan 24;15:493-518. doi: 10.1146/annurev-pathmechdis-012419-032847. Epub 2019 Nov 1. PMID: 31675482.

Zygmunt BM, Węgrzyn A, Gajska W, Yevsa T, Chodaczek G, Guzmán CA. Mannose Metabolism Is Essential for Th1 Cell Differentiation and IFN-γ

Production. J Immunol. 2018 Sep 1;201(5):1400-1411. doi: 10.4049/jimmunol.1700042. Epub 2018 Jul 20. PMID: 30030325.

Glossary of Terms

Aerosol: A suspension of solid or liquid particles in gas.

Airway hyperreactivity: Increased response to bronchoconstrictive stimuli.

Allergen: A substance capable of causing an allergic reaction.

Anaphylaxis: A severe allergic reaction that may be life-threatening.

Anthropogenic: A human caused effect.

Antibody: A protein secreted by B cells that can directly bind an antigen and can neutralize pathogens.

Antigen: A substance that can induce an immune response.

Asian sand dust (ASD): Dust originating in the deserts of Mongolia, Kazakhstan, and northwestern China.

Atopic asthma: IgE-mediated allergic asthma.

B cell receptor (BCR): A transmembrane protein found on B cells that is capable of recognizing antigens. Composed of a heavy and light chain.

Bronchoconstriction: Tightening of smooth muscle around the bronchi, resulting in the narrowing of airways.

Caspase: Protease enzymes that are essential in apoptosis.

Chemokine: Cytokines that recruit cells to the site of infection/inflammation.

Cholinergic: Substances that act on, or mimic, acetylcholine or butyrylcholine.

Corticosteroid: Steroid hormones with anti-inflammatory properties.

Cyanotoxin: Toxins produced by cyanobacteria.

Cytokine: A small molecule that has an effect on the immune system.

Damage-associated molecular pattern (DAMPs): Molecules released under conditions of cellular stress or tissue damage that are capable of eliciting an immune response.

Emphysema: A disease characterized by the destruction of the alveoli.

Endotoxin: Another term for lipopolysaccharide.

Epithelial: Tissue that lines the body's surfaces, canals, and other hollow structures.

Epitopes: The portion of an antigen recognized by an antibody

Fibrosis: The deposition of fibrous connective tissue in response to an insult or injury.

Forced expiratory volume in 1 second (FEV_1): The maximum amount of air that a person can forcibly expel in one second following maximal inhalation.

Forced vital capacity (FVC): The maximum amount of air that a person can forcibly expel from their lungs after maximal inhalation.

Germinal center: Site of antibody affinity maturation.

Gram-negative: Bacteria that are characterized by a thin peptidoglycan cell wall and an outer membrane containing lipopolysaccharides

Gram-positive: Bacteria that are characterized by a thick peptidoglycan cell wall with lipoteichoic acid.

Hematopoietic cells: Cells derived from hematopoietic stem cells that are found in the blood. Includes red blood cells, lymphocytes, and myeloid cells.

House dust mite (HDM): Common mites that are commonly associated with allergies.

Hyperplasia: Excessive cell division.

Immunoglobulin (Ig): Another name for antibodies

Integrin: Transmembrane receptors that aid in cell-cell and cell-extracellular matrix adhesion

Lipopolysaccharide (LPS): A component of the outer membrane of gram-negative bacteria.

Lipoteichoic acid (LTA): A major component of gram-positive bacterial cell walls.

Major histocompatibility complex class I (MHC class I): Ubiquitous cell surface molecule where intracellular antigens are presented for recognition by immune cells.

Major histocompatibility complex class II: Surface molecules present on antigen-presenting cells where extracellular antigens are presented for recognition by immune cells.

Microcystin: A cyanotoxin known to cause liver damage.

Mononuclear cells: Blood cells with a single, round nucleus. Includes lymphocytes and monocytes.

Neutrophil extracellular traps (NETs): Extracellular DNA fibers secreted by neutrophils that bind pathogens.

Nucleoside-binding and oligomerization domain like receptors (NLRs): A class of pathogen recognition receptors that are associated with inflammasome formation.

Opsonization: The binding of opsonins to aid in phagocytosis.

Ovalbumin (OVA): The major protein of chicken egg whites that is commonly used in immunologic studies.

Particulate matter (PM): Solid and liquid droplets in air. Often categorized by size, with PM_{10} (particulate matter smaller than 10 μm in aerosol diameter), $PM_{2.5}$ (particulate matter smaller than 2.5 μm in aerosol diameter), and $PM_{0.1}$ (particulate matter smaller than 0.1 μm in aerosol diameter) being the most common categories.

Pathogen-associated molecular patterns (PAMPs): Conserved pathogenic molecules that are recognized by pattern recognition receptors.

Pattern Recognition Receptors (PRRs): Germline immune receptors capable of recognizing conserved pathogenic or tissue-damaged associated molecules.

Paucigranulocytic: Lacking granulocytes.

Peak expiratory flow (PEF): The maximum flow rate generated during a forced exhalation following a maximal inhalation.

Peptidoglycan: A polysaccharide found in bacterial cell walls.

Playa: Dried lakebed.

Polymorphonuclear (PMN) cells: Immune cells with granules and a nucleus with multiples lobes.

Protease: An enzyme that breaks down proteins and peptides.

Reactive oxygen species (ROS): An oxygen containing molecule that easily reacts with other molecules, causing damage.

Selectin: Sugar-binding transmembrane proteins that aid in cell adhesion.

Skin prick test: A test for allergies that involves scratching or puncturing the skin with a potential allergen and measuring the response.

Somatic hypermutation (SHM): The accumulation of point mutation in the variable region of the heavy and light chain of antibodies. Necessary for affinity maturation.

Sphingolipid: A class of lipids found in cell membrane. Their metabolites are important mediators in many signaling cascades.

Spirometry: A common pulmonary function test that measures the amount and speed of air that can be inhaled and exhaled from the lungs.

T cell receptor (TCR): A surface receptor found on T cells responsible for the recognition of antigens presented in MHC class I or MHC class II.

Type 2 response (T2): An immune response towards parasitic helminth infection characterized by production of IL-4, -5, and -13. Also responsible for allergic responses. Alternatively known as the Th2 response.

Toll-like receptors (TLRs): Membrane associated pattern recognition receptors responsible for recognition of a wide variety of pathogenic molecules.

Type-I interferon (IFN): Cytokines that play an essential role in some types of inflammation, such as viral infection.

Vasoactive: Affecting blood vessel diameter.

Chapter 2: Investigation into the pulmonary health effects of sea spray from a decaying inland sea: An *in vivo* study of aerosolized Salton Sea water exposure in mice

Trevor A. Biddle[1,4], Qi Li[2,3], Mia R. Maltz[1,4,5], Purvi N. Tandel[1], Rajrupa Chakraborty[1,4], Keziyah Yisrael[1,4], Ryan Drover[2,3], David R. Cocker III[2,3], David D. Lo[1,4,5,*]

*Corresponding Author: David D. Lo; Postal Address: 900 University Ave, Riverside, CA 92521; Email: david.lo@medsch.ucr.edu

Abstract

In communities surrounding the Salton Sea, high rates of asthma are associated with high aerosol dust levels. However, the Salton Sea itself may play an additional role in pulmonary health. Therefore, to investigate a potential role of the Salton Sea on pulmonary health, we exposed mice to aerosolized Salton Sea water for 7 days and assessed tissue responses, including cellular infiltration and gene expression changes. For reference, mice were also exposed to aerosolized

[1]: Division of Biomedical Sciences, University of California, Riverside School of Medicine, Riverside, California, USA
[2]: Department of Chemical and Environmental Engineering, University of California, Riverside, Riverside, California, USA
[3]: College of Engineering-Center for Environmental Research and Technology (CE-CERT), University of California, Riverside, Riverside, California, USA
[4]: BREATHE Center, University of California, Riverside, Riverside, California, USA
[5]: Center for Health Disparities Research, University of California, Riverside, Riverside, California, USA

fungal allergen (*Alternaria* sp.) and Pacific Ocean aerosols. Exposure to aerosolized *Alternaria* sp. induced dramatic allergic inflammation, including neutrophil and eosinophil recruitment to the bronchoalveolar lavage fluid (BALF) and lung tissue. By contrast, Salton Sea “spray” induced only B cell recruitment to the lung tissue without increased inflammatory cell numbers in BALF. However, there were consistent gene expression changes suggestive of an inflammatory response. The response to the Salton Sea spray was notably distinct from the response to Pacific Ocean water, which induced some B cell recruitment but without an inflammatory gene expression profile. Our studies suggest that soluble components in Salton Sea water promote induction of a unique inflammation-associated response, though any relationship to asthma remains to be explored.

Abbreviations: BALF, bronchoalveolar lavage fluid; IgE, immunoglobulin E; PM, particular matter; SMPS, scanning mobility particle sizer; PCA, Principal Component Analysis; AMS, aerosol mass spectrometer; ROS, reactive oxygen species

Introduction

The Salton Sea is a 345 mi^2 inland body of water located in California’s Riverside and Imperial counties. The Sea is primarily fed by agricultural runoff as well as inflow from the Alamo, New, and Whitewater rivers. In recent decades,

the Sea has been undergoing a rapid retreat, exposing dry lakebed (playa), and producing increased dusts, spreading throughout the region and influencing the surrounding population. The drying Sea has become hypersaline, at approximately 74 parts per thousand, over twice that of Pacific Ocean water (Bureau of Reclamation, 2020). The rapid change in the Sea's ecology has resulted in periodic algal blooms, and fish and migratory bird die-offs (Carmichael and Li, 2006; Xu et al., 2016). Pesticide and herbicide use from agricultural areas located to the southeast and northwest of the Sea (Xu et al, 2016), as well as heavy metal contamination from elements such as selenium (Zhou et al., 2017), paint an overall picture of ill-health in the Sea itself.

This ecosystem's ill health is also reflected in the surrounding communities. The human population surrounding the Salton Sea includes a high proportion of migrant workers, with high rates of poverty and poor access to health care. Area residents suffer from one of the highest rates of childhood asthma in California at 20%-22.4%, compared to an average of 14.5% for the rest of the State (Farzan et al., 2019). Predictably, the surrounding area also has one of the highest rates of hospitalization for asthma (California Environmental Protection Agency, 2018), making it a serious health crisis in an already underserved community.

Asthma is a disease of airway restriction, defined as an increase in airway hyperreactivity, and usually associated with allergies (referred to as "atopic" asthma), characterized by increased immunoglobulin E (IgE) production, Th2

cytokine secretion and the recruitment of eosinophils to the lungs (Bousquet et al., 2000). Atopic asthma exacerbations can occur in response to exposure to environmental or household allergens (Wark and Gibson, 2006). High levels of particulate matter (PM) have also been known to exacerbate asthma (Guarnieri and Balmes, 2014). Unfortunately for the communities surrounding the Salton Sea, there are many potential allergens and asthma exacerbating particles. The region has consistently high levels of particulate matter between 10μm and 2.5μm in diameter (PM_{10}) and under 2.5μm in diameter ($PM_{2.5}$; Environmental Protection Agency, 2012; Evan, 2019; Frie et al., 2019). Indoor household allergens, such as *Alternaria alternata*, and other fungi, are also prevalent (Sinclair et al., 2018). Up to 70% of patients with fungal allergies show a positive skin test response to *Alternaria* (Bush and Prochnau, 2004). Additionally, household *Alternaria* exposure is linked to an increased odds ratio for developing asthma symptoms (Salo et al, 2006).

However, the region's rampant asthma may have more complex origins than simple dust levels, largely pointing to the Salton Sea itself. Studies have identified a variety of pesticides, including DDT, organophosphates and pyrethroid, in both the water and the sediment of sites around and within the Sea (LeBlanc and Kuivila, 2008). Organophosphates have been linked to increased risk of childhood asthma (Shaffo et al., 2018). Additionally, the Sea experiences periodic algal blooms and has been shown to contain low levels of microcystin-LR and YR, cyanotoxins known to cause ill-health (Carmichael and Li, 2006).

These microcystins have been shown to cause damage to the lungs after chronic exposure (Li et al., 2016; Wang et al., 2016). Some algal blooms, such as red tides off the coast of Florida, have also been directly linked to the development of asthma and asthma exacerbations (Fleming et al., 2007; Zaias et al., 2011). Additionally, cyanobacteria, which make up a large part of algal blooms, may serve directly as sensitizing allergens, exacerbating the harmful effects of the algae (Bernstein et al., 2011).

Despite suggestive associations between the Salton Sea and asthma, more direct mechanistic information on Salton Sea aerosols and their potential impact on pulmonary health is still needed. To address this issue, we began studies to simulate chronic aerosol exposures in a mouse model of pulmonary inflammation. In the present study, we focused on the direct effect of Salton Sea "spray" aerosols on lung responses.

Materials and methods

Water Sample Collection

Two batches of Salton Sea water were collected at the edge of Salton City. The first was collected on March 2nd, 2019 (33°19'25.9"N 115°56'18.3"W) and the second was collected on May 13th, 2020 (33°19'53.2"N 115°56'30.0"W). Water samples were collected with a homemade raft. Four sampling ports were square distributed, sticking out of the bottom of the raft at a length of 2 inches, to ensure sampling surface water only and avoiding floating debris. Two 4.96 m

poles were installed and used to move the raft to places with large depth. Water samples were taken by a hand pump on the shore. The whole system was sterilized thoroughly by bleach solution and flushed by MilliQ water before being used on site. More than 2 L of water samples were taken before sample collection to rinse the system. The collected water was stored on ice while transported to the University of California, Riverside campus. Once there, water samples were stored at 4°C until processed.

Pacific Ocean water was also collected in two batches. The first was collected at Torrey Pines on March 9th, 2019. The second was also collected at Torrey Pines on October 2nd, 2020 (32°55'51.4"N 117°15'37.7"W). Water was collected directly by containers without using the raft since ocean water is relatively well mixed due to tides. Samples were stored at 4°C until processed.

Water Processing

Before using for aerosolization studies, the water was filtered through an acid-washed, sterilized glass funnel using a sterile 0.2 μm filter (47-mm diameter; Pall Supor 200 Sterile Grid filters, Pall Corporation, Por Washington) into an acid-washed sterilized collecting flask below via vacuum filtration. After filtration, filtrate was either stored at 4°C or as aliquots archived at -80°C for long-term storage. The pH of all filtrates was measured; all filtrates were approximately pH 7.0 (±0.8%).

Animals

Animal studies were performed in accordance with UCR institutional IACUC and NIH guidelines and approved protocols. Adult male and female (8-9 weeks old) C57BL/6J mice were purchased from Jackson Labs, Sacramento. Mice were acclimated for one week in the University of California, Riverside SPF vivarium before being placed into the exposure chamber when they were 9-10 weeks old. Mice were kept 3-4 to a cage and given food and water *ad libitum*, with bedding being changed at least once weekly. A 12-hour day/night cycle was provided.

Exposure studies were performed in dual animal chambers (an exposure chamber and a control chamber) developed from the chamber described in Peng, 2019.[23] When in the exposure chamber, mice were given a mixture of dry filtered air (0.5-1 lpm) and aerosolized spray (dried by silica gel, 3.5-4.5 lpm) with a total particle concentration of approximately 1,500 μg m^{-3}. The three types of PM were generated from solutions of *Alternaria alternata* and *Alternaria tenius* filtrate (Greer Laboratories, Lenoir, NC, USA; 0.4g/L), Salton Sea water (133-200x dilution), or Pacific Ocean water (40x dilution) with proper concentrations or dilution ratios, respectively. Example of typical exposure PM levels for different PM types are shown in Figure 2.1a with weekly averaged PM level being 1,425 μg m^{-3} for *Alternaria*, 1,377 μg m^{-3} for Pacific Ocean spray, and 1,523 μg m^{-3} for Salton Sea spray. Sample aerosolization was accomplished by using a homemade nebulizer with silica-gel dryers (Peng et al., 2019). Mice in the control

chamber were given filtered dry air (5.0 lpm) only, with other conditions the same as the exposure chamber, including bedding replacement, food and water supplies, and corresponding day/night cycle. Particulate matter was only monitored within the exposure chamber by a scanning mobility particle sizer (SMPS, including Series 3080 Electrostatic Classifier and Ultrafine Condensation Particle Counter 3776, TSI) to assist in maintaining stable PM concentration of 1500 μg m^{-3}. Concentration was similar to our previous study in Peng et al 2018,[24] where 1500 μg m^{-3} of *Alternaria* was sufficient to generate neutrophil and eosinophil recruitment to the lungs. Relative humidity (40-60%) and ammonia (weekly averaged $[NH_4]$ < 25ppm) were selectively measured in some of the exposures to ensure consistent quality control. For each exposure, we used an equal number of male and female mice. Each exposure had a control air cohort that matched the number and sex of the exposure group. The number of mice for each exposure is as follows: 8 mice for the 3/2/2019 Salton Sea collection, 10 mice for the 5/13/2020 Salton Sea Collection, 4 mice for the 3/9/2019 Pacific Ocean collection, 6 mice for the 10/2/2020 Pacific Ocean collection, 10 mice for the *Alternaria* exposure.

After 7 days, the mice were removed from the chamber, anesthetized via isoflurane and sacrificed by cervical dislocation. The mice were then processed for either RNA extraction and flow cytometry or histological analysis. For the RNA extraction/flow cytometry mice, BALF was collected via 3 injections of 0.8 mL PBS, after which the right lung lobe was extracted and flash frozen in liquid

nitrogen and kept at -80°C until RNA extraction, while the left lobe was digested using 0.5 mg/mL collagenase D (Roche Diagnostics, Mannheim, Germany), 50 U/mL DNAse I (Sigma Aldrich, St. Louis, USA) in RPMI 1640 (Gibco, Grand Island, USA) supplemented with 10% heat-inactivated FBS (Gibco, Grand Island, USA) preheated to 37°C. The lung was left to digest for 30 minutes at 37°C before being diced into small (~1-2mm) sections and pushed through a cell strainer (Corning, Corning, USA). The cell strainer was rinsed with RPMI 1640 with 10% heat-inactivated FBS before being centrifuged and resuspended for use in Flow Cytometry. For the histological mice, the lung was inflated with 0.7 mL of a 1:1 OCT:PBS mixture before being flash frozen via liquid nitrogen in an OCT block.

Flow Cytometry

BALF and post-digested lungs were centrifuged at 1500 rpm before being resuspended in 100 uL of a 1:50 dilution of Mouse BD FC block (BD Pharmingen, San Jose, USA; Clone 2.4G2) in FACS Buffer. Cells were stained using fluorescent antibodies: anti-CD45 FITC (BioLegend, San Diego, USA; Clone 30-F11), anti-CD19 PE-Cy5 (eBioscience, San Diego, USA; Clone MB19-1), anti-CD3 Alexa Fluor 700 (BioLegend, San Diego, USA; Clone 17A2), anti-Ly6G BV510 (BioLegend, San Diego, USA; Clone 1A8), anti-CD11b BV421 (BioLegend, San Diego, USA; Clone M1/70), anti-CD11c PE-Cy7 (BioLegend, San Diego, USA; Clone N418) and anti-SiglecF APC (BioLegend, San Diego,

USA; Clone S17007L). Samples were run on a MoFlo Astrios (Beckman Coulter, Carlsbad, USA). Gating and analysis were performed using FlowJo (Version 10.71, Ashland, USA).

RNA Extraction

RNA was extracted using TRIzol© (Ambion, Carlsbad, USA). Briefly, ~100 mg of frozen lung tissue was placed in a mortar, covered with liquid nitrogen, then ground into dust using a pestle before adding to TRIzol©. Chloroform was added, mixed and centrifuged. The aqueous phase was removed and mixed with isopropanol and centrifuged, leaving a pellet which was then washed 3x with 75% ethanol before drying at room temperature. The pellet was resuspended in DEPC-Treated water (Ambion, Austin, USA). Concentration and purity of RNA was checked via NanoDrop 2000 (Thermo Scientific, Carlsbad, USA).

NanoString Analysis

Purified RNA was analyzed using an nCounter® Sprint Profiler (NanoString Technologies, Seattle, USA) with the nCounter® Mouse Immunology Panel according to manufacturer protocols. Gene expression was analyzed using the nSolver® 4.0 software (NanoString Technologies, Seattle, USA). Statistical analysis was done using nSolver® Advanced Analysis 2.0 (NanoString Technologies, Seattle, USA); false discovery rates (FDR) were calculated, using the Benjamini-Hochberg method.

Differences in lung immune gene expression profiles (from nCounter® Mouse Immunology Panel) for each mouse sampled were analyzed using Principal Component Analyses (PCA; Pielou 1984) using the “prcomp” function in R version 4.0.3 (R version 4.0.3; R Core Team 2020). Normalized and log transformed gene expression data matrices were constructed as data points were projected onto the 2-D plane, such that the variance is maximized. As dimensions were reduced, they spread out in two directions to explain most of the differences in the data. X-axes (labeled as PC1) in the ordination space represent the first principal component, which separates data points to represent the most variation in the dataset; y-axes (labeled as PC2) are orthogonal to PC1 and separate data points to represent the next greatest amount of variation within these gene expression datasets, across exposure types. We used the *ggplot2* package (Wickham, 2009) and the “stat ellipse” function, with 95% confidence intervals, to visualize these PCA plots in R (R version 3.2.1; R Core Team 2017).

Histology

OCT embedded lungs were sectioned at 20 µm in a Cryostat. Sections were stored at -80°C until staining. Before staining with H&E, slides were fixed with 4% PFA for 10 minutes. Histological images were taken using a Keyence BZ-X710 (Keyence Corporation of America, Itasca, USA).

Aerosol Mass Spectrometry

Chemical composition of aerosolized particles were measured by an HR-ToF-AMS (DeCarlo et al., 2006) Particles were generated using the same atomizer system as chamber exposures, as described by Peng et al., 2018. The outlet of our atomizer system was split into two ports, with one connected to the sampling inlet of the aerosol mass spectrometer (AMS) and the other venting through a HEPA filter. The Salton Sea and Pacific Ocean stock samples were diluted 10x with MilliQ water to generate particles at suitable concentrations. *Alternaria* solutions were the same concentrations as those used in chamber exposures. ToF-AMS Analysis Toolkit 1.57 and PIKA 1.16 on Igor Pro 6.36 were used in data processing.

Statistical Analysis

All statistical analysis was done using GraphPad Prism 6 (GraphPad, San Diego, USA). P-value was calculated using the Mann-Whitney U test for nonparametric data. We analyzed multivariate homogeneity of group dispersions (variances) using PERMDISP2 procedures in the R package *vegan*, with the function “betadisper” (Oksanen et al., 2016) in R. Euclidean distances between objects and group centroids were handled by reducing the original distances to principal coordinates. We used Tukey’s Honest Significant Difference methods as “TukeyHSD.betadisper” to create 95% confidence intervals on differences

between mean distance-to-centroids across exposures, as compared with mice in chambers containing control air.

Results

Control of exposure to aerosol particulate levels

To ensure consistent levels of simulated chronic environmental aerosol exposures, our environmental chamber system was set up to continuously monitor suspended aerosols by particulate size as well as steady-state mass concentrations. In this study, we performed exposure studies using aerosolized suspensions generated from aqueous solutions of *Alternaria* filtrate, Salton Sea water, and Pacific Ocean water. Mass concentrations of PM generated from different sources were stable over 7 days, with averaged mass concentrations around 1,500 μg m^{-3} (± 10%; Figure 2.1a). Average size distributions of the different types of PM were generated using the same atomizer system, under identical conditions (Figure 2.1b). Only minor differences in average particle size were observed between samples; peak particle mobility diameter for Pacific Ocean PM was 79.1 nm; *Alternaria* PM was 88.2 nm, and Salton Sea PM was 94.7 nm. Because the injection method was consistent between each exposure, minor differences in PM size distribution were primarily due to composition differences of each aerosolized solution. Moreover, differences in particle densities were seen with higher “salty” PM densities, as compared to the “organic” PM (*Alternaria* PM 1.36g cm^{-3} < Pacific Ocean PM 1.96 g cm^{-3} < Salton

Sea PM 2.07 g cm^{-3}). Importantly, a majority of PM was either fine (PM with a diameter between 0.1 μm-2.5 μm) or ultrafine (PM with a diameter of less than 0.1 μm), with the vast majority of PM under 1 μm in mobility diameter. This is critical to consistent exposure effects, as ultrafine PM is expected to be able to travel deep into lung tissue down to the alveoli.

PM surface area has been proposed to be an important factor in studies on the health effects of PM on lungs. However, as all three types of PM used in this experiment were generated from aqueous solutions, with no inert components; the particles were – by their nature – highly water soluble. Accordingly, particle size could change within the lung due to the high relative humidity of the lung microenvironment (Löndahl et al., 2007); therefore, for comparability across different material exposures, we chose to control the total mass concentration of the different types of PM instead of total surface area.

Due to the complexity of multiple factors, including particle size and depth of penetration into lung tissue, as well as the extent of animal activity, age, or relative humidity fluctuation, it is difficult to estimate the actual dose of material deposited in the lung of a mouse over the course of a 7-day exposure. Since we maintained a target mass concentration in the chamber, with similar particle size distributions across each of three aerosol suspensions, we expect that particle suspensions of all three materials were delivered in similar fashion. Moreover, since the particles were all generated using aqueous solutions, it is likely that all particles coming into direct contact with lung tissue (i.e., alveolar or airway

epithelium) will similarly fully dissolve and release their components to diffuse into the tissue.

PM chemical composition analysis by aerosol mass spectrometer

Since the aerosol suspensions of particles were all using aqueous solutions with no inert particulate matter, the biological impacts of the exposures are expected to be based on the release of soluble components of particulates into the tissue, rather than on the particulate physical properties. Thus, we determined the soluble composition of the aqueous solutions using AMS. There was a large difference in the organic fraction between PM from the Salton Sea (5.9-6.6%), Pacific Ocean (12-20%) and the *Alternaria* (82%). Additionally, *Alternaria* PM had a notable fraction of NO_3 (10%) compared to the others (< 0.1%). Detectable levels of NH_4 (1.01%) were only measured for the *Alternaria* PM. There were also key differences between the “salty” PMs (Salton Sea and Pacific Ocean). The Salton Sea PM was lower in organic content than the Pacific Ocean PM. In contrast, the fraction of metal ions and other inorganics were higher in the Salton Sea PM than in the Pacific Ocean PM (Figure 2.1c).

Alternaria elicited allergic immune cell recruitment to lungs

To assess whether Salton Sea exposure can trigger allergic asthma, it was important to establish reference characteristics of a canonical allergic lung inflammation. Thus, we exposed C57BL/6J mice to *Alternaria alternata* and

Alternaria tenuis filtrate mixture (hereafter referred to as "*Alternaria*") at a chamber mass concentration of approximately 1500 μg m^{-3} for 7 days. A group of mice were held in the exposure chamber, while a control group was simultaneously held in a parallel chamber that had only filtered air pumped into it. Following the exposure, BALF and lung tissues were assessed for inflammatory cell infiltration. H&E staining of the lung showed marked cellular infiltration around the airways compared to the controls (Figure 2.2a), indicating an inflammatory response to the *Alternaria*. Additionally, there was a significant increase in the number of cells in the BALF ($1.7 \times 10^6 \pm 2.7 \times 10^5$ vs. $2.5 \times 10^5 \pm 4.9 \times 10^4$ control, $p<0.0001$; Figure 2.2b) compared to the controls.

BALF cells were stained for analysis by flow cytometry to identify infiltrating inflammatory cells. The differential proportions of neutrophils ($CD11b^+$, $Ly6G^+$), eosinophils ($CD11c^-$, Siglec F^+), T cells (SSC^{low}, $CD3^+$), and B cells (SSC^{low}, $CD19^+$) were quantified as a proportion of $CD45^+$ cells, with the remaining cells mainly being alveolar macrophages. Similar to our previous studies (Peng et al., 2018), the BALF of *Alternaria* exposed mice showed an expected increase in neutrophils (72.1 ± 11.1% vs. 0.2 ± 0.1% control, $p<0.0001$; Figure 2.2d) and eosinophils (8.3 ± 1.7% vs. ~0% control, $p<0.0001$; Figure 2.2c). T cells made up a higher, though small, percent of the BALF after *Alternaria* exposure (2.5 ± 0.4% vs 0.2 ± 0.1% control, $p<0.0001$; Figure 2.2f). B cells were essentially undetectable in the BALF (0.2 ± 0.1% vs. 0.2 ± 0.1% control; Figure 2.2e).

Infiltrating inflammatory cells may be limited to the interstitial compartment of the tissue, and so might not be detected among lung lavage cells. Differences in BALF versus tissue infiltrating cells may also reveal differences in the way inflammatory cells are recruited as well as differences in their impact on tissue remodeling, which has a critical impact on airway resistance. Thus, tissue infiltrating cells were also isolated by enzymatic digestion of lung tissues and stained for analysis by flow cytometry. Interestingly, we found that while there were some similarities in the types of cells detected, the proportions of different infiltrating cell types were notably different. For example, the proportion of neutrophils in *Alternaria* exposed lungs, while higher than in the control lungs (21.8 $\pm$ 1.3% vs. 11.1 $\pm$ 1.8% control, $p<0.01$; Figure 2.2d), was nonetheless smaller than the 70%+ proportion of neutrophils in the BALF. In the case of eosinophils, there also were low numbers of cells detected in controls; however, *Alternaria*-exposed lung actually showed a higher proportion in the digested tissue (12.3 $\pm$ 1.0% vs. 3.6 $\pm$ 0.3% control $p<0.01$; Figure 2,2c) compared to ~8.3% in the BALF. These contrasting ratios of neutrophils and eosinophils in BALF versus digested tissue are consistent with the possibility that neutrophils may play a more important role in clearing microbes from alveolar and airway spaces, while eosinophils are more important in the interstitial spaces, where they may contribute to tissue remodeling.

Lymphocytes were also more easily detected in lung digests compared to BALF. T cells were higher in digested tissue (13.6 $\pm$ 0.9% vs. 13.9 $\pm$ 1.4%

control) compared to BALF, but the *Alternaria* exposed lungs showed no significant difference compared to controls (Figure 2.2f); an expected increase in recruited CD4 T cells was likely diluted by the infiltrating granulocytes. The percentage of B cells was also higher in digests (8.8 $\pm$ 0.6% vs. 17.4 $\pm$ 1.0% control, $p<0.01$) than in BALF, but the proportion of B cells detected in exposed lungs was decreased relative to controls, also possibly due to the increased proportion of granulocytes (Figure 2.2e).

Response to Salton Sea and Pacific Ocean water

With the inflammatory response to *Alternaria* exposure as a reference, we exposed mice to filtered and aerosolized Salton Sea water. Exposures were performed using water samples collected at different times and sites at the Sea, but all exposures were performed at a similar mass concentration. Following the exposures, mice were analyzed in the same manner as the *Alternaria* exposure. In contrast to the picture in *Alternaria* exposed mice, the lungs from mice exposed to aerosolized Salton Sea water did not contain granulocyte recruitment in either the BALF or digested lung tissue. Moreover, H&E stained lung sections (Figure 2.3a) showed no evidence for cellular recruitment after exposure to aerosolized Salton Sea water. Total BALF cell counts also showed no differences between exposure and control ($5.2 \times 10^5 \pm 1.6 \times 10^5$ vs. $3.8 \times 10^5 \pm 7.9 \times 10^4$ control; Figure 2.3b). Flow cytometry analysis of digested lung tissue revealed minimal inflammatory cell recruitment: eosinophils (3.7 $\pm$ 0.6% vs. 2.4 $\pm$ 0.5%

control; Figure 2.3c), neutrophils (12.2 ± 1.2 vs. 15.3 ± 2.7% control; Figure 2.3d), and T cells (10.7 ± 0.7% vs. 10.2 ± 0.8% control; Figure 2.3f) showed no significant differences. Interestingly, B cells in digested lung tissue were increased after exposure to the Salton Sea water (18.5 ± 1.5% vs. 12.3 ± 0.7% control, $p<0.05$; Figure 2.3e). All four cell types were essentially not present in the BALF (data not shown).

To determine whether this response was due to unique characteristics of the Salton Sea spray particles or a general response to Sea spray, we exposed mice to aerosolized Pacific Ocean water, also collected at multiple dates. Communities living near the Pacific Ocean do not show the high asthma rates found near the Salton Sea, so any differences observed may provide clues to potential links between Salton Sea aerosols and asthma. Inflammatory cell recruitment from Salton Sea and Pacific Ocean exposures turned out to be very similar, as there was no difference in the BALF cell counts ($3.8 \times 10^5 \pm 7.6 \times 10^4$ vs $2.6 \times 10^5 + 3.3 \times 10^4$ control; Figure 2.3b) nor increase in the percentage of tissue digest eosinophils (2.6 ± 0.3% vs. 2.8 ± 0.3% control; Figure 2.3c), neutrophils (11.9 ± 2.7% vs. 16.8 ± 6.8% control; Figure 2.3d), or T cells (15.5 ± 1.3% vs. 10.7 ± 1.4% control; Figure 2.3f). Moreover, there was a similar significant increase in B cell percentage (21.1 ± 1.2% vs. 13.9 ± 1.9% control, $p<0.05$; Figure 2.3e). Once again, all four cell types were essentially absent in the BALF (data not shown).

Gene expression changes in the response to aerosols

While assays for cellular infiltrates and histological changes can reveal significant inflammatory responses to exposures, more subtle tissue responses were revealed from analyses of gene expression profiles. In these studies, we focused on a subset of immune-associated genes assayed using a panel of short sequence tag probes (NanoString). This method quantifies expressed genes by direct counting of hybridized tagged gene probes and includes a set of general "housekeeping gene" probes. As a set, this approach allowed broad internal normalization of the assayed gene expression profiles, which in turn enabled direct comparisons of different RNA profiles from different samples and studies. Principal Component Analysis (PCA) of gene expression profiles collapses the complex gene expression data sets and helps provide overall comparisons among individual mice in different treatment groups.

Our reference allergic inflammatory response to *Alternaria* exposure illustrates a reproducible and characteristic gene expression pattern, as seen by the distance between centroids from the control air group to the *Alternaria* group (d=19.84) in this PCA ordination; we observed tight clustering within the control air group and *Alternaria* groups and clear differentiation between the groups in the PCA, despite multiple replicates (Figure 2.4a). We identified 213 differentially regulated genes (FDR < 0.10) of which 166 were significantly upregulated vs 47 which were significantly downregulated (Figure 2.4b). These genes are diverse in function, but the strongest change in regulation falls into immune defense

responses and chemokine production, consistent with the observed recruitment of inflammatory cells into the lung. Among the top 20 regulated genes are Ig receptors (*Fcgr2b, Pigr, Fcgr3*), chemokines (*Cxcl3, Ccl9, Ccl8, Ccl3 Ccl22*), immune regulatory genes (*Tgfbi, Lilrb4, IL33, Ctss, Ptafr, Ctsc*) and innate immune genes (*Cfb, Muc1*).

By contrast, analysis of gene expression profiles from exposures to aerosolized Salton Sea water revealed a distinctively different pattern (Figure 2.5a). The PCA shows an overall distinction between control air and Salton Sea exposed groups; however, the extent of these orthogonal axes did not explain as much of the variance, nor did they illustrate as great of a separation as was detected for the *Alternaria* exposures. Euclidean distance between centroids of control air and Salton Sea exposed groups (d = 3.08) within the PCA ordination was shorter than was found in the PCA for the *Alternaria* exposures.

This exposure triggered significant gene expression changes, with 151 differentially expressed genes (Figure 2.5b). Of these, 146 genes were significantly upregulated while only 5 were significantly downregulated (FDR < 0.10). The regulated genes were primarily associated with phosphorylation pathways (Jak1, Jak2, Jak3, Stat5b, Tnfrsf14), T cell activation (Ifnar1, Ifngr1), and NF-KB signaling (Ikbkb). Additionally, a preference toward MHC I/Th1 response predominates (Ifnar1, Ifngr1, Tap1), although there were some Th2-related receptors upregulated (Il6ra). It should be noted that the magnitude of gene expression changes, while statistically significant, were relatively small, with

the vast majority (134 of the 146 upregulated genes) showing less than 0.5 Log_2 fold change. Despite the lower magnitude changes, the regulated genes were consistent across replicate exposures and multiple Salton Sea samples, illustrated by the clustering of the Salton Sea data points relative to control data in the PCA.

As noted above, both Salton Sea and Pacific Ocean exposures induced some recruitment of B cells into lung tissue. Interestingly, this similarity was not seen in the gene expression profiles; in replicate studies with different Pacific Ocean samples, aerosolized Pacific Ocean exposed mice showed no significant changes in gene expression compared to controls (Figure 2.S2). It is likely that if there were any induced genes related to B cell recruitment, they were not represented in the probe set used. More importantly however, these comparisons suggest that Salton Sea water exposures had a characteristic biological effect, unrelated to any general effect of exposure to sea water.

Our analysis of gene regulation in response to *Alternaria* versus Salton Sea exposures showed that each induced a reproducible and characteristic set of gene expression changes, with tight clustering within the groups and little intergroup overlap. Additionally, both Salton Sea and *Alternaria* produced responses distinct from the Pacific Ocean exposed mice (Figure 2.6a). It is especially notable, however, that the *Alternaria* and Salton Sea exposures each induced strikingly different sets of genes (Figure 2.6b; Pacific Ocean excluded due to a lack of differentially expressed genes). Of the 166 upregulated genes in

Alternaria exposed mice and the 146 in the Salton Sea exposed mice, only 55 are upregulated in both. Even more notable is that of the 47 downregulated genes in the *Alternaria* exposed mice and 5 downregulated genes in the Salton Sea exposed, only 1 was downregulated in both. Additionally, 13 genes which were upregulated in Salton Sea exposed mice were downregulated in *Alternaria* while 2 genes which were upregulated in *Alternaria* exposed mice were downregulated in mice exposed to aerosolized Salton Sea. Thus, while it appeared that both types of exposures regulated genes associated with at least some aspect of innate and adaptive immunity, their overall impacts were on rather different components of the immune or inflammatory response.

Discussion

The studies reported here were principally aimed at determining whether the aqueous components in Salton Sea water might have effects on pulmonary tissues in response to chronic delivery into the lung as aerosolized particles. We found that aerosolized Salton Sea water was able to induce a distinct inflammatory gene expression profile despite a lack of cell recruitment to the BALF as well as neutrophil and eosinophil recruitment to the lung tissue.

To investigate the effect that Salton Sea spray may have on the communities surrounding the Sea, we exposed C57BL/6 mice to approximately 1500 μg m^{-3} of aerosolized Salton Sea for 7 days. While this is meant to simulate a chronic exposure condition, there are still some limitations associated with our

model. Residents surrounding the Salton Sea are exposed to variable levels of aerosols over a period of years, unlike the consistent 7-day exposure in our study. As perfectly matching both the exposure time and aerosol concentration the residents are exposed to is impractical, we focused on a reasonable timeframe and aerosol concentration that showed demonstrable results. As this timeframe and concentration was sufficient to reliably induce large changes in *Alternaria* exposed mice and gene expression changes in Salton Sea exposed mice while the Pacific Ocean exposed mice showed no change, we believe our methodology is capable of providing real insights into the health effects of these aerosols. While direct measurement of airway hyperreactivity was beyond the scope of this study, our initial results call for future studies into this topic.

For this study, we used aerosols generated from filtered aqueous solutions. While this excluded the potential effects of larger inert dust particles, it allowed us to specifically focus on the effects of the dissolved components in the water. Separating the effects of the dissolved aqueous components and inert dust particles is critical as inert dust particles can have their own biological effects, including triggering of airway irritant receptors (Sellick and Widdicombe, 1971). Additionally, larger dust particles (e.g., 1 μm or larger) may affect the delivery of soluble components carried on their surface, since they would not be as capable of penetrating deep into alveolar spaces. Exclusion of these larger particles was also important for generating a consistent PM (all PM in the study had a mobility diameter well under 1 μm); thus, particle size was unlikely to be a

limiting factor for distribution. Effects due directly to minor differences in particle size are most likely negligible, as exposure to Pacific Ocean water failed to induce gene expression changes, indicating that the specific composition of the aerosol is the primary driving agent for gene expression changes and cell recruitment. Our AMS breakdown was unable to pinpoint a broad category for reactive agents, as there was no consistent ratio between the composition and the effects. Thus, future studies should focus on specific components that may be present in the Salton Sea water. As we found some aspects of the NF-KB pathway upregulated (Ikbkb, RelA), care should be taken to investigate sources of reactive oxygen species (ROS). In particular, pesticides (LeBlanc and Kuivila, 2008) and heavy metal ions (Frie et al., 2019; D'Evelyn et al., 2021), both of which have been detected in the Salton Sea, should be investigated, as they are known to induce ROS (Abdollahi et al., 2004; Leikauf et al, 2020).

The main observation reported here is that soluble components of Salton Sea water are able to induce a unique pattern of gene expression changes in chronically exposed lungs, and that this pattern is strikingly distinct from the characteristic allergic inflammation induced by the common household fungal allergens in *Alternaria* filtrate. In the context of the observed high incidence of asthma in the Salton Sea region, our findings suggest that the Salton Sea water soluble components by themselves appear to induce significant lung responses, but they are clearly distinct from the characteristic allergic inflammatory responses typified by *Alternaria* exposures.

However, the distinctive effect of Salton Sea exposures does not entirely rule out potential impacts on asthma. A number of receptors were significantly upregulated, including Il6r, CD97, Ifngr1 and Ifnar1. IL-6 is associated with IL-4 production, which is critical for Th2 differentiation (Rincon and Irvin, 2012). The soluble form of Il6r has also been associated with asthma severity (Peters et al., 2017). CD97 is a known costimulatory factor on CD4+ T cells (Capasso et al., 2006). In contrast to the previous receptors, Ifngr1 and Ifnar1 are associated with Th1 response. However, Th1-polarization has been linked to nonallergic asthma (Zorrati et al., 2014). Additionally, our previous studies showed that Th1 inflammatory responses could not only co-exist with allergic Th2 inflammatory responses, they could show additive effects (Li et al., 1998). Salton Sea exposures also induced a number of genes associated with signaling pathways, such Jak1, Jak2 and Jak3. As these signaling pathways are known to have critical roles in pulmonary eosinophilia, airway hyperreactivity and mucus hypersecretion (Hoshino et al., 2004), upregulation of these components could potentially provide additive or synergistic effects in the presence of other triggers, including environmental or household allergens.

Conclusions

Our results suggest two main points. First, Salton Sea exposure is unable to generate an inflammatory response similar to a potent allergen, as characterized in our study by *Alternaria*. However, aerosolized Salton Sea was

able to trigger an inflammatory response distinct from a potent allergen, unlike aerosolized Pacific Ocean water, which did not trigger an inflammatory response. Thus, while Salton Sea spray may not be sufficient to generate asthma alone, it could play a key role in the progression to asthma or other inflammatory diseases. Future studies should explore the role of this inflammatory response in the context of the full range of aerosols to which the communities surrounding the Salton Sea are exposed.

Acknowledgments

Research reported in this publication was supported by the National Institute On Minority Health And Health Disparities of the National Institutes of Health under Award Number U54MD013368. The content is solely the responsibility of the authors and does not necessarily represent the official views of the National Institutes of Health. The authors thank Mary Hamer, Director of the School of Medicine Research Instrumentation Core facility for assistance with flow cytometry data collection, and Dr. Meera Nair for assistance in establishing flow cytometry parameters for lung cell populations, and for helpful comments on the manuscript.

Author contributions

TAB, designed and set up exposure studies, collected field samples and animal samples, collected flow cytometry and gene expression data and

performed data analysis, prepared manuscript and data figures; QL, designed and carried out chamber exposure studies, analysis of aerosols parameters and components; MRM, designed and implemented PCAs; PNT, contributed lung histology and analysis; RC, assisted with animal sample collection, and data analyses; KY, assisted with animal sample collection, and data analyses; RD, contributed sample collections, chamber exposure management; DRC, assisted with chamber design and oversight of exposure studies; DDL, overall experimental design, sample collection, data analysis, manuscript and data figure assembly and editing.

References

Abdollahi, M., Ranjbar, A., Shadnia, S., Nikfar, S., & Rezaie, A. (2004). Pesticides and oxidative stress: A review. *Medical Science Monitor*, *10*(6), 141–148.

Bernstein, J. A., Ghosh, D., Levin, L. S., Zheng, S., Carmichael, W., Lummus, Z., & Bernstein, I. L. (2011). Cyanobacteria: An unrecognized ubiquitous sensitizing allergen? *Allergy and Asthma Proceedings*, *32*(2), 106–110. https://doi.org/10.2500/aap.2011.32.3434

Bousquet J, Jeffery PK, Busse WW, Johnson M, Vignola AM. Asthma. From bronchoconstriction to airways inflammation and remodeling. Am J Respir Crit Care Med. 2000 May;161(5):1720-45. doi: 10.1164/ajrccm.161.5.9903102.

Bureau of Reclamation (2020). *Salton Sea.* Retrieved March 02, 2021, from https://www.usbr.gov/lc/region/programs/saltonsea.html

Bush, R. K., & Prochnau, J. J. (2004). Alternaria-induced asthma. *Journal of Allergy and Clinical Immunology*, *113*(2), 227–234. https://doi.org/10.1016/j.jaci.2003.11.023

California Environmental Protection Agency, Office of Environmental Health Hazard Assessment. (2018, June 25). *CalEnviroScreen 3.0*. Retrieved from https://oehha.ca.gov/calenviroscreen/report/calenviroscreen-30

Capasso, M., Durrant, L. G., Stacey, M., Gordon, S., Ramage, J., & Spendlove, I. (2006). Costimulation via CD55 on Human CD4 + T Cells Mediated by CD97 . *The Journal of Immunology*, *177*(2), 1070–1077. https://doi.org/10.4049/jimmunol.177.2.1070

Carmichael, W. W., & Li, R. H. (2006). Cyanobacteria toxins in the Salton Sea. *Saline Systems*, *2*, 5. https://doi.org/10.1186/1746-1448-2-5

D'Evelyn, S. M., Vogel, C. F. A., Bein, K. J., Lara, B., Laing, E. A., Abarca, R. A., Zhang, Q., Li, L., Li, J., Nguyen, T. B., & Pinkerton, K. E. (2021). Differential inflammatory potential of particulate matter (PM) size fractions from imperial valley, CA. *Atmospheric Environment*, *244*(January 2020). https://doi.org/10.1016/j.atmosenv.2020.117992

DeCarlo, P. F., Kimmel, J. R., Trimborn, A., Northway, M. J., Jayne, J. T., Aiken, A. C., Gonin, M., Fuhrer, K., Horvath, T., Docherty, K. S., Worsnop, D. R., & Jimenez, J. L. (2006). Field-deployable, high-resolution, time-of-flight aerosol

mass spectrometer. *Analytical Chemistry*, *78*(24), 8281–8289. https://doi.org/10.1021/ac061249n

Environmental Protection Agency, (2012) *Nonattainment Areas for the Criteria Pollutants.* Retrieved from https://www.arcgis.com/apps/MapSeries/index.html?appid=8fbf9bde204944eeb422eb3ae9fde765

Evan, A. T. (2019). Downslope winds and dust storms in the salton basin. *Monthly Weather Review*, *147*(7), 2387–2402. https://doi.org/10.1175/MWR-D-18-0357.1

Farzan, S. F., Razafy, M., Eckel, S. P., Olmedo, L., Bejarano, E., & Johnston, J. E. (2019). Assessment of respiratory health symptoms and asthma in children near a drying saline lake. *International Journal of Environmental Research and Public Health*, *16*(20). https://doi.org/10.3390/ijerph16203828

Fleming, L. E., Kirkpatrick, B., Backer, L. C., Bean, J. A., Wanner, A., Reich, A., Zaias, J., Cheng, Y. S., Pierce, R., Naar, J., Abraham, W. M., & Baden, D. G. (2007). Aerosolized red-tide toxins (brevetoxins) and asthma. *Chest*, *131*(1), 187–194. https://doi.org/10.1378/chest.06-1830

Frie, A. L., Garrison, A. C., Schaefer, M. V., Bates, S. M., Botthoff, J., Maltz, M., Ying, S. C., Lyons, T., Allen, M. F., Aronson, E., & Bahreini, R. (2019). Dust Sources in the Salton Sea Basin: A Clear Case of an Anthropogenically Impacted Dust Budget. *Environmental Science and Technology*, *53*(16), 9378–9388. https://doi.org/10.1021/acs.est.9b02137

Guarnieri, M., & Balmes, J. R. (2014). Outdoor air pollution and asthma. *The Lancet*, *383*(9928), 1581–1592. https://doi.org/10.1016/S0140-6736(14)60617-6

Hoshino, A., Tsuji, T., Matsuzaki, J., Jinushi, T., Ashino, S., Teramura, T., Chamoto, K., Tanaka, Y., Asakura, Y., Sakurai, T., Mita, Y., Takaoka, A., Nakaike, S., Takeshima, T., Ikeda, H., & Nishimura, T. (2004). STAT6-mediated signaling in Th2-dependent allergic asthma: Critical role for the development of eosinophilia, airway hyper-responsiveness and mucus hypersecretion, distinct from its role in Th2 differentiation. *International Immunology*, *16*(10), 1497–1505. https://doi.org/10.1093/intimm/dxh151

Jakob Löndahl, Andreas Massling, Joakim Pagels, Erik Swietlicki, Elvira Vaclavik & Steffen Loft (2007) Size-Resolved Respiratory-Tract Deposition of Fine and Ultrafine Hydrophobic and Hygroscopic Aerosol Particles During Rest and Exercise, Inhalation Toxicology, 19:2, 109-116, DOI: 10.1080/08958370601051677

LeBlanc, L. A., & Kuivila, K. M. (2008). Occurrence, distribution and transport of pesticides into the Salton Sea Basin, California, 2001-2002. *Hydrobiologia*, *604*(1), 151–172. https://doi.org/10.1007/s10750-008-9316-1

Leikauf, G. D., Kim, S. H., & Jang, A. S. (2020). Mechanisms of ultrafine particle-induced respiratory health effects. *Experimental and Molecular Medicine*, *52*(3), 329–337. https://doi.org/10.1038/s12276-020-0394-0

Li, L., Xia, Y., Nguyen, A., Feng, L., & Lo, D. (1998). Th2-induced eotaxin expression and eosinophilia coexist with Th1 responses at the effector stage of lung inflammation. *Journal of Immunology (Baltimore, Md. : 1950)*, *161*(6), 3128–3135. http://www.ncbi.nlm.nih.gov/pubmed/9743380

Li, X., Xu, L., Zhou, W., Zhao, Q., & Wang, Y. (2016). Chronic exposure to microcystin-LR affected mitochondrial DNA maintenance and caused pathological changes of lung tissue in mice. *Environmental Pollution*, *210*, 48–56. https://doi.org/10.1016/j.envpol.2015.12.001

Oksanen, O., Blanchet, F.G., Kindt, R., et al. (2016) Vegan: Community Ecology Package. R Package Version 2.3-5. http://CRAN.R-project.org/package=vegan

Peng, X., Madany, A. M., Jang, J. C., Valdez, J. M., Rivas, Z., Burr, A. C., Grinberg, Y. Y., Nordgren, T. M., Nair, M. G., Cocker, D., Carson, M. J., & Lo, D. D. (2018). Continuous Inhalation Exposure to Fungal Allergen Particulates Induces Lung Inflammation While Reducing Innate Immune Molecule Expression in the Brainstem. *ASN Neuro*, *10*, 175909141878230. https://doi.org/10.1177/1759091418782304

Peng, X., Maltz, M. R., Botthoff, J. K., Aronson, E. L., Nordgren, T. M., Lo, D. D., & Cocker, D. R. (2019). Establishment and characterization of a multi-purpose large animal exposure chamber for investigating health effects. *Review of Scientific Instruments*, *90*(3), 1–7. https://doi.org/10.1063/1.5042097

Peters, M. C., Mcgrath, K. W., Hawkins, G. A., Ph, D., Hastie, T., Ph, D., Levy, B. D., Israel, E., Phillips, B. R., Mauger, T., Ph, D., Comhair, S. A., Ph, D., Erzurum, S. C., Johansson, M. W., Wenzel, S. E., Woodruff, P. G., & Bleecker, E. R. (2017). Plasma IL6 levels, metabolic dysfunction, and asthma severity: a cross-sectional analysis of two cohorts. *Lancet Respir Med*, *4*(7), 574–584. https://doi.org/10.1016/S2213-2600(16)30048-0.Plasma

Pielou, E.C. (1984) The Interpretation of Ecological Data: A Primer on Classification and Ordination. J. Wiley and Sons, New York.

Rincon, M., & Irvin, C. G. (2012). Role of IL-6 in asthma and other inflammatory pulmonary diseases. *International Journal of Biological Sciences*, *8*(9), 1281–1290. https://doi.org/10.7150/ijbs.4874

Salo, P. M., Arbes, S. J., Sever, M., Jaramillo, R., Cohn, R. D., London, S. J., & Zeldin, D. C. (2006). Exposure to Alternaria alternata in US homes is associated with asthma symptoms. *Journal of Allergy and Clinical Immunology*, *118*(4), 892–898. https://doi.org/10.1016/j.jaci.2006.07.037

Sellick, H., & Widdicombe, J. G. (1971). Stimulation of lung irritant receptors by cigarette smoke, carbon dust, and histamine aerosol. *Journal of Applied Physiology*, *31*(1), 15–19. https://doi.org/10.1152/jappl.1971.31.1.15

Shaffo, F. C., Grodzki, A. C., Fryer, A. D., & Lein, P. J. (2018). Mechanisms of organophosphorus pesticide toxicity in the context of airway hyperreactivity and asthma. *American Journal of Physiology - Lung Cellular and Molecular Physiology*, *315*(4), L485–L501. https://doi.org/10.1152/ajplung.00211.2018

Sinclair, R., Russell, C., Kray, G., & Vesper, S. (2018). Asthma risk associated with indoor mold contamination in hispanic communities in Eastern Coachella Valley, California. *Journal of Environmental and Public Health*, *2018*. https://doi.org/10.1155/2018/9350370

Wang, C., Gu, S., Yin, X., Yuan, M., Xiang, Z., Li, Z., Cao, H., Meng, X., Hu, K., & Han, X. (2016). The toxic effects of microcystin-LR on mouse lungs and alveolar type II epithelial cells. *Toxicon*, *115*, 81–88. https://doi.org/10.1016/j.toxicon.2016.03.007

Wark PA, Gibson PG. Asthma exacerbations . 3: Pathogenesis. Thorax. 2006 Oct;61(10):909-15. doi: 10.1136/thx.2005.045187.

Wickham, H. ggplot2: Elegant Graphics for Data Analysis; Springer-Verlag: New York, NY, USA, 2009.

Xu, E. G., Bui, C., Lamerdin, C., & Schlenk, D. (2016). Spatial and temporal assessment of environmental contaminants in water, sediments and fish of the Salton Sea and its two primary tributaries, California, USA, from 2002 to 2012. *Science of the Total Environment*, *559*, 130–140. https://doi.org/10.1016/j.scitotenv.2016.03.144

Zaias, J., Fleming, L. E., Baden, D. G., & Abraham, W. M. (2011). Repeated exposure to aerosolized brevetoxin-3 induces prolonged airway hyperresponsiveness and lung inflammation in sheep. *Inhalation Toxicology*, *23*(4), 205–211. https://doi.org/10.3109/08958378.2011.558936

Zhou, C., Huang, J. C., Liu, F., He, S., & Zhou, W. (2017). Effects of selenite on Microcystis aeruginosa: Growth, microcystin production and its relationship to toxicity under hypersalinity and copper sulfate stresses. *Environmental Pollution*, *223*, 535–544. https://doi.org/10.1016/j.envpol.2017.01.056

Zoratti, E., Havstad, S., Wegienka, G., Nicholas, C., Bobbitt, K. R., Woodcroft, K. J., Ownby, D. R., & Johnson, C. C. (2014). Differentiating asthma phenotypes in young adults through polyclonal cytokine profiles. *Annals of Allergy, Asthma and Immunology*, *113*(1), 25–30. https://doi.org/10.1016/j.anai.2014.04.013

Figures

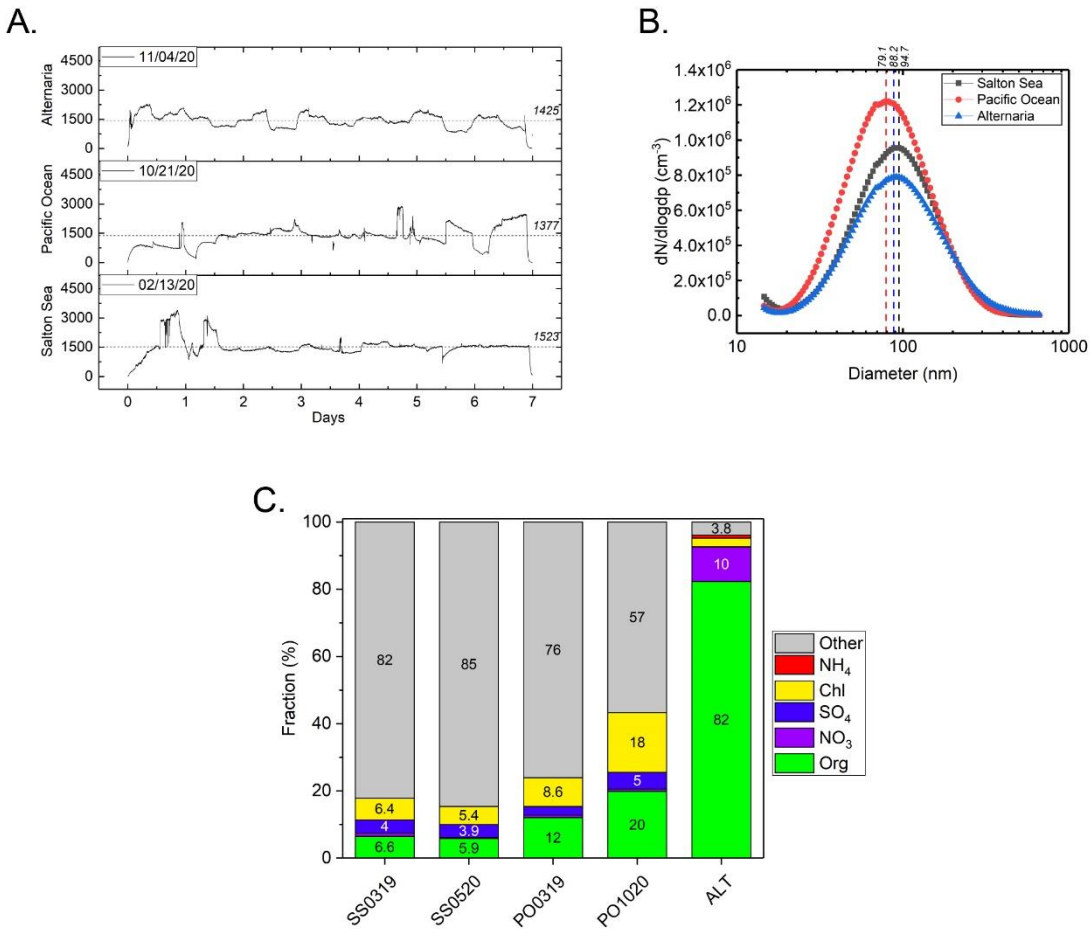
A.
Alternaria
Pacific Ocean
Salton Sea
11/04/20
10/21/20
02/13/20
1425
1377
1523
4500
3000
1500
0
0 1 2 3 4 5 6 7
Days
B.
79.1
88.2
94.7
Salton Sea
Pacific Ocean
Alternaria
dN/dlogdp (cm-3)
1.4x10^6
1.2x10^6
1.0x10^6
8.0x10^5
6.0x10^5
4.0x10^5
2.0x10^5
0.0
10
100
1000
Diameter (nm)
C.
Fraction (%)
100
80
60
40
20
0
82
85
76
57
82
6.4
4
6.6
5.4
3.9
5.9
8.6
12
18
5
20
10
3.8
Other
NH4
Chl
SO4
NO3
Org
SS0319
SS0520
PO0319
PO1020
ALT

Figure 2.1 - Quantification of Alternaria (ALT), Pacific Ocean (PO) and Salton Sea (SS) aerosols

PM mass concentration was measured by a scanning mobility particle sizer. Chemical composition was determined by AMS. (A) PM mass concentration during 7-day exposure of SS, PO and ALT. Dash line shows the 7-day averaged mass concentration of PM. All units are in μg m^{-3}. (B) Averaged mobility diameter distribution of different PM used in exposure experiments. (C) Chemical composition of dry particulate matters generated from different materials collected in different season (mm/yr). Other includes metals (sodium, calcium, magnesium), trace metals and other inorganics. (Key: SS0319, Salton Sea/March 2019; SS0520, Salton Sea/May 2020; PO0319, Pacific Ocean/March 2019; PO1020, Pacific Ocean/October 2020; ALT, Alternaria filtrate).

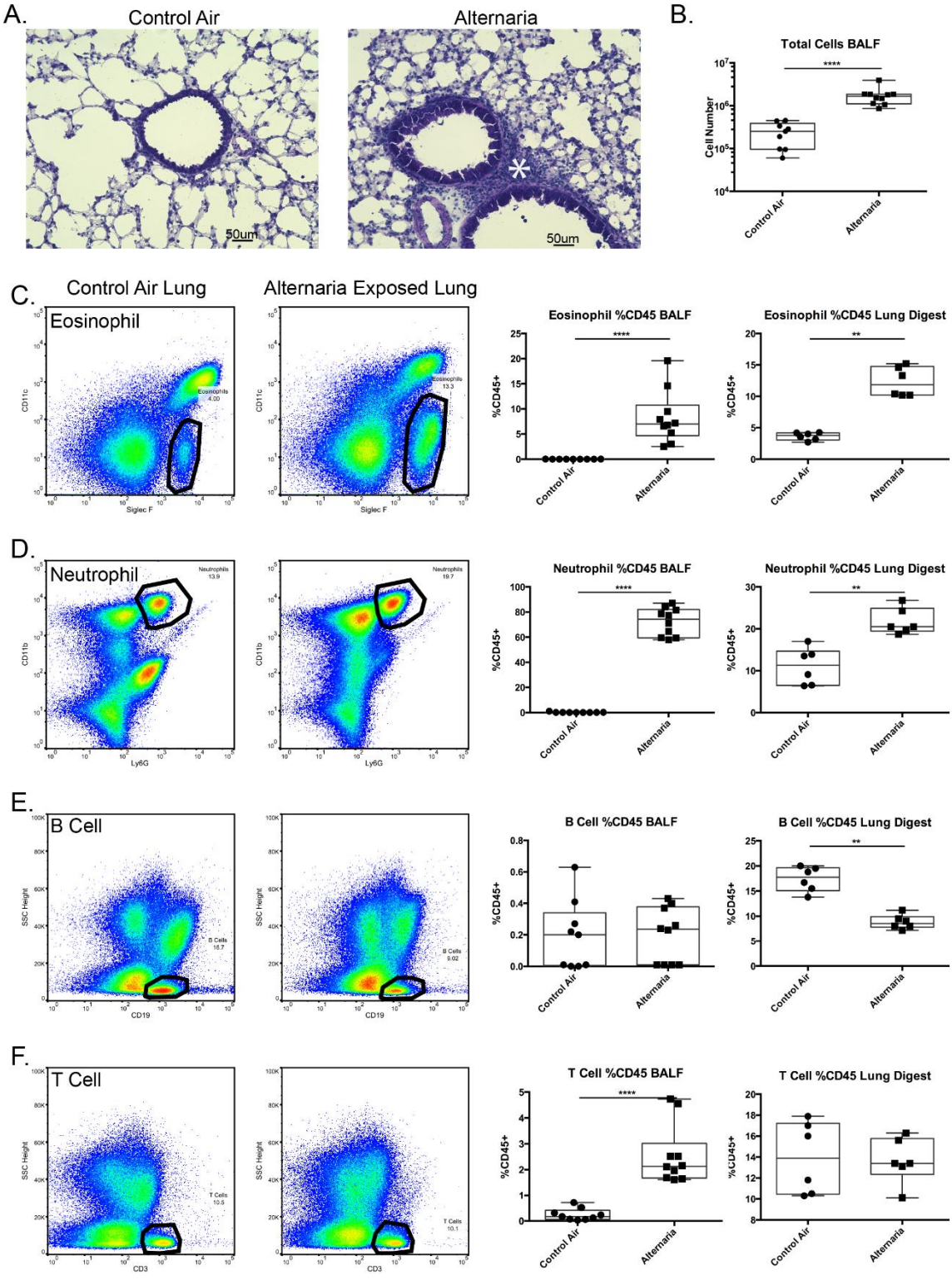
A.
Control Air
Alternaria
50um
50um
B.
Total Cells BALF
****
Cell Number
Control Air
Alternaria
C.
Control Air Lung
Alternaria Exposed Lung
Eosinophil
CD11c
Siglec F
Eosinophils
4.00
Eosinophils
13.3
Eosinophil %CD45 BALF
Eosinophil %CD45 Lung Digest
%CD45+
**
D.
Neutrophil
CD11b
Ly6G
Neutrophils
13.9
Neutrophils
19.7
Neutrophil %CD45 BALF
Neutrophil %CD45 Lung Digest
E.
B Cell
SSC Height
CD19
B Cells
16.7
B Cells
9.02
B Cell %CD45 BALF
B Cell %CD45 Lung Digest
F.
T Cell
CD3
T Cells
10.5
T Cells
10.1
T Cell %CD45 BALF
T Cell %CD45 Lung Digest

Figure 2.2 - Inflammatory cell recruitment due to Alternaria aerosols

Mice were exposed to either filtered control air or aerosolized *Alternaria* filtrate for 7 days in dual environmental chambers. Following exposure, bronchoalveolar lavage fluid (BALF) was collected and the left lobe was digested and analyzed via flow cytometry. (A) Lungs inflated with a 1:1 OCT:PBS solution and frozen in OCT blocks were sectioned and stained with H&E. (*, Interstitial infiltrate). (B) Total cells in the BALF were counted via hemocytometer (Left, Control air, n=9; Right, *Alternaria*, n=10). (C-F) Cells were represented as a percentage of $CD45^+$ cells in digested lungs or BALF. Representative dot plots for control air and *Alternaria* exposed are shown. Eosinophils are $CD45^+CD11c^-$ $SiglecF^+$ (Left diagram: Left, Control air BALF, n=9; Right, *Alternaria* BALF, n=10; Right diagram: Left, Control Air Lung, n=6, Right, *Alternaria* Lung, n=6). Neutrophils are $CD45^+CD11b^+Ly6G^+$ (Left diagram: Left, Control air BALF, n=9; Right, *Alternaria* BALF, n=10; Right diagram: Left, Control air, n=6, Right, *Alternaria,* n=6). B cells are $CD45^+SSC^{low}CD19^+$ (Left diagram: Left, Control air BALF, n=9; Right, *Alternaria* BALF, n=10; Right diagram: Left, Control air, n=6, Right, *Alternaria,* n=6). T cells are $CD45^+SSC^{low}CD3^+$ (Left diagram: Left, Control air BALF, n=9; Right diagram: Right, *Alternaria* BALF, n=10; Left, Control air, n=6, Right, *Alternaria,* n=6). ** = $p<0.01$; **** = $p<0.0001$

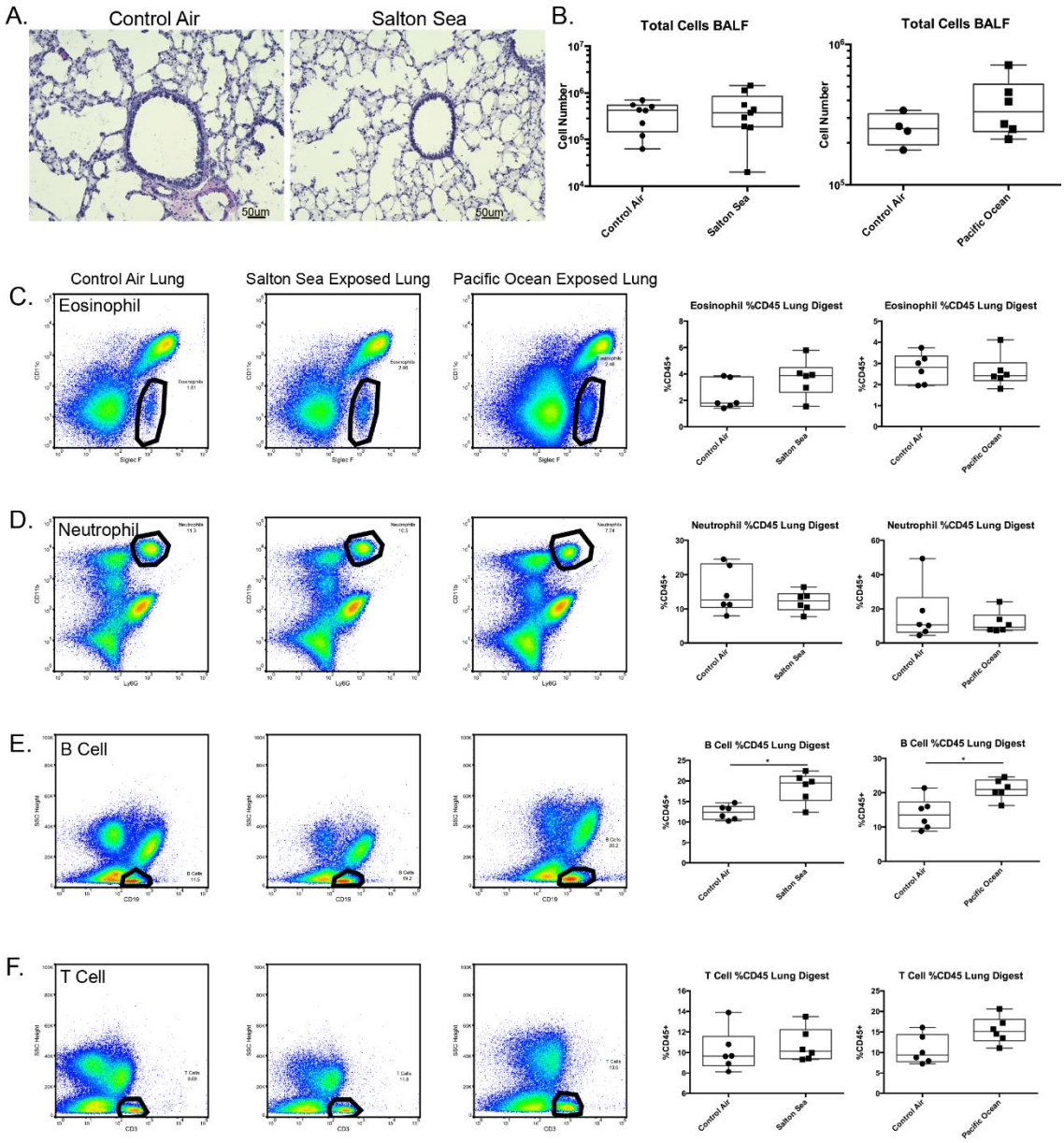
A.
Control Air
Salton Sea
50um
50um
B.
Total Cells BALF
Cell Number
Control Air
Salton Sea
Total Cells BALF
Cell Number
Control Air
Pacific Ocean
Control Air Lung
Salton Sea Exposed Lung
Pacific Ocean Exposed Lung
C.
Eosinophil
Siglec F
Eosinophil %CD45 Lung Digest
%CD45+
Control Air
Salton Sea
Eosinophil %CD45 Lung Digest
%CD45+
Control Air
Pacific Ocean
D.
Neutrophil
Ly6G
Neutrophil %CD45 Lung Digest
%CD45+
Control Air
Salton Sea
Neutrophil %CD45 Lung Digest
%CD45+
Control Air
Pacific Ocean
E.
B Cell
CD19
B Cell %CD45 Lung Digest
%CD45+
Control Air
Salton Sea
B Cell %CD45 Lung Digest
%CD45+
Control Air
Pacific Ocean
F.
T Cell
CD3
T Cell %CD45 Lung Digest
%CD45+
Control Air
Salton Sea
T Cell %CD45 Lung Digest
%CD45+
Control Air
Pacific Ocean

Figure 2.3 - Inflammatory cell recruitment due to Salton Sea and Pacific Ocean aerosols

Mice were exposed to filtered control air, filtered and aerosolized Salton Sea water, or filtered and aerosolized Pacific Ocean water for 7 days. BALF was collected and tissue was digested for flow cytometry. (A) Lungs were inflated with a 1:1 OCT:PBS mixture and frozen, sectioned and stained with H&E. (B) Total cells in the BALF were counted via hemocytometer (Left diagram: Left, Control air, n=8; Right, Salton Sea, n=9; Right diagram: Left, Control Air, n=4; Right, Pacific Ocean, n=6). (C-F) Digested lung was stained and analyzed via flow cytometry. Cells populations are represented as the percentage of $CD45^+$ cells. Representative dot plots for the control air, Salton Sea exposed, and Pacific Ocean exposed mice are shown. Aerosolized Salton Sea and Pacific Ocean exposed mice are compared to their contemporaneous controls. Eosinophils are $CD45^+CD11c^-SiglecF^+$ (Left diagram: Left, Control air, n=6; Right, Salton Sea, n=6; Right Diagram: Left, Control air, n=6; Right, Pacific Ocean, n=6). Neutrophils are $CD45^+CD11b^+Ly6G^+$ (Left diagram: Left, Control air, n=6; Right, Salton Sea, n=6; Right Diagram: Left, Control air, n=6; Right, Pacific Ocean, n=6). B cells are $CD45^+SSC^{low}CD19^+$ (Left diagram: Left, Control air, n=6; Right, Salton Sea, n=6; Right Diagram: Left, Control air, n=6; Right, Pacific Ocean, n=6). T cells are $CD45^+SSC^{low}CD3^+$ (Left diagram: Left, Control air, n=6; Right, Salton Sea, n=6; Right Diagram: Left, Control air, n=6; Right, Pacific Ocean, n=6). * = $p<0.05$

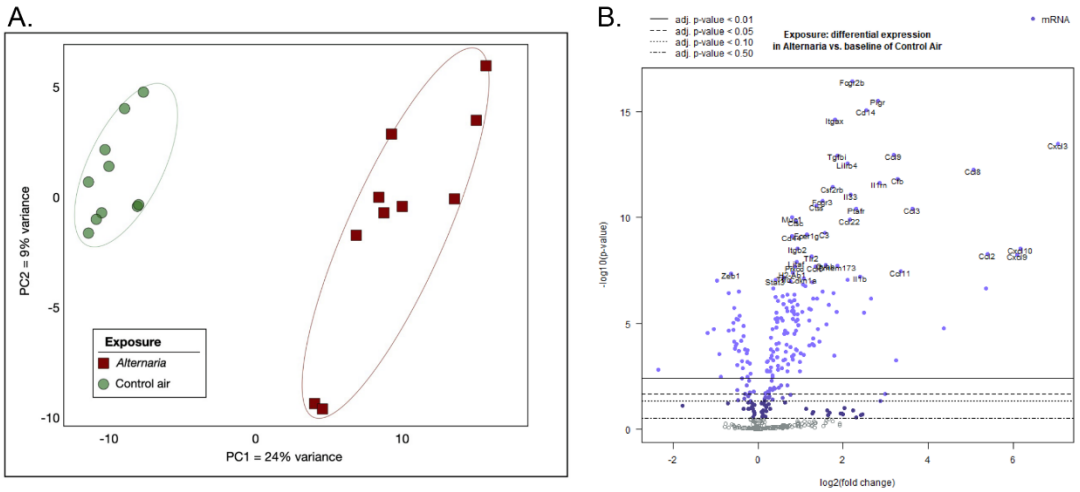

Figure 2.4 - Gene expression changes due to Alternaria aerosol exposure

After a 7-day exposure to either filtered control air (n=10) or *Alternaria* filtrate (n=10), lung RNAs were analyzed for gene expression using a defined immunology gene panel (NanoString); (A) PCA of the gene expression data with red squares representing mouse lung immune gene expression profiles from individual animals exposed to aerosolized *Alternaria* sp., as compared to green circles, which are from mouse samples exposed to control air. (B) Volcano plot depicting the differential expression profile of the *Alternaria* exposed mice compared to a baseline of control air. The X-axis depicts the log2 fold change while the Y-axis depicted the -log10 (Benjamini-Hochberg adjusted p-value). The 40 most significant gene by Benjamini-Hochberg adjusted p-value are labeled.

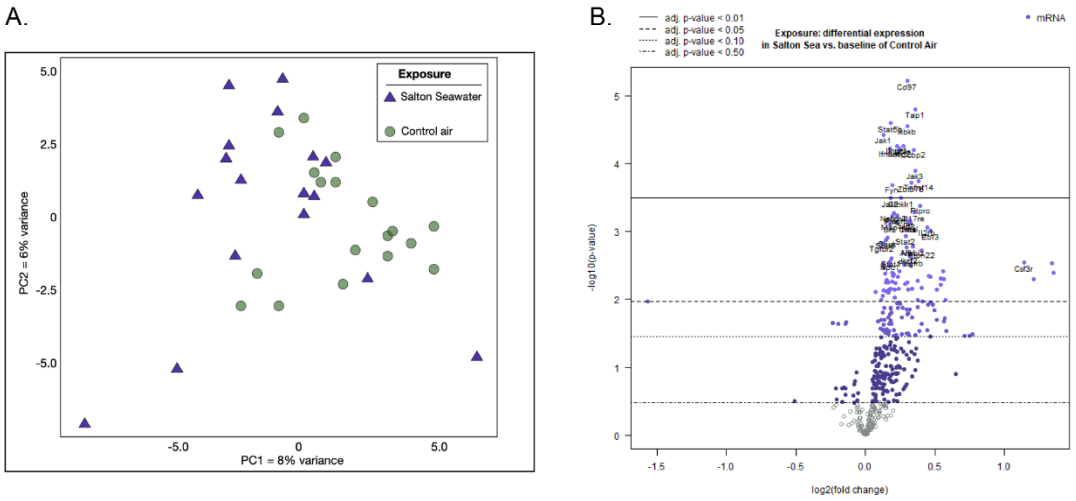

Figure 2.5 - Gene expression changes due to Salton Sea aerosol exposure

After a 7-day exposure to either filtered control air (n=18) or aerosolized Salton Sea water (n=17), lung RNAs were analyzed for gene expression using a defined immunology gene panel (NanoString). (A) PCA of the gene expression data with purple triangles representing mouse lung immune gene expression profiles from individual animals exposed to aerosolized Salton Sea water, as compared to green circles, which are from mouse samples exposed to control air. (B) Volcano plot depicting the differential expression profile of the aerosolized Salton Sea exposed mice compared to a baseline of control air. The X-axis depicts the log2 fold change while the Y-axis depicted the -log10 (Benjamini-Hochberg adjusted p-value). The 40 most significant gene by Benjamini-Hochberg (BH) adjusted p-value are labeled.

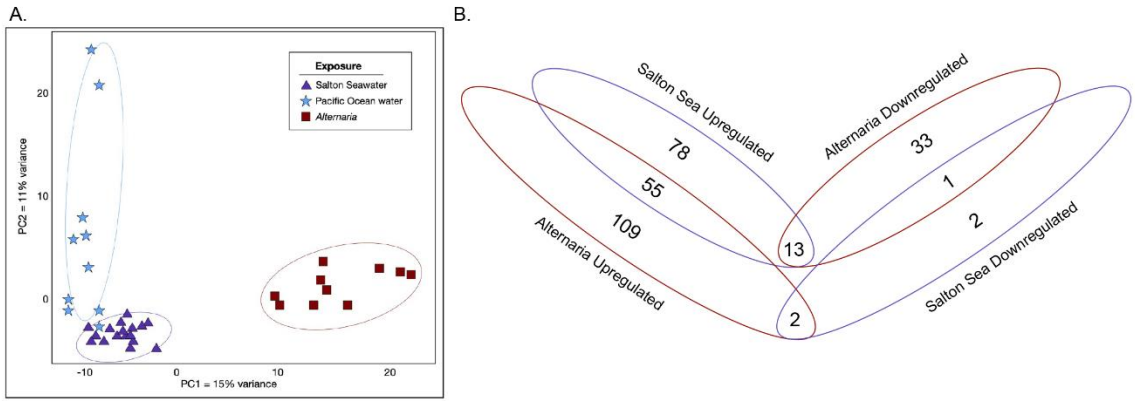

Figure 2.6 - Comparisons between Alternaria, Salton Sea and Pacific Ocean exposures

Mice were exposed to either control air, *Alternaria*, or aerosolized Salton Sea for 7-days before lung tissue was collected. Extracted RNA was analyzed using a Mouse Immunology Panel (NanoString). (A) PCAs were generated using the “prcomp” function in R (version 4.0.3), to compare Pacific Ocean (blue stars), Salton Sea (purple triangles) and *Alternaria* (red squares) exposures, and visualized PCA as in Methods. Comparisons are made between *Alternaria* exposed mice (n=10) and their contemporaneous controls (n=10) or aerosolized Salton Sea exposed mice (n=17) and their contemporaneous controls (n=18). 213 genes were differentially regulated in the *Alternaria* comparison (FDR < 0.10), of which 166 were upregulated and 47 were downregulated. 151 genes were differentially regulated in the Salton Sea comparison (FDR < 0.10), of which 146 were upregulated and 5 were downregulated. 55 genes were upregulated in both comparisons, 1 gene was downregulated in both comparisons, 13 were upregulated in the Salton Sea comparison but downregulated in the *Alternaria*

comparison while 2 were upregulated in the *Alternaria* comparison but downregulated in the Salton Sea comparison. 78 genes were uniquely upregulated, and 2 genes were uniquely downregulated in the Salton Sea comparison while 109 genes were uniquely upregulated and 33 were uniquely downregulated in the *Alternaria* comparison

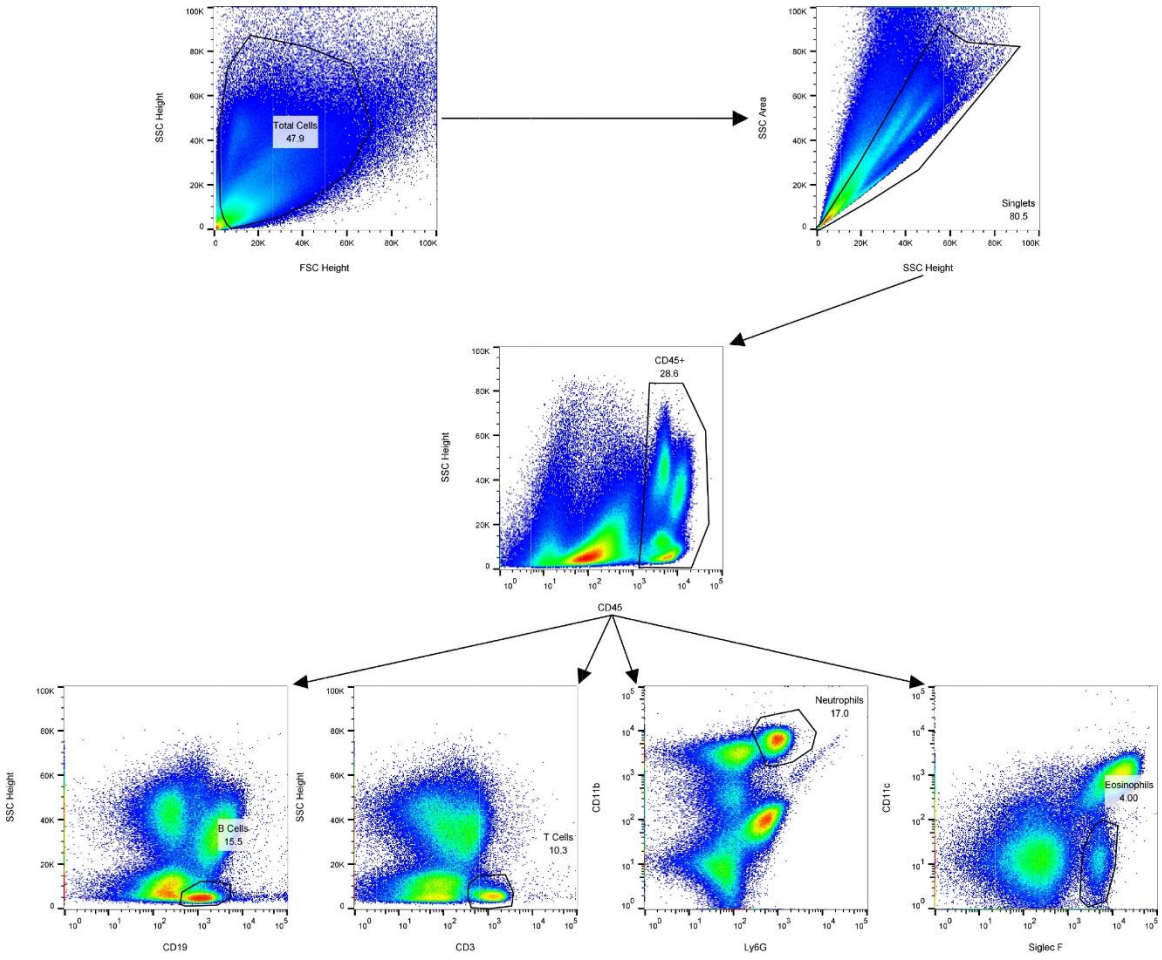
SSC Height
FSC Height
Total Cells
47.9
SSC Area
SSC Height
Singlets
80.5
SSC Height
CD45
CD45+
28.6
SSC Height
CD19
B Cells
15.5
SSC Height
CD3
T Cells
10.3
CD11b
Ly6G
Neutrophils
17.0
CD11c
Siglec F
Eosinophils
4.00

Figure 2.S1 - Gating strategy for flow cytometry

Lungs of mice were collected and digested after 7 days of a given exposure condition. The digested lungs were treated with BD FC Block in order to prevent nonspecific binding. Afterwards, the digested lung was stained with anti-$CD45^+$ FITC, anti-CD19 PE-Cy5, anti-CD3 Alexa Fluor 700, anti-CD11b BV421, anti-Ly6G BV510 or anti-SiglecF APC. The gating strategy used to identify different immune cell subpopulations are shown above. First, debris is gated out using SSC and FSC height. Following that, doublets are gated out using SSC area and SSC height. Then $CD45^+$ cells are selected. These $CD45^+$ cells are then subdivided into B cells (SSC^{low}, $CD19^+$), T cells (SSC^{low}, $CD3^+$), neutrophils ($CD11b^+$, $Ly6G^+$) and eosinophils ($CD11c^-$, Siglec F^+).

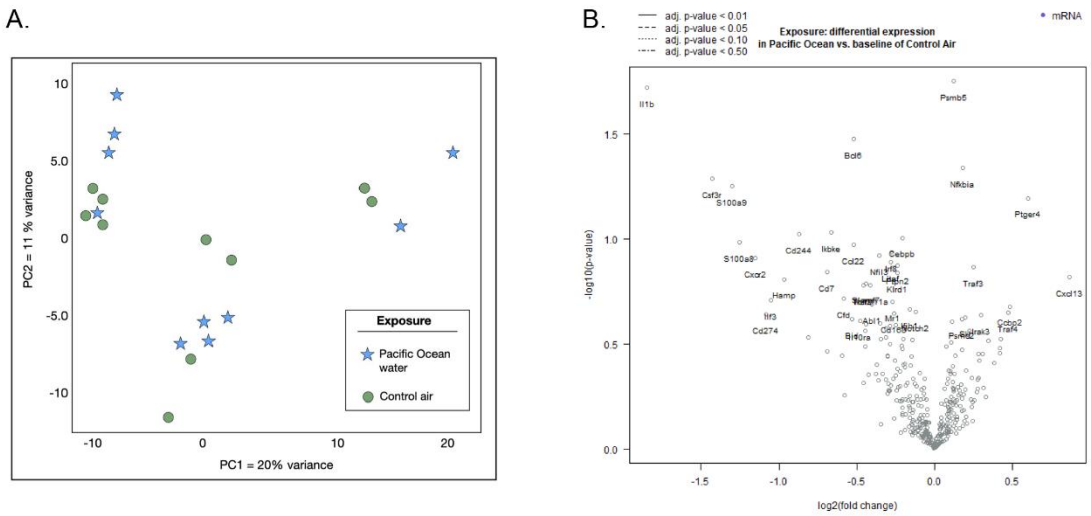

Figure 2.S2 - Gene expression changes due to Pacific Ocean aerosols

After a 7-day exposure to either filtered control air (n=10) or aerosolized Pacific Ocean exposed (n=10), lung RNAs were analyzed for gene expression using a defined immunology gene panel (NanoString). (A) PCA of the gene expression data with blue stars representing mouse lung immune gene expression profiles from individual animals exposed to aerosolized Pacific Ocean, as compared to green circles, which are from mouse samples exposed to control air. PCAs were generated as described in Methods. (B) Volcano plot depicting the differential expression profile of the aerosolized Pacific Ocean exposed mice compared to a baseline of control air. The X-axis depicts the log2 fold change while the Y-axis depicted the -log10 (Benjamini-Hochberg adjusted p-value). The 40 most significant gene by Benjamini-Hochberg adjusted p-value are labeled.

Chapter 3: The Effect of Preexposure to Salton Sea Water on Asthma Development

Trevor A. Biddle[11,4], Keziyah Yisrael[1,4], Ryan Drover[2,3], Diana Del Castillo[1], Daniel Gonzales[2,3], Malia L. Shapiro[1], David R. Cocker III[2,3], David D. Lo[1,4,5]

Abstract

Our previous study using aerosolized Salton Sea Water indicated a change in inflammatory gene regulation without inflammatory cell recruitment to the lungs or airways. This was distinct in both the types of genes and magnitude of inflammation when compared to a type-2-like response to *Alternaria sp.* In this study, we investigated if there exposure to aerosolized Salton Sea Water was capable of predisposing mice to allergic development. To do so, we exposed mice to 1500 μg/m^3 of filtered and aerosolized Salton Sea Water for 7 days and then a subclinical 150 μg/m^3 aerosolized dose of a mixture of *Alternaria alternata* and *Alternaria tenuis*. We found no change in inflammatory gene expression, inflammatory cell recruitment to the airways and lung tissue, and no significant

[1]: Division of Biomedical Sciences, University of California, Riverside School of Medicine, Riverside, California, USA
[2]: Division of Biomedical Sciences, University of California, Riverside School of Medicine, Riverside, California, USA
[3]: College of Engineering-Center for Environmental Research and Technology (CE-CERT), University of California, Riverside, Riverside, California, USA
[4]: BREATHE Center, University of California, Riverside, Riverside, California, USA
[5]: Center for Health Disparities Research, University of California, Riverside, Riverside, California, USA

change in airway hyperreactivity compared to contemporaneous mice exposure to filtered house air. Our results indicate that Salton Sea Water is unlikely to be the primary culprit behind the elevated asthma rates in the regions surrounding the Salton Sea.

Introduction

The Salton Sea is a terminal lake located on the borders of Riverside and Imperial Counties. This lake was formed from a breach in the Colorado River canal in 1905 and has since primarily been maintained by agricultural runoff. However, due to water diversion towards cities and away from agriculture, along with increasing temperatures due to climate change, the Salton Sea is rapidly drying. The Salton Sea has a current salinity of over 70 parts per thousand, which is approximately double the salinity of the Pacific Ocean (Bureau of Reclamation, 2020). This, along with pollution from agricultural activities, has dramatically changed the local ecology. The region is subject to frequent algal blooms, which can release deadly cyanotoxins which have been implicated in large fish and migratory bird die-offs (Carmichael and Li, 2006; Xu et al., 2016). Additionally, historical and current use pesticides, such as DDT, organophosphates, and pyrethroids, have been found at detectable levels in the waters and sediments of the Salton Sea (LeBlanc and Kuivila, 2008; Xu et al., 2016). Due to the geochemical composition of the region, the Salton Sea also contains heavy metals such as selenium (Zhou et al., 2017).

The communities surrounding the Salton Sea are in poor health, particularly with regards to asthma. This region suffers from one of the highest rates of childhood asthma in the state of California at 20%-22.4% (Farzan et al., 2019), as well as emergency room visits due to asthma (CalEnviroScreen 4.0). The exact reasons remain to be elucidated, but there are several potential culprits. The region has high levels of particulate matter (California EPA, 2022), with Eastern Coachella Valley (the easternmost portion of Riverside County) and Imperial Counties being designated nonattainment areas for particulate matter between 10μm and 2.5μm (PM_{10}), and particulate matter under 2.5μm ($PM_{2.5}$). Particulate matter from other arid regions has been linked to asthma development when paired with an allergen (Kwon et al., 2002; Chen et al., 2004; Watanabe et al., 2011). Additionally, the aforementioned pollutants in the water, such as cyanotoxins and pesticides, have been independently linked to lung damage and the development and exacerbation of asthma (Fleming et al., 2007; Bernstein et al., 2011; Zaias et al., 2011; Li et al., 2016; Wang et al., 2016 Shaffo et al., 2018).

Our previous work showed that exposure to filtered and aerosolized Salton Sea Water was capable of upregulating several inflammatory genes without active inflammatory cell recruitment (Biddle et al., 2021). However, this inflammatory pattern did not appear to replicate a type-2 allergic response, unlike our *Alternaria sp.* exposed positive controls. Based on this, we sought to determine if prior exposure to Salton Sea Water primed mice for a type-2 allergic

response. To do so, we exposed mice to 1500 μg/m^3 of filtered and aerosolized Salton Sea Water for 7 days followed by an exposure to a subclinical 150 μg/m^3 dose of an *Alternaria alternata* and *Alternaria tenuis* mixture. We found no significant change in inflammatory gene expression between mice pre-exposed to Salton Sea Water. There was also no significant change in inflammatory cell recruitment found in the bronchoalveolar lavage fluid (BALF) and in airway hyperreactivity between exposed mice and those given filtered house air. Taken together, these results indicate that aerosolized Salton Sea Water, such as that in the form of sea spray, is unlikely to sensitize patients to the development of asthma.

Materials and Methods

Sample Collection

Water samples were collected from the southeastern part of the Salton Sea near the Imperial Wister Wildlife Unit (33.2041600, -115.938574) on 12/21/2022. Autoclaved glassware was used to skim water off the top of the Salton Sea. This was then transported back to the University of California, Riverside and kept at 4°C until further processing.

Sample Processing

Samples were centrifuged at 1500 rpm for 7 minutes to pellet large particulate matter. The supernatant was then filtered through a 0.22 μm sterile

filter to remove cells and other debris that would interfere with the aerosolization process. Processed samples were stored at 4°C until used.

Animals

All experiments were performed following the University of California, Riverside's institutional IACUC and NIH guidelines. Wild type C57BL/6J mice were purchased from Jackson Labs, Sacramento and acclimated for one week in the University of California, Riverside's specific pathogen free (SPF) vivarium. Mice were kept 2-4 to a cage and allowed food and water *ad libitum*. Mice were provided a 12-hour day/night cycle. Mice were exposed to either aerosolized Salton Sea Water or filtered house air for 7 days before being exposed to either *Alternaria sp* or filtered house air for 7 additional days. Groups were distributed as follows: 4 female mice and 5 male mice were exposed to just filtered air; 4 female and 8 male mice were exposed to filtered air followed by *Alternaria sp.*; 4 female and 8 male mice were exposed to aerosolized Salton Sea Water followed by *Alternaria sp.*

Chamber Operation

Exposure studies were performed in dual 540 L animal chambers, with one connected to an aerosolizer and silica driers as describe in Peng et al., 2019, and one connected to filtered house air. Relative humidity, temperature, and atmospheric pressure were measured and kept at acceptable levels during

the exposure. Mice in the exposure chamber were continuously fed a mixture of dry filtered air (0.5–1 lpm) and aerosolized spray (dried by two in-line silica gel columns, 3.5–4.5 lpm). The PM was generated from solutions of *Alternaria alternata* and *Alternaria tenuis* filtrate (Greer Laboratories, Lenoir, NC, USA; 0.4 g/L) and from Salton Sea Water that was diluted to give the appropriate aerosol mass concentration. The aerosol sources for the exposure were each tested in advance in order to determine chemical composition (high-resolution time-of-flight aerosol mass spectrometer (HR-ToF-AMS), Aerodyne) and aerosol density (aerosol particle mass analyzer (APM), Kanomax) to prepare the solutions to yield the targeted particle mass concentration. Sample aerosolization was accomplished by using a homemade nebulizer with silica-gel dryers. Mice in the control chamber were given filtered dry air (5.0 lpm) only, with other conditions matching the exposure chamber, including bedding replacement, food and water supplies, and corresponding day/night cycle. Particulate matter was only monitored within the exposure chamber by a scanning mobility particle sizer (SMPS, including Series 3080 Electrostatic Classifier and Ultrafine Condensation Particle Counter 3776, TSI) to assist in maintaining stable PM concentration. The PM concentrations used in this study were 1500 $\mu g/m^3$ for the Salton Sea Water (matching the dose from Biddle et al., 2021) and 150 $\mu g/m^3$ for *Alternaria sp.* (which was determined to be a subclinical level of *Alternaria* based on a pilot experiment).

Animal Processing

After the two 7-day exposures, mice were removed from the environmental exposure chamber for processing. Mice were either set aside to recover overnight for FlexiVent analysis or were processed immediately for cell infiltrate and inflammatory gene expression analysis.

For the cell infiltrate and inflammatory gene expression processing, mice (n = 5-6) were anesthetized using isoflurane and euthanized by cervical dislocation. Bronchoalveolar lavage fluid (BALF) was collected by washing the lung with 0.8 mL of PBS 3 times. The lungs were then excised and used for either RNA extraction or for analyzing cell infiltrates. The right lobe was flash frozen in liquid nitrogen and kept at -80°C until RNA extraction. The left lobe minced into small (~1-2 mm) sections and digested using 0.5 mg/mL collagenase D (Roche Diagnostics, Mannheim, Germany) and 50 U/mL DNase I (Sigma Aldrich, St. Louis, USA) in RPMI 1640 (Gibco, Grand Island, USA) fortified with 10% heat-inactivated FB (Gibco, Grand Island, USA) preheated to 37°C. The lung and digestion mixture incubated at 37°C for 30 minutes at 150 rpm prior to agitation using an 18-gauge needle. The lung and digestion mix was then incubate for 15 additional minutes under the same conditions. Following digestion, the lung was pushed through a 100 µm cell strainer (Corning, Corning, USA), which was then washed with the fortified RPMI 1640. This solution was then centrifuged and resuspended in PBS for use in flow cytometry.

Lung Measurements

Male mice (n = 2-3) were left to recover overnight from the two 7-day exposures. Prior to intubation on a FlexiVent (Scireq, Montreal, Canada), mice were anesthetized using intraperitoneal (IP) injection of an 80mg/kg ketamine 12mg/kg xylazine mixture. Once intubated, mice were given an IP injection of 1mg/kg Pancuronium Bromide as a paralytic agent to prevent interference with the mechanical ventilation. Lung measurements were recorded using the NPFE Mouse Mechanics program and the Dose Response program. Methacholine at 0, 6.25, 12.5, 25, and 50 mg/mL were used for analysis of airway hyperreactivity. After the final measurement, mice were euthanized via cervical dislocation.

3.2.7 Flow Cytometry:

BALF and post-digested lungs were centrifuged at 1500 rpm before resuspension in 100 µL of a 1:100 dilution of Zombie Yellow™ dye (Biolegend, San Diego, USA). After staining, cells were washed in FACS Buffer, centrifuged, and resuspended in 100 µL of a 1:50 dilution of Mouse BD FC block (BD Pharmigen, San Joe, USA). Cells were then stained using the following fluorescent antibodies: anti-CD45 FITC (BioLegend, San Diego, USA; Clone 30-F11), anti-CD19 Percp-Cy5.5 (eBioscience, San Diego, USA; Clone eBio1D3), anti-CD3 Alexa Fluor 700 (BioLegend, San Diego, USA; Clone 17A2), anti-Ly6G BV510 (BioLegend, San Diego, USA; Clone 1A8), anti-CD11b APC-eFluor 780 (eBioscience, San Diego, USA; Clone M1/70), anti-CD11c PE-Cy7 (BioLegend, San Diego, USA; Clone N418), anti-SiglecF APC (BioLegend, San Diego, USA;

Clone S17007L), anti-CD4 BV711 (BioLegend, San Diego, USA; Clone RM4-5), anti-CD8 PE-CF594 (BD Biosciences, San Diego, USA; Clone 53-6.7), and anti-IgE PE (BioLegend, San Diego, USA; Clone RME-1).

Cells stained with Zombie Yellow™ dye were excluded from further analysis. Cell populations were determined using the following surface markers: neutrophils were $CD45^{+}CD11b^{+}Ly6G^{+}SiglecF^{-}CD11c^{-}$, eosinophils were $CD45^{+}CD11b^{+}SiglecF^{+}CD11c^{-}$, T cells were $CD45^{+}CD3^{+}SiglecF^{-}CD11c^{-}$, and were further divided based on CD4 and CD8 staining, and B cells were $CD45^{+}CD19^{+}SiglecF^{+}CD11c^{-}$ and further divided based on IgE staining.

Samples were run on a NovoCyte Quanteon (Agilent Technologies, Santa Clara, USA). Gating and analysis were performed using FlowJo (Version 10.81, Ashland, USA).

RNA Extraction

RNA was purified from the frozen right lung lobes using a TRIzol© (Ambion, Carlsbad, USA) based method. ~100 mg of frozen lung tissue (half of the right lobe) was placed in a mortar, frozen with liquid nitrogen, and ground into dust using a pestle. After, the ground lung tissue was placed in TRIzol©. Manufacturer protocol was followed except the RNA pellet was washed 3 times with 75% ethanol rather than once. The pellet was resuspended in DEPC-Treated water (Ambion, Austin, USA). Concentration and purity of the RNA was checked via NanoDrop 2000 (Thermo Scientific, Carlsbad, USA).

NanoString Analysis

RNA was analyzed using an nCounter® Sprint Profiler (NanoString Technologies, Seattle, USA) with the nCounter® Mouse Immunology Panel according to manufacturer protocols. The nSolver® 4.0 software (NanoString Technologies, Seattle, USA) was used to normalize gene counts based on housekeeping genes and positive controls. Differential expression was calculated using the nSolver® Advanced Analysis 2.0 software (NanoString Technologies, Seattle, USA), and p-values were adjusted using the Benjamini-Hochberg method.

nSolver® 4.0 normalized log2 gene counts and nSolver® Advanced Analysis 2.0 software differential expression data was imported into R version 4.2.2 (R Core Team, 2022) using *readr* (Wickham et al., 2022) and *readxl* (Wickham and Bryan, 2022) and visualized using *ggplot2* (Wickham, 2016) and *Khroma* (Frerebeau, 2022). Principal component analyzed were calculated from the normalized log2 gene counts and the built-in “prcomp” function. This was visualized using *ggfortify* (Tang et al., 2016).

Statistical Analysis

Statistical analysis for inflammatory cell infiltration and lung measurements was performed using GraphPad Prism 9 (GraphPad, San Diego, USA). For the inflammatory cell analysis: P-value was calculated using a one-way ANOVA with

Holm-Šídák's multiple comparisons test. For the lung measurements: A two-way ANOVA with Tukey's correction was used to analyze the response for each group at each dose of methacholine. Results shown include all mice, along with the average ± the standard error (SE). P-value for gene expression was calculated using nSolver® 4.0 and was false discovery rate (FDR) adjusted using the Benjamini-Hochberg method. A p-value of less than 0.05 and an FDR adjusted p-value of less than 0.1 were considered significant.

Results

Changes in Cell Profile of the BALF and Digested Lung Tissue

To determine the extent to which Salton Sea Water may contribute to allergic development, we exposed mice to either filtered house air or filtered and aerosolized Salton Sea Water for 7 days, followed by a 7-day exposure to a subclinical dose of aerosolized *Alternaria alternata* and *Alternaria tenuis*. We ended up with three final groups: Mice exposed to filtered house air for both 7-day exposures (control air mice), mice exposed to control air and then *Alternaria sp.* (Alternaria mice), and mice exposed to Salton Sea Water and then *Alternaria sp.* (Salton Sea Water mice). We used a flow cytometry-based analysis to obtain cell differentials in both the BALF and the digested lung tissue.

We found that there was no significant difference in inflammatory cell profile in the BALF. The majority of cells in the BALF were alveolar macrophages (94.5% ± 0.7% control air; 93.8% ± 1.6% Alternaria; 94.4% ± 2.1% Salton Sea

Water; Figure 3.1a) as measured by percentage of $CD45^+$ cells. There were negligible numbers of eosinophils (0.04 ± 0.02% control air; 0.2% ± 0.1% Alternaria; 0.1% ± 0.04% Salton Sea Water; Figure 3.1b) and neutrophils (0.6% ± 0.1% control air; 0.9% ± 0.2% Alternaria; 0.7% ± 0.2% Salton Sea Water; Figure 3.1c).

There were minimal changes in the inflammatory cell profile in the lung tissue. Alveolar macrophages (12.6% ± 1.6% control air; 9.9% ± 1.0% Alternaria; 10.3% ± 0.5% Salton Sea Water; Figure 3.2a), eosinophils (4.5% ± 0.3% control air; 4.2% ± 0.4% Alternaria; 3.4% ± 0.4% Salton Sea Water; Figure 3.2b), neutrophils (16.4% ± 4.0% control air; 10.6% ± 0.8% Alternaria; 9.4% ± 0.9% Salton Sea Water; Figure 3.2c), and T cells (20.8% ± 2.2% control air; 19.53% ± 1.4% Alternaria; 20.5% ± 1.8% Salton Sea Water; Figure 3.2d) showed no significant difference between the control and exposure groups. Additionally, there was no significant difference between percentage of $CD4^+$ (46.2% ± 1.0% control air; 46.6% ± 1.4% Alternaria; 46.5% ± 0.8% Salton Sea Water; Figure 3.2e) vs $CD8^+$ (45.7% ± 1.3% control air; 44.0% ± 1.1% Alternaria; 43.4% ± 1.0% Salton Sea Water; Figure 3.2f) T cells as percentage of total T cells. The only change detected in the lung tissue was an elevated percentage of B cells in the exposed mice (22.3% ± 1.2% control air; 31.6% ± 1.3% Alternaria; 28.9% ± 1.6% Salton Sea Water; Figure 3.2g); however, there was no significant difference between mice pretreated with Salton Sea Water and those exposed to just Alternaria. There was also no significant difference in percentage IgE+ B cells as

percent of total B cells (0.6% ± 0.1% control air; 1.4% ± 1.0% Alternaria; 0.6% ± 0.04% Salton Sea Water; Figure 3.2h).

Inflammatory Gene Expression Between Exposure Groups

To determine the potential differences in whole lung tissue gene expression between the different exposure groups, we ran the Salton Sea Water and Alternaria groups on an NanoString Sprint Profiler using their Mouse Immunology Panel. No genes reached our FDR adjusted significance threshold of 0.1 (Figure 3.3a). There was an overall trend towards lower inflammatory gene expression in mice pretreated with Salton Sea Water, but once again, no genes were significantly differentially regulation. The individual mice also tended to cluster together in PCA analysis (Figure 3.3b). Taken together, these indicate that there was no significant difference in inflammatory gene regulation to mice pre-exposed to Salton Sea Water.

Changes in Airway Hyperreactivity

To test for changes in airway hyperreactivity in the different groups, we rested a set number of male mice overnight before measuring airway hyperreactivity on a FlexiVent. We found that there was no significant difference between the control and exposed groups at any dose of methacholine. However, we did detect a significant change at the 50mg/mL methacholine dose between

mice between the exposure groups, as mice pretreated with Salton Sea Water having lower reactivity compared to mice exposed to just Alternaria (Figure 3.4).

Discussion

Based on the results from our previous paper (Biddle et al., 2021), we hypothesized that aerosolized Salton Sea Water may contribute to the high rates of asthma in the communities surrounding the Salton Sea by sensitizing individuals towards asthma development. However, based on our current experiment, that seems unlikely to be the case. We had minimal overall impact from pre-exposing mice to Salton Sea Water, with the only significant change between the Salton Sea Water and Alternaria groups being a reduction in airway reactivity to 50mg/mL of methacholine. Otherwise, we detected no change between the exposure groups and minimal changes between the control and exposure groups.

Our results indicate that the sea spray is unlikely to be the primary culprit behind the elevated asthma rates in the region. Based on these results, we believe that it is better to focus on other potential sources of pollution, such as dust, and the role they may play in asthma development.

Despite our findings, the Salton Sea may still serve as a reservoir for various pollutants. Previous studies have found that pollutants such as DDT, organophosphates, pyrethroids, heavy metals, and cyanotoxins are present in the Salton Sea (LeBlanc and Kuivila, 2008; Xu et al, 2016; Zhou et al., 2017).

These pollutants tend to be hydrophobic, and preliminary data collected from other labs at the University of California, Riverside, indicate that there may be an enrichment from the water to the sediment to the dust. Thus, the role of the Salton Sea in asthma development may be that it serves to concentrate pollutants into the sediments, which are exposed as playa as the Salton Sea dries. Playa has been linked to increased levels of particulate matter (Reheis, MC, 1997; Reynolds et al., 2007; Bullar et al., 2008; Hossein et al., 2018), and will be an increasing source of dust in the future. Based on this and our findings, we believe that it is more pertinent to focus on the health impacts of the dust in the region, as it is likely more relevant to the pulmonary health in the region.

References

Biddle, T. A., Li, Q., Maltz, M. R., Tandel, P. N., Chakraborty, R., Yisrael, K., Drover, R., Cocker, D. R., & Lo, D. D. (2021). Salton Sea aerosol exposure in mice induces a pulmonary response distinct from allergic inflammation. *Science of The Total Environment*, *792*, 148450. https://doi.org/10.1016/j.scitotenv.2021.148450

Bullard, J., Baddock, M., McTainsh, G., Leys, J., 2008. Sub-basin scale dust source geomorphology detected using MODIS. Geophysical Research Letters 35. doi:10.1029/2008GL033928

Bureau of Reclamation. *Annual Report on the Salton Sea*. (Online). February 2022. Available: https://saltonsea.ca.gov/wp-content/uploads/2022/02/2022-Annual-Report_English_Feb-24-2022_Final.pdf. Referenced: March 10, 2023

California Environmental Protection Agency, Office of Environmental Health Hazard Assessment, 2021, October 20. CalEnviroScreen 4.0. Retrieved from. https://oehha.ca.gov/calenviroscreen/report/calenviroscreen-40

Carmichael WW, Li R. Cyanobacteria toxins in the Salton Sea. Saline Syst. 2006 Apr 19;2:5. doi: 10.1186/1746-1448-2-5. PMID: 16623944; PMCID: PMC1472689.

Chen YS, Sheen PC, Chen ER, Liu YK, Wu TN, Yang CY. Effects of Asian dust storm events on daily mortality in Taipei, Taiwan. Environ Res. 2004 Jun;95(2):151-5. doi: 10.1016/j.envres.2003.08.008.

Environmental Protection Agency. (2022, August 31). *Nonattainment Areas for Criteria Pollutants (Green Book)*. https://www.epa.gov/green-book

Farzan, S. F., Razafy, M., Eckel, S. P., Olmedo, L., Bejarano, E., & Johnston, J. E. (2019). Assessment of respiratory health symptoms and asthma in children near a drying saline lake. International Journal of Environmental Research and Public Health, 16(20). https://doi.org/10.3390/ijerph16203828

Fleming, L. E., Kirkpatrick, B., Backer, L. C., Bean, J. A., Wanner, A., Reich, A., Zaias, J., Cheng, Y. S., Pierce, R., Naar, J., Abraham, W. M., & Baden, D. G. (2007). Aerosolized red-tide toxins (brevetoxins) and asthma. *Chest*, *131*(1), 187–194. https://doi.org/10.1378/chest.06-1830

Frerebeau N (2022). *khroma: Colour Schemes for Scientific Data Visualization*. Université Bordeaux Montaigne, Pessac,

France. doi:10.5281/zenodo.1472077, R package version 1.9.0, https://packages.tesselle.org/khroma/.

Hossein Mardi, A., Khaghani, A., MacDonald, A. B., Nguyen, P., Karimi, N., Heidary, P., Karimi, N., Saemian, P., Sehatkashani, S., Tajrishy, M., & Sorooshian, A. (2018). The Lake Urmia environmental disaster in Iran: A look at aerosol pollution. *The Science of the total environment*, *633*, 42–49. https://doi.org/10.1016/j.scitotenv.2018.03.148.

Kwon, H. J., Cho, S. H., Chun, Y., Lagarde, F., & Pershagen, G. (2002). Effects of the Asian dust events on daily mortality in Seoul, Korea. *Environmental Research*, *90*(1), 1–5. https://doi.org/10.1006/enrs.2002.4377

LeBlanc, L. A., & Kuivila, K. M. (2008). Occurrence, distribution and transport of pesticides into the Salton Sea Basin, California, 2001-2002. *Hydrobiologia*, *604*(1), 151–172. https://doi.org/10.1007/s10750-008-9316-1

Peng, X., Maltz, M. R., Botthoff, J. K., Aronson, E. L., Nordgren, T. M., Lo, D. D., & Cocker, D. R. (2019). Establishment and characterization of a multi-purpose large animal exposure chamber for investigating health effects. *Review of Scientific Instruments*, *90*(3), 1–7. https://doi.org/10.1063/1.5042097

R Core Team. (2022). *R: A Language and Environment for Statistical Computing*. Vienna, Austria. Retrieved from https://www.R-project.org/

Reheis, M. C. (1997), Dust deposition downwind of Owens (dry) Lake, 1991–1994: Preliminary findings, *J. Geophys. Res.*, 102(D22), 25999– 26008, doi:10.1029/97JD01967.

Reynolds, R.L., Yount, J.C., Reheis, M., Goldstein, H., Chavez, P., Jr., Fulton, R., Whitney, J., Fuller, C. and Forester, R.M. (2007), Dust emission from wet and dry playas in the Mojave Desert, USA. Earth Surf. Process. Landforms, 32: 1811-1827. https://doi.org/10.1002/esp.1515

Shaffo, F. C., Grodzki, A. C., Fryer, A. D., & Lein, P. J. (2018). Mechanisms of organophosphorus pesticide toxicity in the context of airway hyperreactivity and asthma. *American Journal of Physiology - Lung Cellular and Molecular Physiology*, *315*(4), L485–L501. https://doi.org/10.1152/ajplung.00211.2018

Tang Y, Horikoshi M, Li W (2016). “ggfortify: Unified Interface to Visualize Statistical Result of Popular R Packages.” *The R Journal*, **8**(2), 474–485. doi: 10.32614/RJ-2016-060, https://doi.org/10.32614/RJ-2016-060.

Wang, C., Gu, S., Yin, X., Yuan, M., Xiang, Z., Li, Z., Cao, H., Meng, X., Hu, K., & Han, X. (2016). The toxic effects of microcystin-LR on mouse lungs and alveolar type II epithelial cells. *Toxicon*, *115*, 81–88. https://doi.org/10.1016/j.toxicon.2016.03.007

Watanabe, M., Yamasaki, A., Burioka, N., Kurai, J., Yoneda, K., Yoshida, A., Igishi, T., Fukuoka, Y., Nakamoto, M., Takeuchi, H., Suyama, H., Tatsukawa, T., Chikumi, H., Matsumoto, S., Sako, T., Hasegawa, Y., Okazaki, R., Horasaki, K., & Shimizu, E. (2011). Correlation between Asian dust storms and worsening asthma in Western Japan. *Allergology International*, *60*(3), 267–275. https://doi.org/10.2332/allergolint.10-OA-0239

Wickham H (2016). *ggplot2: Elegant Graphics for Data Analysis*. Springer-Verlag New York. ISBN 978-3-319-24277-4, https://ggplot2.tidyverse.org.

Wickham H, Bryan J (2022). *readxl: Read Excel Files*. https://readxl.tidyverse.org, https://github.com/tidyverse/readxl.

Wickham H, Hester J, Bryan J (2022). *readr: Read Rectangular Text Data*. https://readr.tidyverse.org, https://github.com/tidyverse/readr.

Xu EG, Bui C, Lamerdin C, Schlenk D. Spatial and temporal assessment of environmental contaminants in water, sediments and fish of the Salton Sea and its two primary tributaries, California, USA, from 2002 to 2012. Sci Total Environ. 2016 Jul 15;559:130-140. doi: 10.1016/j.scitotenv.2016.03.144. Epub 2016 Apr 6. PMID: 27058132.

Zaias, J., Fleming, L. E., Baden, D. G., & Abraham, W. M. (2011). Repeated exposure to aerosolized brevetoxin-3 induces prolonged airway hyperresponsiveness and lung inflammation in sheep. *Inhalation Toxicology*, *23*(4), 205–211. https://doi.org/10.3109/08958378.2011.558936

Zhou, C., Huang, J. C., Liu, F., He, S., & Zhou, W. (2017). Effects of selenite on Microcystis aeruginosa: Growth, microcystin production and its relationship to toxicity under hypersalinity and copper sulfate stresses. *Environmental Pollution*, *223*, 535–544. https://doi.org/10.1016/j.envpol.2017.01.056

Figures

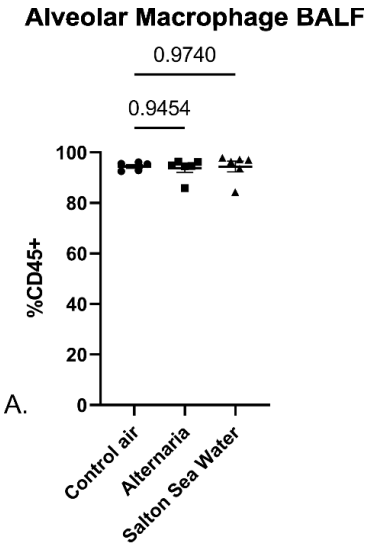
Alveolar Macrophage BALF
0.9740
0.9454
%CD45+
100
80
60
40
20
0
A.
Control air
Alternaria
Salton Sea Water

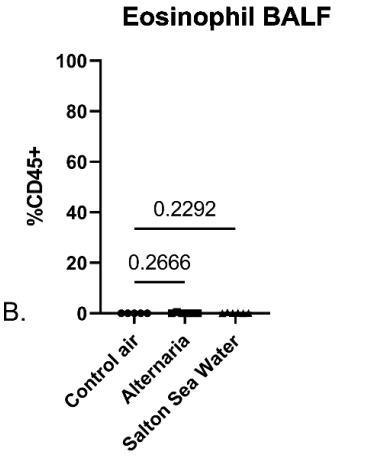
Eosinophil BALF
%CD45+
100
80
60
40
20
0
0.2292
0.2666
B.
Control air
Alternaria
Salton Sea Water

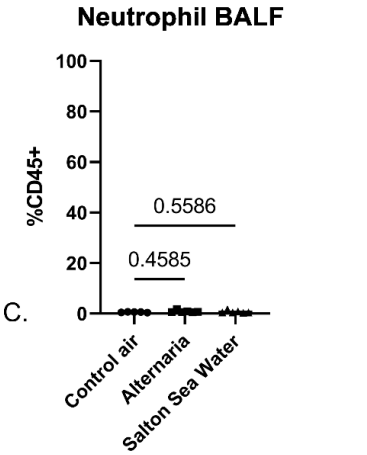
Neutrophil BALF
%CD45+
100
80
60
40
20
0
0.5586
0.4585
C.
Control air
Alternaria
Salton Sea Water

Figure 3.1 - Inflammatory cell recruitment in bronchoalveolar lavage fluid (BALF) of control air, Alternaria exposed, and Salton Sea Water pretreated mice

Control air mice (n = 5) were exposed to filtered house air for two 7-day exposures. Alternaria (n = 6) mice were exposed to filtered house air for 7 days followed by exposure to 150 μg/m^3 of aerosolized *Alternaria alternata* and *Alternaria tenuis* for 7 days. Salton Sea Water (n = 6) mice were exposed to 1500 μg/m^3 of filtered and aerosolized Salton Sea Water for 7 days followed by exposure to 150 μg/m^3 of aerosolized *Alternaria alternata* and *Alternaria tenuis* for 7 days. Number shown were determined by flow cytometry analysis and graphed as percentage of $CD45^+$ cells in the BALF. Cells stained positive with the Zombie Yellow Live/Dead stain were excluded from further analysis. P-values were determined by using a one-way ANOVA with Holm-Šídák's multiple comparisons test. (A) Alveolar macrophages were defined as $CD45^+CD11c^+SiglecF^+$. (B) Eosinophils were defined as $CD45^+CD11c^-CD11b^+SiglecF^+$. (C) Neutrophils were defined as $CD45^+CD11b^+Ly6G^+$. Average ± the standard error. Exact P-values shown.

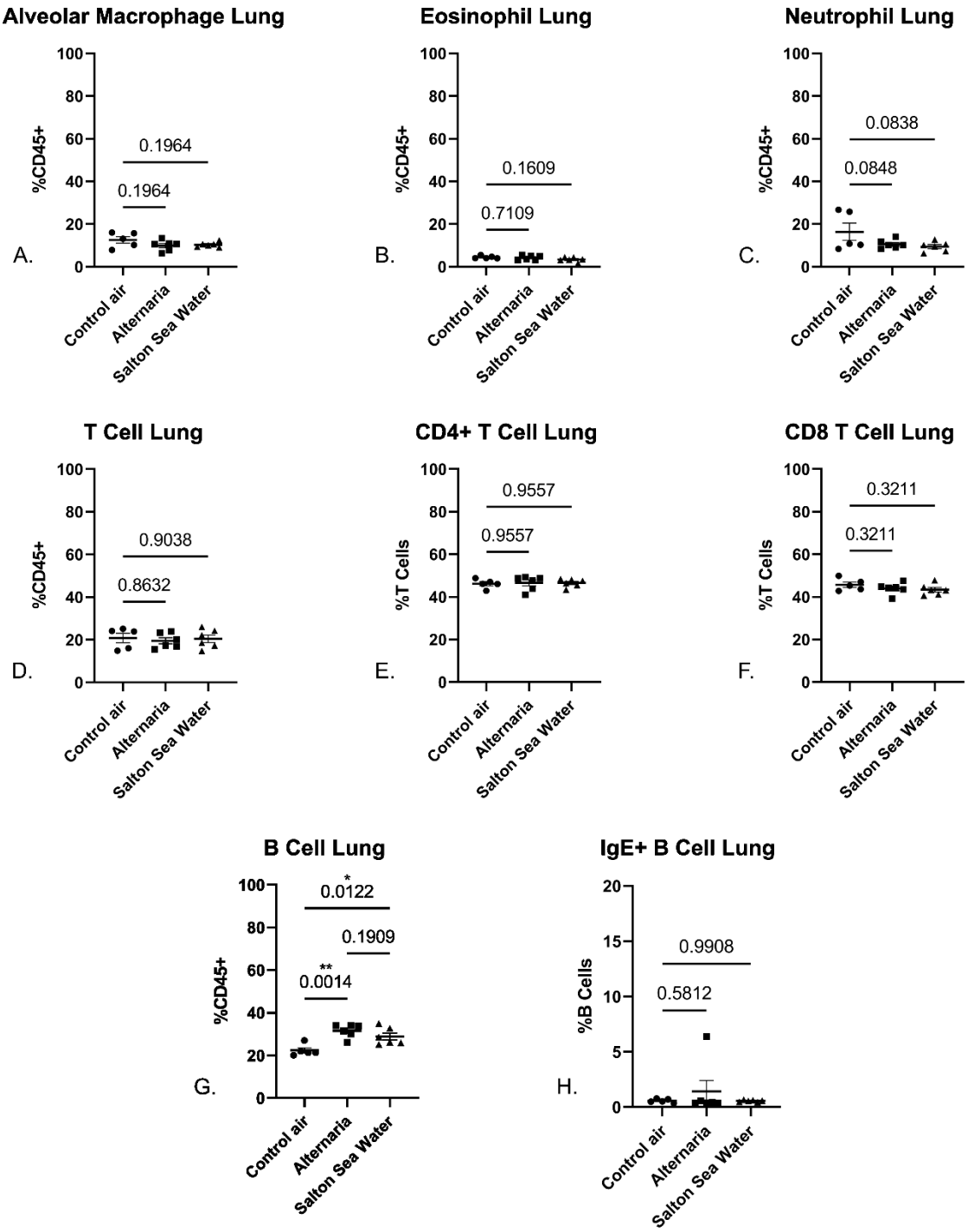
Alveolar Macrophage Lung
%CD45+
0.1964
0.1964
A.
Control air
Alternaria
Salton Sea Water
Eosinophil Lung
%CD45+
0.1609
0.7109
B.
Neutrophil Lung
%CD45+
0.0838
0.0848
C.
T Cell Lung
%CD45+
0.9038
0.8632
D.
CD4+ T Cell Lung
%T Cells
0.9557
0.9557
E.
CD8 T Cell Lung
%T Cells
0.3211
0.3211
F.
B Cell Lung
%CD45+
*
0.0122
0.1909
**
0.0014
G.
IgE+ B Cell Lung
%B Cells
0.9908
0.5812
H.

Figure 3.2 - Inflammatory cell recruitment in digested lung tissue of control air, Alternaria exposed, and Salton Sea Water pretreated mice

Control air mice (n = 5) were exposed to filtered house air for two 7-day exposures. Alternaria (n = 6) mice were exposed to filtered house air for 7 days followed by exposure to 150 μg/m^3 of aerosolized *Alternaria alternata* and *Alternaria tenuis* for 7 days. Salton Sea Water (n = 6) mice were exposed to 1500 μg/m^3 of filtered and aerosolized Salton Sea Water for 7 days followed by exposure to 150 μg/m^3 of aerosolized *Alternaria alternata* and *Alternaria tenuis* for 7 days. Alternaria and Salton Sea Water groups had an even distribution of male and female mice. Control air had 2 male and 3 female mice. Left lung lobes were digested prior to staining. Number shown were determined by flow cytometry analysis and graphed as percentage of $CD45^+$ cells in the lung tissue unless otherwise stated. Cells stained positive with the Zombie Yellow Live/Dead stain were excluded from further analysis. P-values were determined by using a one-way ANOVA with Holm-Šídák's multiple comparisons test. (A) Alveolar macrophages were defined as $CD45^+CD11c^+SiglecF^+$. (B) Eosinophils were defined as $CD45^+CD11c^-CD11b^+SiglecF^+$. (C) Neutrophils were defined as $CD45^+CD11b^+Ly6G^+$. (D) T cells were defined as $CD45^+CD3^+SSC^{low}$. (E-F). $CD4^+$ and $CD8^+$ were determined by the presence of CD4 or CD8 on T cells. Numbers shown are percentage of T cells. (G) B cells were defined as $CD45^+CD19^+SSC^{low}$. (H) IgE^+ B cells were determined by presence of IgE on B cells. Average ± the standard error. Exact P-values shown.

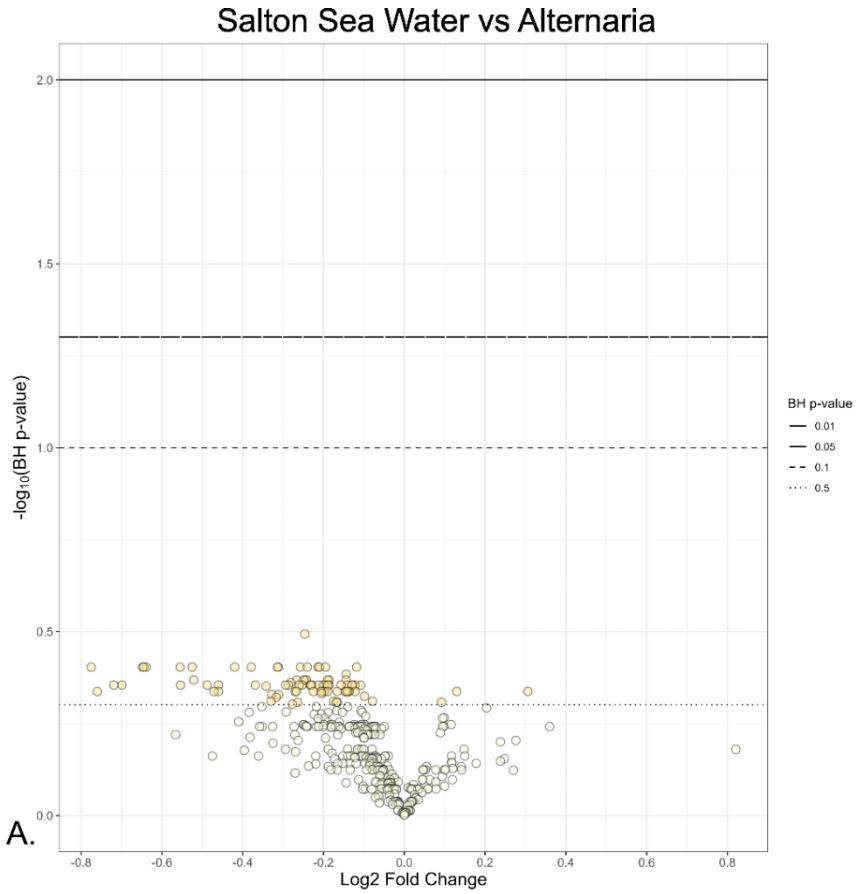
Salton Sea Water vs Alternaria
A.
-log10(BH p-value)
Log2 Fold Change
BH p-value
0.01
0.05
0.1
0.5

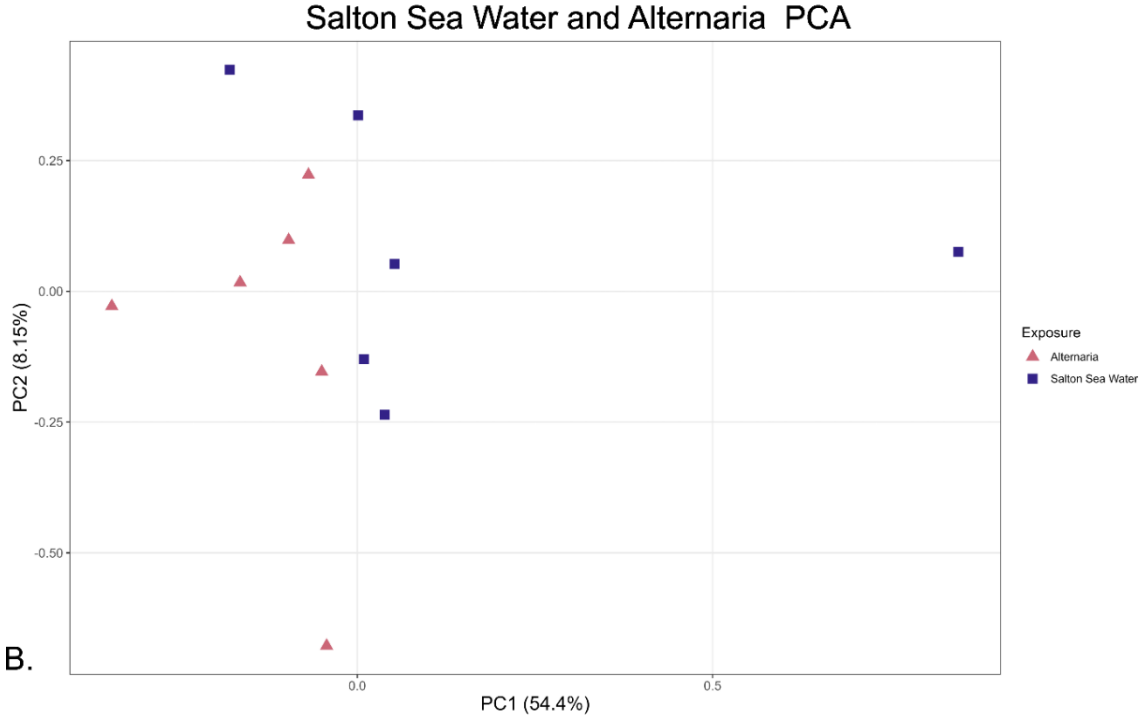
Salton Sea Water and Alternaria PCA
B.
PC2 (8.15%)
PC1 (54.4%)
Exposure
Alternaria
Salton Sea Water

Figure 3.3 - Gene expression analysis comparing Alternaria exposed and Salton Sea Water pretreated groups

RNA was extracted from right lung lobes. Alternaria (n = 6) mice were exposed to filtered house air for 7 days followed by exposure to 150 μg/m^3 of aerosolized *Alternaria alternata* and *Alternaria tenuis* for 7 days. Salton Sea Water (n = 6) mice were exposed to 1500 μg/m^3 of filtered and aerosolized Salton Sea Water for 7 days followed by exposure to 150 μg/m^3 of aerosolized *Alternaria alternata* and *Alternaria tenuis* for 7 days. Each group has an even distribution of male and female mice RNA expression was determined by a NanoString Sprint Profiler using the Mouse Immunology Panel. Differential expression was calculated using the nSolver Advanced Analysis 2.0 software and compared the Salton Sea Water group compared to a baseline of Alternaria. P-values were adjusted using the Benjamini-Hochberg method. PCA was generated using the “prcomp” function built into R 4.2.2 using normalized log2 gene counts calculated using nSolver 4.0. Data was visualized using *ggplot2* for the differential expression data and *ggfortify* for the PCA data. (A) Volcano plot showing the differential expression between the Salton Sea Water and Alternaria Groups. (B) PCA plot showing the difference in overall gene expression between Salton Sea Water and Alternaria mice.

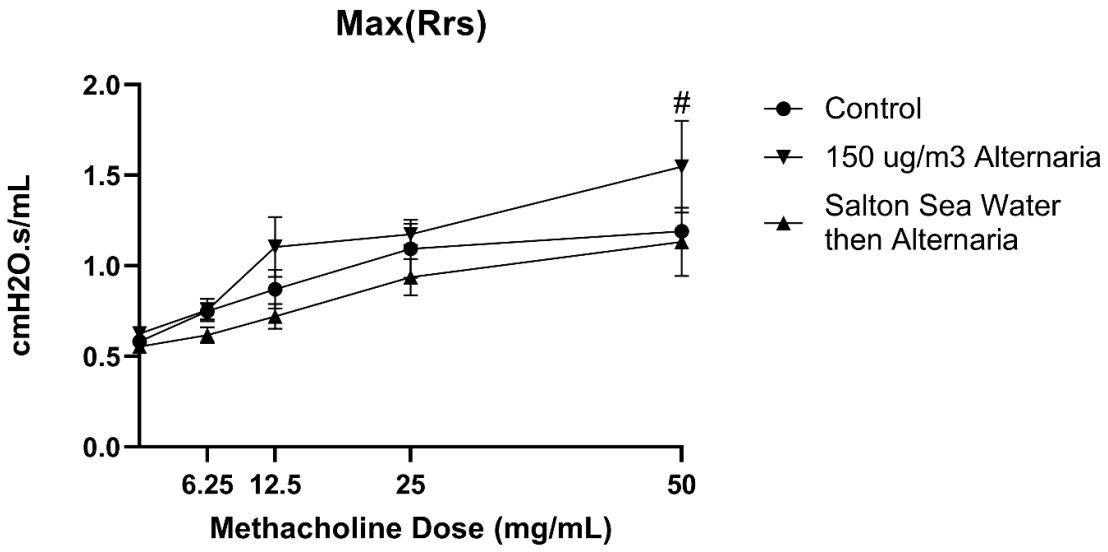

Figure 3.4 - Changes in airway hyperreactivity between the control air, Alternaria exposed, and Salton Sea Water pretreated mice

All mice shown are male. Control air mice (n = 2) were exposed to filtered house air for two 7-day exposures. Alternaria (n = 3) mice were exposed to filtered house air for 7 days followed by exposure to 150 μg/m^3 of aerosolized *Alternaria alternata* and *Alternaria tenuis* for 7 days. Salton Sea Water (n = 3) mice were exposed to 1500 μg/m^3 of filtered and aerosolized Salton Sea Water for 7 days followed by exposure to 150 μg/m^3 of aerosolized *Alternaria alternata* and *Alternaria tenuis* for 7 days. Measurements were collected using a FlexiVent and the dose-response script. Measurements shown are the max airway resistance after exposure to the given dose of methacholine. Points shown are the average with ± the standard error. P-values were calculated using a two-way ANOVA with Tukey's multiple comparison test. # p-value < 0.05 between Alternaria and Salton Sea Water groups.

Chapter 4: Aerosolized Aqueous Dust Extracts Collected Near a Drying Lake Trigger Acute Neutrophilic Pulmonary Inflammation Reminiscent of Microbial Innate Immune Ligands

Trevor A. Biddle[1,4], Keziyah Yisrael[1,4], Ryan Drover[2,3], Qi Li[2,3], Mia R. Maltz[1,4,5], Talyssa M. Topacio[6], Jasmine Yu[7], Diana Del Castillo[1], Daniel Gonzales[2,3], Hannah L. Freund[6], Mark P. Swenson[6], Malia L. Shapiro[1], Jon K. Botthoff[8], Emma Aronson[6], David R. Cocker III[2,3], David D. Lo[1,4,5,*]

*Corresponding Author: David D. Lo; Postal Address: 900 University Ave, Riverside, CA 92521; Email: david.lo@medsch.ucr.edu

Abstract

Background: A high incidence of asthma is prevalent among residents near the Salton Sea, a large inland terminal lake in southern California. This arid region has high levels of ambient particulate matter (PM); yet while high PM levels are often associated with asthma in many environments, it is possible that

[1]: Division of Biomedical Sciences, University of California, Riverside School of Medicine, Riverside, California, USA
[2]: Department of Chemical and Environmental Engineering, University of California, Riverside, Riverside, California, USA
[3]: College of Engineering-Center for Environmental Research and Technology (CE-CERT), University of California, Riverside, Riverside, California, USA
[4]: BREATHE Center, University of California, Riverside, Riverside, California, USA
[5]: Center for Health Disparities Research, University of California, Riverside, Riverside, California, USA
[6]: Department of Microbiology, University of California, Riverside, Riverside, California, USA
[7]: School of Medicine, University of California, Riverside, Riverside, California, USA
[8]: Center for Conservation Biology, University of California, Riverside, Riverside, California, USA

the rapidly retreating lake, and exposed playa or lakebed, may contribute components with a specific role in promoting asthma symptoms.

Objectives: Our hypothesis is that asthma may be higher in residents closest to the Salton Sea due to chronic exposures to playa dust. Playa emissions may be concentrating dissolved material from the lake, with microbial components capable of inducing pulmonary innate immune responses. To test this hypothesis, we used a mouse model of aerosol exposures to assess the effects of playa dust.

Methods: From dust collected around the Salton Sea region, aqueous extracts were used to generate aerosols, which were injected into an environmental chamber for mouse exposure studies. We compared the effects of exposure to Salton Sea aerosols, as well as to known immunostimulatory reference materials. Acute 48-hour and chronic 7-day exposures were compared, with lungs analyzed for inflammatory cell recruitment and gene expression.

Results: Dust from sites nearest to the Salton Sea triggered lung neutrophil inflammation that was stronger at 48-hours but reduced at 7-days. This acute inflammatory profile and kinetics resembled the response to innate immune ligands LTA and LPS while distinct from the classic allergic response to *Alternaria*.

Conclusion: Lung inflammatory responses to Salton Sea dusts are similar to acute innate immune responses, raising the possibility that microbial components are entrained in the dust, promoting inflammation. This effect highlights the health risks at drying terminal lakes from inflammatory components in dust emissions from exposed lakebed.

Introduction

The Salton Sea, a 345 mi^2 body of water located in California's Coachella Valley and Imperial Valley, is a site of frequent high levels of dust. Already designated a nonattainment area for particulate matter smaller than 10 μm in aerosol diameter (PM_{10}) and particulate matter under 2.5 μm in aerosol diameter ($PM_{2.5}$), (Environmental Protection Agency, 2022) dust in the region may soon worsen. Due to increasing temperatures and ongoing drought conditions, along with a 2003 ordinance shifting water away from the Sea, it has been estimated that 105,000 acres of additional playa will be exposed between 2003-2045 (Evan, 2019), with the shoreline having retreated substantially between 1985-2020 (Fig. 4.1). Exposed playa has been linked to higher levels of dust in general (Reheis, 1997; Reynolds et al., 2007; Bullard et al., 2008; Hossein Mardi et al., 2018), and, in particular, the dust in the Salton Sea Basin is estimated to increase by 11% between 2018-2030 (Parajuli and Zender, 2018) with changes in composition due to playa emissions (Frie et al., 2017).

Along with high levels of dust, the communities surrounding the Salton Sea have high levels of childhood asthma. Currently, the asthma rate among children is estimated at 20%-22.4%, which is among the highest in the state of California, and noticeably higher than the state average of 14.5% (Farzan et al., 2019). Additionally, the communities surrounding the Salton Sea are among the top percentile for emergency room visits due to asthma (California Environmental Protection Agency and Office of Environmental Health Hazard Assessment, 2021), though whether this is due to more severe asthma, lack of access to healthcare, high asthma rates, or a combination thereof is currently unknown.

Worryingly little is known about how the dust in the Salton Sea Basin may contribute to asthma and pulmonary disease. Asthma is generally defined as a disease of airway restriction, with an increase in airway hyperreactivity due to an allergen, along with immunoglobulin E (IgE) production, Th2 cytokine secretion and eosinophil recruitment (Bousquet et al., 2000). Typically, asthma development is associated with childhood exposure to aeroallergens, which leads to the development of allergies (Simpson et al., 2010; Stoltz et al., 2013; Anderson and Jackson, 2017). However, the exact mechanism for asthma development remain elusive, with risk factors including microbial exposure (Ege et al., 2011; Lynch et al., 2014; Stein et al., 2016), genetic predisposition (Chang et al., 2012), and childhood viral and bacterial infections (Jackson et al., 2008; James et al., 2013). Other pulmonary diseases such as acute lung injury (ALI) instead preferentially recruit neutrophils (Blázquez-Prieto et al., 2018). Large dust

storms, such as those in East Asia, have been linked to increased prevalence of respiratory diseases such as asthma (Kwon et al., 2002; Chen et al., 2004; Watanabe et al., 2011), while organic dust from enclosed swine facilities has been shown to cause neutrophilic inflammation and oxidative stress (Poole and Romberger, 2012). Thus, dust can cause a variety of pulmonary disease; however, it is unclear how Salton Sea dust may be contributing, especially in a location which serves as a reservoir for agricultural runoff. Contaminants such as pesticides, herbicides, heavy metals, along with microbial toxins, have been found in the Salton Sea (Carmichael and Li, 2006; Xu et al., 2016; Zhou et al., 2017). We previously showed that aerosolized Salton Sea water is capable of inducing gene expression changes indicating a mild inflammatory genotype without overt inflammatory cell recruitment (Biddle et al., 2021). However, in that paper we had not examined the potential contributions of dust in pulmonary disease.

While there have been previous studies examining the toxic effects of dust from the Salton Sea Basin, these studies relied on a single collected site and either an *in vitro* model (D'Evelyn et al., 2021), or intranasal administration of whole dust without a control dust site (Burr et al., 2021). As our study used an environmental exposure chamber to examine the potentially harmful effects of dust from multiple sites, including a desert dust control site, using an *in vivo* model while mimicking natural inhalation, we believe it offers a more robust and

accurate look at dust as a source of pulmonary inflammation around the Salton Sea.

To understand the type of pulmonary inflammation caused by Salton Sea dust extracts, we used the aforementioned environmental exposure chamber, flow cytometry, and whole lung tissue gene expression. The inflammatory cell recruitment to the airways and lung tissue, along with changes in gene expression, were analyzed at either a 48-hour or 7-day timepoint. Dust exposed mouse samples were compared to well established acute, innate inflammatory agents lipoteichoic acid (LTA), lipopolysaccharide (LPS), and the chronic, adaptive inflammatory allergen *Alternaria* to determine where the dust extracts fall along these axes.

Methods

Sample Collection

At each of four sites, we collected dust using passive collectors; our collectors consisted of a modified round bundt pan (Nordic Ware, Minneapolis, MN, USA) coated with Teflon (25.4 cm in diameter), which was lined with Kevlar mesh (Industrial Netting, Maple Grove, MN, USA), as described in Aciego et al. (Aciego et al., 2017) and Maltz et al. (Maltz et al., 2022). Glass marbles were suspended from the bottom and rested atop the mesh within the pan. Pans were fitted with overarching cross-braced strapping, which was covered in bird repellent (Bird-X, Elmhurst, IL, USA) to deter bird visitation or roosting. All pans,

marbles, and mesh were acid washed in 2 M HCl, with rinses of 18.2 M Ω water between each reagent cleaning step, prior to deployment or contact with any dust. We deployed each of our collectors atop wooden posts, 2 m above ground level, within open canopy locations at each field site; this minimized the contribution of local dust inputs from nearby vegetation and local saltation.

On August 14th, 2020, we deployed these passive dust collectors at the “Boyd Deep” site, located in the Boyd Deep Canyon Reserve of the University of California (20 miles from the northwest border of the Salton Sea shoreline; see Table 4.1). On August 30th, 2020, dust collectors were deployed at the “Sonny Bono” site, Sonny Bono Salton Sea National Wildlife Refuge, the “Wister” site, in the Wister Unit of the Imperial Wildlife Area, and the “Dos Palmas” site, in the Dos Palmas Preserve of the Bureau of Land Management. There was a second deployment at the “Wister” site starting on September 18th, 2021. These three sites are located at distances of 0.6, 2.0, and 4.0 miles from the nearest border of the Salton Sea lakebed, respectively (Table 4.1; Fig. 4. 4.1). After 81 days (for 2021 Wister dust), 55 days (for Boyd Deep Canyon dust), or 41 days (for Sonny Bono, 2020 Wister, Dos Palmas dust) these dust collectors were taken down, sealed in sterile Whirl-pak collection bags (Nasco, Madison, WI, USA), and transported to the University of California Riverside for further processing. The sampling duration varied due to environmental conditions preventing access to remote areas, and other factors. The Boyd Deep Canyon Site was chosen as a control site as the mountain range protected the site from winds blowing over the

Salton Sea. The Sonny Bono, Wister, and Dos Palmas sites were chosen based to give an idea of the dust over several geographic sites and based on availability of government permits and government lands on which to add the passive dust collectors.

To sample playa, we used sterilized putty knives and flat spatulas to scrape the top layer (3.0 - 5.0 mm) of playa from the muddy exposed surface at 1.0 m - 2.0 m distances from the Salton Sea shoreline at Corvina Beach. From a 0.25 m^2 plot, we slid large flat sterilized spatulas into playa material to sever the top layer of playa from the underlying sediment. We used the sterile putty knife to scrape this playa material into sterile Whirl-pak collection bags. Playa samples were frozen prior to subsequent transport and processing at the University of California Riverside.

Sample Processing

To recover and archive dust samples from collectors across each of these date ranges, we used 18.2 M Ω water to extract the dust. We rinsed the marbles, mesh, and inner pan from each collector, using sterilized gloves to dislodge dust from these surfaces into the water suspension; we then removed the mesh and marbles and transferred the remaining water and dust suspension to acid-washed 1 L bottles (Nalgene Nunc International Corporation, Rochester, NY, USA; high density polyethylene; HDPE), for further processing and subsequent analyses.

All materials used for filtration and storage of samples were sterilized by acid washing, as described above. Frozen wet playa samples were weighed to 100 g and suspended into 1 L of 18.2 M Ω water within a beaker. Playa suspensions were mixed at the lowest speed on a stir plate at ambient temperatures and then filtered through autoclaved cheese cloth. We then filtered our playa suspensions into glass funnels through autoclaved 5.0 µm filters (Millipore-Sigma, Burlington, MA, USA).

We filtered all playa and dust suspensions into glass funnels through sterile 0.2 µm filters (47-mm diameter; Pall Supor 200 Sterile Grid filters, Pall Corporation, Port Washington, New York, USA) into collecting flasks. The remaining flow-through of playa (i.e., playa filtrate) was analyzed and subsequently used for mouse chamber exposures. Dust filtrates were frozen at a 45 ° angle in Fast Freeze Flasks, prior to lyophilization on a Labconco FreeZone 2.5 L -50 °C benchtop freeze dryer (i.e., lyophilizer, Labconco Corp., Kansas City, MO, USA). Lyophilized dust filtrate was subsequently normalized by dust mass (mg) in an aqueous suspension for use in mouse chamber exposures.

Animals

All animal studies were done following the UCR institutional IACUC and NIH guidelines. Both male and female 8–9-week-old C57BL/6J mice were purchased from Jackson Labs, Sacramento and acclimated for one week in the University of California, Riverside SPF vivarium. After acclimation, mice were

placed in an environmental exposure chamber for experimentation. Mice were kept 3-4 to a cage and allowed food and water *ad libitum*. A 12-hour day/night cycle was provided. Exposure lasted for either 48-hours or 7-days. The 48-hour timepoint was chosen to reflect an acute innate response, while the 7-day timepoint was chosen as we found that *Alternaria* was capable of generating an allergic-type response by 7-days (Biddle et al., 2021).

Chamber operation

Exposure studies were performed in dual 540 L animal chambers (an exposure chamber and a control chamber) developed as described in Peng et al. (2019) and as used in Biddle et al. (2021). The relative humidity, temperature, and atmospheric pressure were measured in both chambers, with ammonia selectively measured in some exposures to ensure consistent exposure conditions were maintained. Mice in the exposure chamber were continuously fed a mixture of dry filtered air (0.5–1 lpm) and aerosolized spray (dried by two in-line silica gel columns, 3.5–4.5 lpm). The PM was generated from solutions of *Alternaria alternata* and *Alternaria tenuis* filtrate (Greer Laboratories, Lenoir, NC, USA; 0.4 g/L), lipoteichoic acid (LTA) from *Staphylococcus aureus* (Sigma Aldrich, St. Louis, USA), Lipopolysaccharide (LPS) from *Escherichia coli* O55:B5 (Sigma Aldrich, St. Louis, USA), and playa or dust collected from various sites in the region near the Salton Sea (0.025-0.100 g/L). The aerosol sources for the exposure were each tested in advance in order to determine chemical

composition (high-resolution time-of-flight aerosol mass spectrometer (HR-ToF-AMS), Aerodyne) and aerosol density (aerosol particle mass analyzer (APM), Kanomax) to prepare the solutions to yield the targeted particle mass concentration. Sample aerosolization was accomplished by using a homemade nebulizer with silica-gel dryers (Peng et al., 2019). Mice in the control chamber were given filtered dry air (5.0 lpm) only, with other conditions matching the exposure chamber, including bedding replacement, food and water supplies, and corresponding day/night cycle. Particulate matter was only monitored within the exposure chamber by a scanning mobility particle sizer (SMPS, including Series 3080 Electrostatic Classifier and Ultrafine Condensation Particle Counter 3776, TSI) to assist in maintaining stable PM concentration. The target PM concentrations were as follows: 750 μg/m^3 for the *Alternaria* mixture, 150 μg/m^3 for LTA, 1 μg/m^3 for LPS, and 1500 μg/m^3 for environmental samples. *Alternaria*, LTA, and LPS doses were set at levels that promoted inflammatory cell recruitment without an accompanying cytokine storm (data not shown). The environmental sample concentration was similar to our previous studies in Biddle et al. (2021), where 1500 μg m^{-3} of water from Salton City was capable of inducing differential gene expression in the lungs by 7-days of exposure. For each exposure (n = 6-12), we used an equal number of male and female mice. Each exposure had a control air cohort that matched the number and sex of the exposure group. Mice were kept in the chamber for either 48-hours or 7-days depending on the study.

Animal Processing

After either 48-hour or 7-days, the mice were removed from the environmental exposure chamber. They were then anesthetized using isoflurane and euthanized by cervical dislocation. Bronchoalveolar lavage fluid (BALF) was collected by flushing the lungs 3 times with 0.8 mL of PBS. Afterwards, the lungs were dissected out for digestion or RNA extraction. The right lung lobes were flash frozen in liquid nitrogen and kept at --80°C until RNA extraction. The left lobe minced into small (~1-2 mm) sections and digested using 0.5 mg/mL collagenase D (Roche Diagnostics, Mannheim, Germany) and 50 U/mL DNase I (Sigma Aldrich, St. Louis, USA) in RPMI 1640 (Gibco, Grand Island, USA) fortified with 10% heat-inactivated FB (Gibco, Grand Island, USA) preheated to 37°C. After incubating 30 minutes at 150 rpm in 37°C, the lung was agitated using an 18-gauge needle and incubate for another 15 minutes under the same conditions. Following digestion, the lung was pushed through a 100 µm cell strainer (Corning, Corning, USA). The cell strainer was then washed with RPMI 1640 with 10% heat-inactivated FBS before centrifugation and resuspension for use in flow cytometry.

Some mice were set aside for histology. After being anesthetized and euthanized, the lungs were inflated using 0.7 mL of a 1:1 OCT: PBS mixture. The whole lungs were excised, placed into OCT, and flash frozen in liquid nitrogen before being stored at -80°C until further processing

Histology

OCT embedded lungs were sectioned at 15 µm in a Cryostat. Sections were stored at -80°C until staining. Before staining with H&E, slides were fixed with 4% PFA for 10 minutes. Histological images were taken using a Keyence BZ-X710 (Keyence Corporation of America, Itasca, USA).

Flow Cytometry

BALF and post-digested lungs were centrifuged at 1500 rpm before resuspension in 100 µL of a 1:100 dilution of Zombie Yellow™ dye (Biolegend, San Diego, USA). After staining, cells were washed in FACS Buffer, centrifuged, and resuspended in 100 µL of a 1:50 dilution of Mouse BD FC block (BD Pharmigen, San Joe, USA). Cells were then stained using the following fluorescent antibodies: anti-CD45 FITC (BioLegend, San Diego, USA; Clone 30-F11), anti-CD19 Percp-Cy5.5 (eBioscience, San Diego, USA; Clone eBio1D3), anti-CD3 Alexa Fluor 700 (BioLegend, San Diego, USA; Clone 17A2) or anti-CD3 APC-Cy7 (BioLegend, San Diego, USA; Clone 17A2), anti-Ly6G BV510 (BioLegend, San Diego, USA; Clone 1A8), anti-CD11b BV421 (BioLegend, San Diego, USA; Clone M1/70), anti-CD11c PE-Cy7 (BioLegend, San Diego, USA; Clone N418) and anti-SiglecF APC (BioLegend, San Diego, USA; Clone S17007L).

Cells stained with Zombie Yellow™ dye were excluded from further analysis. Cell populations were determined using the following surface markers:

neutrophils were $CD45^+CD11b^+Ly6G^+SiglecF^-CD11c^-$, eosinophils were $CD45^+CD11b^+SiglecF^+CD11c^-$, T cells were $CD45^+CD3^+SiglecF^-CD11c^-$, and B cells were $CD45^+CD19^+SiglecF^+CD11c^-$

Samples were run on a NovoCyte Quanteon (Agilent Technologies, Santa Clara, USA). Gating and analysis were performed using FlowJo (Version 10.81, Ashland, USA).

RNA Extraction

RNA was purified from the frozen right lung lobes using a TRIzol© (Ambion, Carlsbad, USA) based method. ~100 mg of frozen lung tissue (half of the right lobe) was placed in a mortar, frozen with liquid nitrogen, and ground into dust using a pestle. After, the ground lung tissue was placed in TRIzol©. Chloroform was added, and the solution was mixed and centrifuged. The surface aqueous phase was mixed with isopropyl alcohol and centrifuged. The RNA pellet was then washed 3 times with 75% ethanol before drying at room temperature. This pellet was then resuspended in DEPC-Treated water (Ambion, Austin, USA). Concentration and purity of the RNA was checked via NanoDrop 2000 (Thermo Scientific, Carlsbad, USA).

NanoString Analysis

50 ng of purified RNA was analyzed using an nCounter® Sprint Profiler (NanoString Technologies, Seattle, USA) with the nCounter® Mouse

Immunology Panel according to manufacturer protocols. The nSolver® 4.0 software (NanoString Technologies, Seattle, USA) was used to normalize gene counts based on housekeeping genes and positive controls. Differential expression was calculated using the nSolver® Advanced Analysis 2.0 software (NanoString Technologies, Seattle, USA), and p-values were adjusted using the Benjamini-Hochberg method.

Normalized log2 gene counts and differential expression data were imported into R version 4.1.2 (R Core Team, 2022) using *readr* (Wickham et al., 2022) and *readxl* (Wicham and Bryan, 2022) and visualized using the *ggplot2* (Wickham, 2016) package and the *Khroma* (Frerebeau, 2022) package. Principal Component Analyses (Pielou,1984) were calculated using the normalized log2 gene count and the “prcomp” function. This data was visualized using the *ggforitify* (Tang et al., 2016) package. Dendrograms were generated using the average log2 gene count for each type of exposure and the built-in hclust function using the Ward.D2 method. They were visualized as an unrooted dendrogram using the *ape* (Paradis and Schliep, 2019) package.

Statistical Analysis

Statistical analysis for inflammatory cell infiltration was done using GraphPad Prism 9 (GraphPad, San Diego, USA). P-value was calculated using the Mann-Whitney U test for nonparametric data. Results shown include all mice, along with the average $\pm$ the standard error (SE). P-value for gene expression

was calculated using nSolver® 4.0 and was false discovery rate (FDR) adjusted using the Benjamini-Hochberg method. A p-value of less than 0.05 and an FDR adjusted p-value of less than 0.1 were considered significant.

Results

Pulmonary Inflammation due to Salton Sea Dust Extract Compared to a Desert Dust Extract Control

To assess the biological effects of inhalation of these dusts in the Salton Sea region, we made aqueous extracts from collected dust, filtering out inert and larger particulate material. We injected suspensions of fine aerosols (~100nm diameter) into an environmental chamber for chronic exposures of mice. In previous studies on exposure to aerosols generated from Salton Sea water ("sea spray"), the exposed lungs showed induction of sets of genes associated with low level immune activation; however, no active tissue inflammation (i.e., recruitment of inflammatory cells such as neutrophils, eosinophils, lymphocytes) was detected above background (Biddle et al., 2021). In striking contrast, in mice exposed for 7 days to aerosolized extracts from Salton Sea dust collected at the Imperial Wister Unit, there was infiltration by granulocytes around the major airways (Fig. 4.1b). Additionally, there was dramatic recruitment of neutrophils in bronchoalveolar lavage fluid (BALF) (13.9% $\pm$ 8.8% vs 0.08 $\pm$ 0.04%; Fig. 4.1c). T cells were also preferentially recruited to the airways (2.4 $\pm$ 0.7% vs 0.5 $\pm$ 0.2%; Fig. 4.1e), though B cells (Fig. 4.1f) and eosinophils (Fig. 4.1d) were not

detected above background levels. Moreover, gene expression patterns were consistent with activation of acute immune inflammation (Fig. 4.1h). The most highly expressed genes included several neutrophil chemokines (*Cxcl3*, *Cf2rb*), among other inflammatory chemokine (*Ccl6*, *Ccl9*). Additionally, several innate immune receptors (*Cd14*, *TLR2*) and inflammatory cytokine *Il1a* were upregulated in exposed mice.

For comparison, exposure to extracts of dust collected at Boyd Deep Canyon, a site in the desert distant from the prevailing winds of the Salton Sea, showed no significant inflammation in either the lung tissue (Fig. 4.1a), BALF (Fig. 4.1c,d,e,f), nor a gene expression pattern indicative of active inflammation (Fig. 4.1g). While there were some inflammatory chemokines upregulated (*Cxcl3*, *Ccl9*), they were approximately 25-50% lower than in mice exposed to extract from around the Salton Sea. Additionally, control extracts failed to elicit upregulation in innate immune receptors or cytokines.

Comparison of 48-Hour and 7-Day timepoints for Salton Sea Dust Extract and Reference microbial toxins LTA, LPS, and allergen Alternaria

Interestingly, although communities near the sea appear to suffer from a high incidence of asthma, the inflammatory response seen here did not show eosinophil recruitment nor Th2 gene regulation, which are hallmarks of allergic inflammation. This is not a limitation of the relatively short term (7d) aerosol exposure, as similar exposure to aerosols of the fungal allergen *Alternaria*

produces robust allergic inflammation within 4 to 7 days (Peng et al., 2018; Biddle et al., 2021). Second, exposures of only 48 hours induced the strongest neutrophil recruitment (63.9 ± 3.5% vs 0.1 ± 0.03% in the airways; Fig2a; 41.2 ± 10.4% vs 8.6 ± 0.6% in the digested lung tissue; Fig. 4.2c) with strong but slightly lower persistent inflammation present after 7 days of exposure (Fig. 4.2a) and no recruitment of eosinophils at either timepoint (Fig. 4.2b,d). Allergic stimuli such as *Alternaria* tend to have a stronger response at 7 days, as 48 hours does not appear to be enough to generate an adaptive response. Both neutrophilic and eosinophilic recruitment was greater at 7 days in *Alternaria* exposed mice (Fig. 4.2a,b). Thus, material from dust at the Salton Sea induced strong pulmonary inflammation, but not the allergic profile more commonly associated with clinical asthma.

The kinetics and types of inflammatory cells recruited matched conventional patterns of responses to innate immune triggers such as LPS and LTA, ligands for the innate receptors Toll-like receptor 4 (TLR4) and Toll-like receptor 2 (TLR2) respectively. These microbial components triggered strong, acute neutrophilic inflammation at 48-hours; however, over the course of chronic 7-day exposure the inflammatory response was significantly attenuated. The attenuation over the course of 7 days for Salton Sea dust extracts and innate immune triggers vs the increasing response after exposure to allergen is also shown at the gene expression level. The average log2 fold change decreased in all three exposures, from 0.476 to 0.219 for Wister extract, 0.266 to 0.177 for

LPS, and 0.243 to 0.191 for LTA but increased from 0.226 to 0.683 for *Alternaria*. By the 7-day timepoint, the Salton Sea dust extracts, LPS, and LTA had attenuated to the point that their gene expression patterns clustered closer to the mice given only filtered air while the allergic inflammation gene expression patterns in mice exposed to Alternaria were clearly distinct at 7-days (Fig. 4.2e). This tendency towards resolution is not seen in an allergic model, as the *Alternaria* response matured over the course of 7 days.

Gene Expression Comparison of Multiple Salton Sea Collection Sites

To confirm that neutrophil recruitment and innate immune activation were representative of the entire Salton Sea basin rather than specifically the Imperial Wister Unit, we exposed mice to dust extract collect from two additional sites around the Salton Sea, the Dos Palmas Preserve and Sonny Bono. As the response was higher at 48-hours for dust extract from the Imperial Wister Unit, we used this timepoint for analysis. We found that dust extract from these locations triggered neutrophil infiltration to the BALF and gene expression profiles (Fig. 4.S1) consistent with dust collected from the Imperial Wister Unit. This gene expression profile clustered with the other innate immune triggers and the Alternaria mixture before maturation into a Th2 response (Fig. 4.3a). By contrast, mice exposed to extracts of playa (dry exposed lakebed), one of the major potential sources of dust, failed to recruit significant neutrophil responses

and showed few gene expression changes (Fig. 4.S2), with only *Marco* and *Il1a* being significantly upregulated.

To better characterize the relationship between the chronic exposures, we performed a similar analysis using our 7-day exposures. We found that there was significant overlap between the control air and the Boyd Deep Canyon Dust extract exposed mice. LTA exposed mice, whom had the most significant attenuation of inflammation by 7-days, also overlapped heavily with the control air. The LPS and Wister Dust extract exposed mice were distinct from the controls, but not to the extent of the *Alternaria* exposed mice. Thus, while LPS and Wister Dust do not have a maturation of the immune response by 7-days, they appear to have not fully resolved, indicating a potential for low-level inflammation over a longer time course (Fig. 4.3b). It should be noted that LPS and Wister responses were distinct from each other, with minimal overlap. Thus, they are unlikely to be triggering inflammation through the same mechanism.

The relationship between the different exposures is summarized in the dendrograms in Fig. 4.3c and Fig. 4.3d. For the 48-hour exposures, the response to playa is at one end, with the majority of exposures on the other branch. The Wister dust has the longest branch, as it has the strongest response and is unique among the other exposures. The others are closely related, with minor separation. For the 7-day exposures, Alternaria is entirely separated from the other exposures. The control dust extract is on the opposite side from the innate immune-like responses, which all have little distinction from each other.

Discussion

The response to Salton Sea dust showed similarities to innate immune ligands LTA and LPS in the overall kinetics and patterns of gene induction. These responses started with high levels of neutrophil, but not eosinophil, recruitment to the airways before decreasing to nonexistent (LTA) or minimal (LPS) levels by 7 days of continuous exposure, along with an attenuation of inflammatory gene expression. This is wholly distinct from an adaptive immune Th2 response to the allergen Alternaria which started with a low level of neutrophil recruitment before maturing into a stronger response highlighted by high levels of neutrophils, eosinophils, and an increase in genes related to Th2 responses. As the Salton Sea dust followed the kinetics of the innate immune ligands, it appears unlikely to be triggering an adaptive response.

Yet the effects of Salton Sea dust did not strictly match reference innate ligands. Salton Sea dust triggered neutrophil recruitment that was persistent for at least 7 days, which was not the case in mice exposed to LTA. Additionally, we found upregulation of *TLR2* in our Salton Sea Dust exposed mice, but not in LTA or LPS exposed mice, indicating potential for exacerbation after dust exposure, even in the case of selective tolerance to the dust. All Salton Sea dusts induced persistent upregulation of *Il1a* through 7 days of exposure; no other 7-day exposure in our study induced significant upregulation of *Il1a*. *Il1a* has been associated with neutrophil recruitment by cigarette smoke (Botelho et al., 2011), as well as promoting inflammatory cytokine release and inhibiting fibrotic

extracellular matrix (ECM) release and healing by lung fibroblasts (Suwara et al., 2014; Osei et al., 2016). The persistent upregulation of *Il1a* could be a key culprit in the pattern of inflammation caused by chronic Salton Sea dust exposure and contribute to long term lung pathology without conforming to either microbial toxin-driven innate nor adaptive immune patterns of immunity. This is important as other innate immune triggers such as LPS tend to attenuate and provide immune tolerance (Natarajan et al., 2010), which may not be the case in Salton Sea dust exposure.

It is important to clarify that the patterns of inflammation compared in this study are similar to familiar innate immune triggers composed of microbial components (cell wall, endotoxin, etc.) that are not by themselves directly toxic, and are mediated instead through innate immune receptors such as TLR2 and TLR4. These should be viewed as rather distinct from the effects of actual microbial toxins (e.g., cyanotoxins, microbicidins, etc.), produced by a variety of microbes including both bacteria and algae. The effects of these types of toxins on lung inflammation are not within the scope of this study, and while Salton Sea water is known to have detectable levels of some cyanotoxins (Carmichael and Li, 2006), it is not known if the cyanotoxins can aerosolize and cause pulmonary inflammation nor it is known whether Salton Sea dust contains harmful concentrations of these toxins. However, studies have cited the potential impact of microbial toxins in triggering or exacerbating asthma symptoms when present in red tides (Fleming et al., 2007; Zaias et al., 2011).

In addition to the ways that Salton Sea dust may directly cause pulmonary disease, the dust may interact with allergens to modify asthma development. Exposure to LPS during allergic sensitization to ovalbumin or house dust mite can worsen Th2 asthma or shift it towards a corticosteroid resistant Th17-type asthma (Li et al., 1998; Barboza et al., 2013; Yu and Chen, 2018; Sadakane et al., 2019; Thakur et al., 2019). As Salton Sea dust triggers inflammation similar to LPS, it may work in similar ways. This would have significant implications for the communities surrounding the Salton Sea, as different forms of asthma require different treatments.

The similarity of the Salton Sea dust responses to innate immunity that can be triggered by “Pathogen-Associated Molecular Patterns” – that is, bacterial components such as endotoxin, cell wall, and other materials – raises the question of whether specific microbial species in the Salton Sea or accompanying playa dust are particularly pro-inflammatory in lungs. While a comprehensive microbiome analysis of the aeolian microbiota has yet to be published, several studies have analyzed the composition of the Salton Sea and the sediment. Proteobacteria, particularly Gammaproteobacteria and Alphaproteobacteria, make up the majority of the bacteria in the Salton Sea and in the sediment, followed by Bacteroidetes (Dillon et al., 2009; Swan et al., 2010; Hawley et al., 2014). These types of bacteria are known major contributors to LPS in the gut (d’Hennezel et al., 2017), and can be carried on dust particles over large distances (Tang et al., 2018), indicating a potential source of microbial

inflammatory substances, particularly LPS. Understanding the interplay between the water, playa and aeolian microbiota is likely critical to understanding the pulmonary inflammation due to Salton Sea Dust (Freund et al., 2022).

As our preparation method filters out whole bacteria, our results would be due to the products produced by the bacteria rather than an immune response towards the bacteria itself. The diverse bacteria and other microorganisms in the dust and playa samples we processed for these exposures produce a wide and diverse range of primary and secondary compounds. While our induced pulmonary inflammation results from dust extracts were similar to LPS, there were clear differences. Thus, while LPS may be a contributing compound to dust-driven pulmonary inflammation, it is unlikely to be the only factor.

Conclusions

In summary, our results provide insight into the pulmonary health effects of a drying terminal lake. The dust collected from around the Salton Sea was uniquely toxic when compared to desert dust collected from a location protected from the prevailing winds around the sea. While there is likely a unique ecology and contaminants to the Salton Sea Basin, we believe the more general features of the drying lake, associated aerosol dusts, and consequent health impact, has broad relevance to other regions plagued by chronic drought and drying lakes. These regions are unique as they have rapidly increasing levels of dust, which has the unique property of triggering high levels of pulmonary inflammation that

is likely to worsen the pulmonary health of already vulnerable nearby communities. By understanding the inflammation triggered by the dust, the mechanisms behind the inflammation, and how it interacts with allergens and allergic development, we may be better equipped to handle the negative health impacts of the dust and developed tailored strategies to address them.

Acknowledgments

TAB led experiments and was the primary author of the manuscript. KY, TMT, DDC and MLS helped with mouse dissections and processing. RD, QL, and DG ran and monitored environmental exposure chamber. HF, MPS, MRM collected and processed dust. JY assisted in creation of figure 1 JKB designed environmental dust collectors. EA and DRCIII helped with experimental design and processing. DDL assisted with experimental design and editing the manuscript. This research used the site and facilities of the University of California, Natural Reserve System, Philip L. Boyd Deep Canyon Desert Research Center, doi:10.21973/N3V66D.

Funding Sources

The research presented in this publication was supported by the National Institute On Minority Health And Health Disparities of the National Institutes of Health under Award Number U54MD013368. The content is solely the

responsibility of the authors and does not necessarily represent the official views of the National Institutes of Health.

References

Aciego SM, Riebe CS, Hart SC, Blakowski MA, Carey CJ, Aarons SM, Dove NC, Botthoff JK, Sims KW, Aronson EL. Dust outpaces bedrock in nutrient supply to montane forest ecosystems. Nat Commun. 2017 Mar 28;8:14800. doi: 10.1038/ncomms14800.

Anderson, Halie M.; Jackson, Daniel J.. Microbes, allergic sensitization, and the natural history of asthma. Current Opinion in Allergy and Clinical Immunology: April 2017 - Volume 17 - Issue 2 - p 116-122. doi: 10.1097/ACI.0000000000000338

Barboza, R., Câmara, N. O. S., Gomes, E., Sá-Nunes, A., Florsheim, E., Mirotti, L., Labrada, A., Alcântara-Neves, N. M., & Russo, M. (2013). Endotoxin Exposure during Sensitization to Blomia tropicalis Allergens Shifts TH2 Immunity Towards a TH17-Mediated Airway Neutrophilic Inflammation: Role of TLR4 and TLR2. *PLoS ONE*, *8*(6). https://doi.org/10.1371/journal.pone.0067115

Biddle, T. A., Li, Q., Maltz, M. R., Tandel, P. N., Chakraborty, R., Yisrael, K., Drover, R., Cocker, D. R., & Lo, D. D. (2021). Salton Sea aerosol exposure in mice induces a pulmonary response distinct from allergic inflammation. *Science of The Total Environment*, *792*, 148450. https://doi.org/10.1016/j.scitotenv.2021.148450

Blázquez-Prieto J, López-Alonso I, Huidobro C, Albaiceta GM. The Emerging Role of Neutrophils in Repair after Acute Lung Injury. Am J Respir Cell Mol Biol. 2018 Sep;59(3):289-294. doi: 10.1165/rcmb.2018-0101PS.

Botelho FM, Bauer CM, Finch D, Nikota JK, Zavitz CC, Kelly A, Lambert KN, Piper S, Foster ML, Goldring JJ, Wedzicha JA, Bassett J, Bramson J, Iwakura Y, Sleeman M, Kolbeck R, Coyle AJ, Humbles AA, Stämpfli MR. IL-1α/IL-1R1 expression in chronic obstructive pulmonary disease and mechanistic relevance to smoke-induced neutrophilia in mice. PLoS One. 2011;6(12):e28457. doi: 10.1371/journal.pone.0028457.

Bousquet J, Jeffery PK, Busse WW, Johnson M, Vignola AM. Asthma. From bronchoconstriction to airways inflammation and remodeling. Am J Respir Crit Care Med. 2000 May;161(5):1720-45. doi: 10.1164/ajrccm.161.5.9903102.

Bullard, J., Baddock, M., McTainsh, G., Leys, J., 2008. Sub-basin scale dust source geomorphology detected using MODIS. Geophysical Research Letters 35. doi:10.1029/2008GL033928

Burr, A. C., Velazquez, J. V., Ulu, A., Kamath, R., Kim, S. Y., Bilg, A. K., Najera, A., Sultan, I., Botthoff, J. K., Aronson, E., Nair, M. G., & Nordgren, T. M. (2021). Lung inflammatory response to environmental dust exposure in mice suggests a link to regional respiratory disease risk. *Journal of Inflammation Research*, *14*, 4035–4052. https://doi.org/10.2147/JIR.S320096

California Environmental Protection Agency, Office of Environmental Health Hazard Assessment, 2021, October 20. CalEnviroScreen 4.0. Retrieved from. https://oehha.ca.gov/calenviroscreen/report/calenviroscreen-40

Carmichael, W. W., & Li, R. H. (2006). Cyanobacteria toxins in the Salton Sea. *Saline Systems*, *2*, 5. https://doi.org/10.1186/1746-1448-2-5

Chen YS, Sheen PC, Chen ER, Liu YK, Wu TN, Yang CY. Effects of Asian dust storm events on daily mortality in Taipei, Taiwan. Environ Res. 2004 Jun;95(2):151-5. doi: 10.1016/j.envres.2003.08.008.

D'Evelyn, S. M., Vogel, C. F. A., Bein, K. J., Lara, B., Laing, E. A., Abarca, R. A., Zhang, Q., Li, L., Li, J., Nguyen, T. B., & Pinkerton, K. E. (2021). Differential inflammatory potential of particulate matter (PM) size fractions from imperial valley, CA. *Atmospheric Environment*, *244*(January 2020). https://doi.org/10.1016/j.atmosenv.2020.117992

d'Hennezel E, Abubucker S, Murphy LO, Cullen TW. Total Lipopolysaccharide from the Human Gut Microbiome Silences Toll-Like Receptor Signaling. mSystems. 2017 Nov 14;2(6):e00046-17. doi: 10.1128/mSystems.00046-17.

Dillon JG, McMath LM, Trout AL. Seasonal changes in bacterial diversity in the Salton Sea. Hydrobiologia. 2009. 632:49-64. https://doi.org/10.1007/s10750-009-9827-4

Ege MJ, Mayer M, Normand AC, et al. Exposure to environmental microorganisms and childhood asthma. N Engl J Med 2011; 364:701–709.

Environmental Protection Agency. (2022, August 31). *Nonattainment Areas for Criteria Pollutants (Green Book)*. https://www.epa.gov/green-book

Evan, A. T. (2019). Downslope winds and dust storms in the salton basin. *Monthly Weather Review*, *147*(7), 2387–2402. https://doi.org/10.1175/MWR-D-18-0357.1

Farzan, S. F., Razafy, M., Eckel, S. P., Olmedo, L., Bejarano, E., & Johnston, J. E. (2019). Assessment of respiratory health symptoms and asthma

in children near a drying saline lake. *International Journal of Environmental Research and Public Health*, *16*(20). https://doi.org/10.3390/ijerph16203828

Fleming, L. E., Kirkpatrick, B., Backer, L. C., Bean, J. A., Wanner, A., Reich, A., Zaias, J., Cheng, Y. S., Pierce, R., Naar, J., Abraham, W. M., & Baden, D. G. (2007). Aerosolized red-tide toxins (brevetoxins) and asthma. *Chest*, *131*(1), 187–194. https://doi.org/10.1378/chest.06-1830

Frerebeau N (2022). *khroma: Colour Schemes for Scientific Data Visualization*. Université Bordeaux Montaigne, Pessac, France. doi:10.5281/zenodo.1472077, R package version 1.9.0, https://packages.tesselle.org/khroma/.

Freund* H, Maltz* M, Swenson M, Topacio T, Montellano V, Porter W, Aronson E. 2022. Microbiome interactions and their ecological implications at the Salton Sea. Calif Agr 76(1):16-26. https://doi.org/10.3733/ca.2022a0002.

Frie, A. L., Dingle, J. H., Ying, S. C., & Bahreini, R. (2017). The Effect of a Receding Saline Lake (The Salton Sea) on Airborne Particulate Matter Composition. *Environmental Science and Technology*, *51*(15), 8283–8292. https://doi.org/10.1021/acs.est.7b01773

Hawley ER, Schackwitz W, Hess M. Metagenomic sequencing of two Salton Sea microbiomes. Genome Announc. 2014. 2:2010-1. https://doi.org/10.1128/genomeA.01208-13

Hossein Mardi, A., Khaghani, A., MacDonald, A. B., Nguyen, P., Karimi, N., Heidary, P., Karimi, N., Saemian, P., Sehatkashani, S., Tajrishy, M., & Sorooshian, A. (2018). The Lake Urmia environmental disaster in Iran: A look at aerosol pollution. *The Science of the total environment*, *633*, 42–49. https://doi.org/10.1016/j.scitotenv.2018.03.148.

Jackson DJ, Gangnon RE, Evans MD, et al. Wheezing rhinovirus illnesses in early life predict asthma development in high-risk children. Am J Respir Crit Care Med 2008; 178:667–672.

James KM, Gebretsadik T, Escobar GJ, et al. Risk of childhood asthma following infant bronchiolitis during the respiratory syncytial virus season. J Allergy Clin Immunol 2013; 132:227–229.

Jen-Chieh Chang, Lin Wang, Rong-Fu Chen, Chieh-An Liu, "Perinatal Gene-Gene and Gene-Environment Interactions on IgE Production and Asthma Development", Journal of Immunology Research, vol. 2012, Article ID 270869, 9 pages, 2012. https://doi.org/10.1155/2012/270869

Kwon, H. J., Cho, S. H., Chun, Y., Lagarde, F., & Pershagen, G. (2002). Effects of the Asian dust events on daily mortality in Seoul, Korea. *Environmental Research*, *90*(1), 1–5. https://doi.org/10.1006/enrs.2002.4377

Li, L., Xia, Y., Nguyen, A., Feng, L., & Lo, D. (1998). Th2-induced eotaxin expression and eosinophilia coexist with Th1 responses at the effector stage of lung inflammation. *Journal of Immunology (Baltimore, Md. : 1950)*, *161*(6), 3128–3135. http://www.ncbi.nlm.nih.gov/pubmed/9743380

Lynch SV, Wood RA, Boushey H, et al. Effects of early-life exposure to allergens and bacteria on recurrent wheeze and atopy in urban children. J Allergy Clin Immunol 2014; 134:593–601.

Maltz, M. R., Carey, C. J., Freund, H. L., Botthoff, J. K., Hart, S. C., Stajich, J. E., Aarons, S. M., Aciego, S. M., & Meyer, K. M. (2022). *Landscape Topography and Regional Drought Alters Dust Microbiomes in the Sierra Nevada of California*. *13*(June), 1–19. https://doi.org/10.3389/fmicb.2022.856454

Natarajan S, Kim J, Remick DG. Chronic pulmonary LPS tolerance induces selective immunosuppression while maintaining the neutrophilic response. Shock. 2010 Feb;33(2):162-9. doi: 10.1097/SHK.0b013e3181aa9690.

Osei, E. T., Noordhoek, J. A., Hackett, T. L., Spanjer, A. I. R., Postma, D. S., Timens, W., Brandsma, C.-A., & Heijink, I. H. (2016). Interleukin-1α drives the dysfunctional cross-talk of the airway epithelium and lung fibroblasts in COPD. *European Respiratory Journal*, *48*(2), 359 LP – 369. https://doi.org/10.1183/13993003.01911-2015

Paradis E, Schliep K (2019). “ape 5.0: an environment for modern phylogenetics and evolutionary analyses in R.” *Bioinformatics*, **35**, 526-528.

Parajuli, S. P., & Zender, C. S. (2018). Projected changes in dust emissions and regional air quality due to the shrinking Salton Sea. *Aeolian Research*, *33*(June), 82–92. https://doi.org/10.1016/j.aeolia.2018.05.004

Peng, X., Madany, A. M., Jang, J. C., Valdez, J. M., Rivas, Z., Burr, A. C., Grinberg, Y. Y., Nordgren, T. M., Nair, M. G., Cocker, D., Carson, M. J., & Lo, D. D. (2018). Continuous Inhalation Exposure to Fungal Allergen Particulates Induces Lung Inflammation While Reducing Innate Immune Molecule Expression in the Brainstem. *ASN Neuro*, *10*, 175909141878230. https://doi.org/10.1177/1759091418782304

Peng, X., Maltz, M. R., Botthoff, J. K., Aronson, E. L., Nordgren, T. M., Lo, D. D., & Cocker, D. R. (2019). Establishment and characterization of a multi-

purpose large animal exposure chamber for investigating health effects. *Review of Scientific Instruments*, *90*(3), 1–7. https://doi.org/10.1063/1.5042097

Pielou, E.C. (1984) The Interpretation of Ecological Data: A Primer on Classification and Ordination. J. Wiley and Sons, New York.

Poole, J. A., & Romberger, D. J. (2012). Immunological and inflammatory responses to organic dust in agriculture. *Current Opinion in Allergy and Clinical Immunology*, *12*(2), 126–132. https://doi.org/10.1097/ACI.0b013e3283511d0e

R Core Team. (2022). *R: A Language and Environment for Statistical Computing*. Vienna, Austria. Retrieved from https://www.R-project.org/

Reheis, M. C. (1997), Dust deposition downwind of Owens (dry) Lake, 1991–1994: Preliminary findings, *J. Geophys. Res.*, 102(D22), 25999– 26008, doi:10.1029/97JD01967.

Reynolds, R.L., Yount, J.C., Reheis, M., Goldstein, H., Chavez, P., Jr., Fulton, R., Whitney, J., Fuller, C. and Forester, R.M. (2007), Dust emission from wet and dry playas in the Mojave Desert, USA. Earth Surf. Process. Landforms, 32: 1811-1827. https://doi.org/10.1002/esp.1515

Sadakane, K., Ichinose, T., & Nishikawa, M. (2019). Effects of co-exposure of lipopolysaccharide and β-glucan (Zymosan A) in exacerbating murine allergic asthma associated with Asian sand dust. *Journal of Applied Toxicology*, *39*(4), 672–684. https://doi.org/10.1002/jat.3759

Simpson A, Tan VY, Winn J, et al. Beyond atopy: multiple patterns of sensitization in relation to asthma in a birth cohort study. Am J Respir Crit Care Med 2010; 181:1200–1206.

Stein MM, Hrusch CL, Gozdz J, et al. Innate immunity and asthma risk in Amish and Hutterite farm children. N Engl J Med 2016; 375:411–421

Stoltz DJ, Jackson DJ, Evans MD, et al. Specific patterns of allergic sensitization in early childhood and asthma & rhinitis risk. Clin Exp Allergy 2013; 43:233–241.

Suwara, M., Green, N., Borthwick, L. *et al.* IL-1α released from damaged epithelial cells is sufficient and essential to trigger inflammatory responses in human lung fibroblasts. *Mucosal Immunol* **7**, 684–693 (2014). https://doi.org/10.1038/mi.2013.87

Swan BK, Ehrhardt CJ, Reifel KM, et al. Archaeal and bacterial communities respond differently to environmental gradients in anoxic sediments

of a California hypersaline lake, the Salton Sea. Appl Environ Microbiol. 2010. 76:757-68. https://doi.org/10.1128/aem.02409-09

Tang Y, Horikoshi M, Li W (2016). “ggfortify: Unified Interface to Visualize Statistical Result of Popular R Packages.” *The R Journal*, **8**(2), 474–485. doi: 10.32614/RJ-2016-060, https://doi.org/10.32614/RJ-2016-060.

Tang, K., Huang, Z., Huang, J., Maki, T., Zhang, S., Shimizu, A., Ma, X., Shi, J., Bi, J., Zhou, T., Wang, G., and Zhang, L.: Characterization of atmospheric bioaerosols along the transport pathway of Asian dust during the Dust-Bioaerosol 2016 Campaign, Atmos. Chem. Phys., 18, 7131–7148, https://doi.org/10.5194/acp-18-7131-2018, 2018.

Thakur, V. R., Khuman, V., Beladiya, J. V., Chaudagar, K. K., & Mehta, A. A. (2019). An experimental model of asthma in rats using ovalbumin and lipopolysaccharide allergens. *Heliyon*, *5*(11), e02864. https://doi.org/10.1016/j.heliyon.2019.e02864

Watanabe, M., Yamasaki, A., Burioka, N., Kurai, J., Yoneda, K., Yoshida, A., Igishi, T., Fukuoka, Y., Nakamoto, M., Takeuchi, H., Suyama, H., Tatsukawa, T., Chikumi, H., Matsumoto, S., Sako, T., Hasegawa, Y., Okazaki, R., Horasaki, K., & Shimizu, E. (2011). Correlation between Asian dust storms and worsening asthma in Western Japan. *Allergology International*, *60*(3), 267–275. https://doi.org/10.2332/allergolint.10-OA-0239

Wickham H (2016). *ggplot2: Elegant Graphics for Data Analysis*. Springer-Verlag New York. ISBN 978-3-319-24277-4, https://ggplot2.tidyverse.org.

Wickham H, Bryan J (2022). *readxl: Read Excel Files*. https://readxl.tidyverse.org, https://github.com/tidyverse/readxl.

Wickham H, Hester J, Bryan J (2022). *readr: Read Rectangular Text Data*. https://readr.tidyverse.org, https://github.com/tidyverse/readr.

Xu, E. G., Bui, C., Lamerdin, C., & Schlenk, D. (2016). Spatial and temporal assessment of environmental contaminants in water, sediments and fish of the Salton Sea and its two primary tributaries, California, USA, from 2002 to 2012. *Science of the Total Environment*, *559*, 130–140. https://doi.org/10.1016/j.scitotenv.2016.03.144

Yu, Q. L., & Chen, Z. (2018). Establishment of different experimental asthma models in mice. *Experimental and Therapeutic Medicine*, *15*(3), 2492–2498. https://doi.org/10.3892/etm.2018.5721

Zaias, J., Fleming, L. E., Baden, D. G., & Abraham, W. M. (2011). Repeated exposure to aerosolized brevetoxin-3 induces prolonged airway hyperresponsiveness and lung inflammation in sheep. *Inhalation Toxicology*, *23*(4), 205–211. https://doi.org/10.3109/08958378.2011.558936

Zhou, C., Huang, J. C., Liu, F., He, S., & Zhou, W. (2017). Effects of selenite on Microcystis aeruginosa: Growth, microcystin production and its relationship to toxicity under hypersalinity and copper sulfate stresses. *Environmental Pollution*, *223*, 535–544. https://doi.org/10.1016/j.envpol.2017.01.056

Figures

Figure 4.1 - Collection Sites and Changes in Exposed Playa Over Time

Map showing the 3 dust collection sites (Wister, Dos Palmas, Sonny Bono) from around the Salton Sea, along with the desert dust control collection site (Boyd Deep Canyon), playa collection site (Corvina Beach), and water collection site from Biddle et al., 2021 (Salton City). Map also shows the change in playa exposure between 1985-2020 due to evaporation of the Salton Sea.

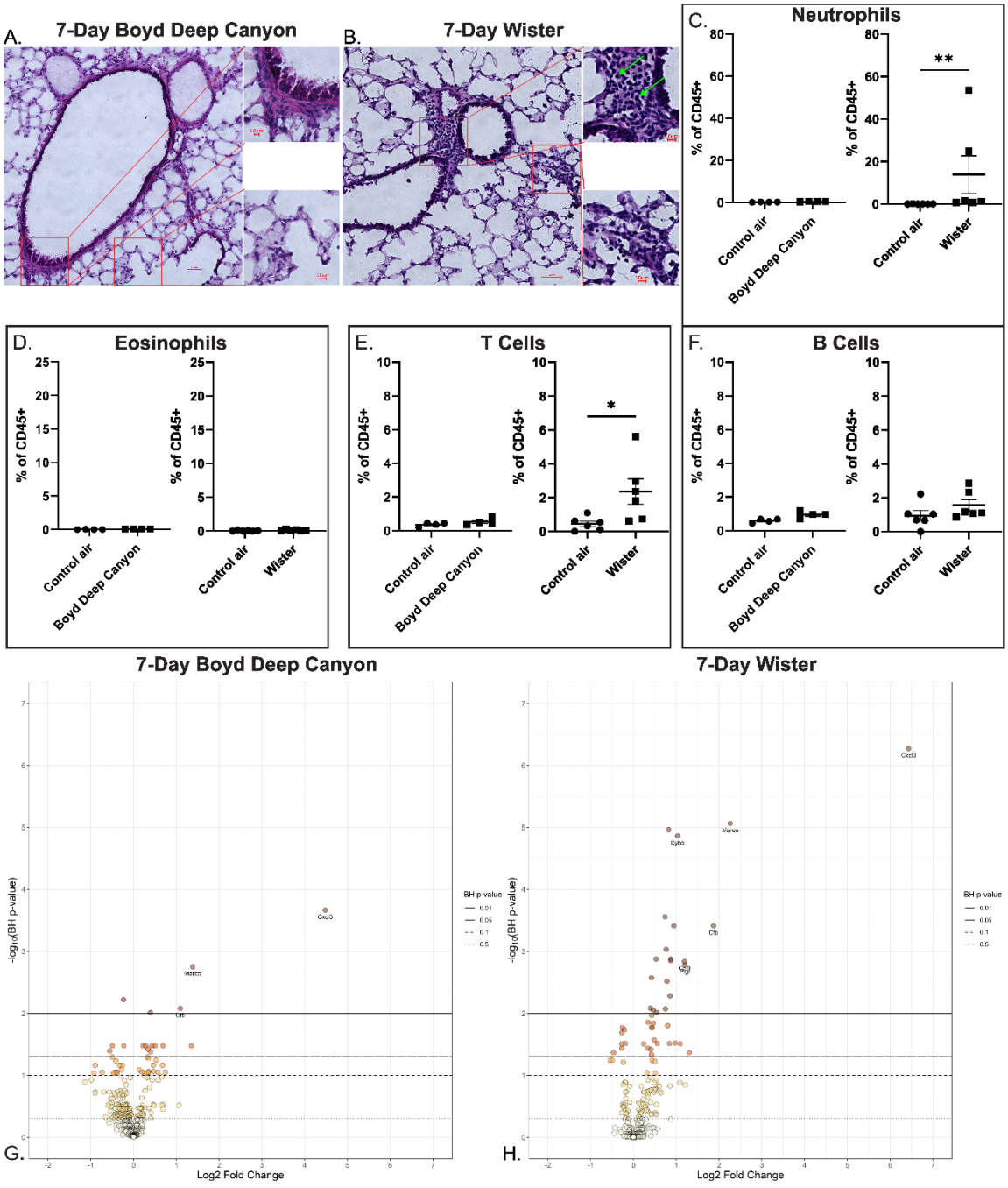
A.
7-Day Boyd Deep Canyon
B.
7-Day Wister
C.
Neutrophils
D.
Eosinophils
E.
T Cells
F.
B Cells
% of CD45+
Control air
Boyd Deep Canyon
Wister
**
*
7-Day Boyd Deep Canyon
7-Day Wister
G.
H.
-log10(BH p-value)
Log2 Fold Change
BH p-value
Cxcl3
Marco
Cfb
Cybb

Figure 4.2 - Pulmonary inflammation triggered by Salton Sea (Wister) Dust extract and by Desert (Boyd Deep Canyon) Dust extract

(A) 20X magnification H&E stain of lung tissue from mice exposed to Boyd Deep Canyon Dust extract. Insets are 60X magnification. (B) 20X magnifcation H&E stain of lung tisue from mice exposed to Wister Dust extract. Insets are 60X magnification. (C) Neutrophilic infiltration into the bronchoalveolar lavage fluid measured as a percentage of total immune cells (CD45+) as determined by flow cytometry. Neutrophil were defined as $CD45^{+}CD11b^{+}Ly6G^{+}SiglecF^{-}CD11c^{-}$. (D) Eosinophilic infiltration into the bronchoalveolar lavage fluid measured as a percentage of total immune cells (CD45+) as determined by flow cytometry. Eosinophils were defined as $CD45^{+}CD11b^{+}SiglecF^{+}CD11c^{-}$. (E) T cell infiltration into the bronchoalveolar lavage fluid measured as a percentage of total immune cells (CD45+) as determined by flow cytometry. T cells were defined as $CD45^{+}CD3^{+}SiglecF^{-}CD11c^{-}$. (F) B cell infiltration into the bronchoalveolar lavage fluid measured as a percentage of total immune cells (CD45+) as determined by flow cytometry. B cells were defined as $CD45^{+}CD19^{+}SiglecF^{+}CD11c^{-}$. All Boyd Deep Canyon Dust extract (*n = 4*) and Wister Dust extract (*n = 6*) exposed mice were compared to contemporaneous sex- and age-matched mice exposed to filtered house air. (G) Differential expression plot for Boyd Deep Canyon Dust extract exposed mice (*n = 6*) compared to contemporaneous sex- and age-matched mice exposed to filtered house air (*n = 6*). (F) Differential expression plot for Wister Dust extract exposed mice (*n = 9*) compared to contemporaneous

sex- and age-matched mice exposed to filtered house air (*n = 9)*. Gene expression was measured by a Nanostring Sprint Profiler using the mouse immunology panel; analysis was done using the accompanying nSolver software and visualized using *ggplot2*. Labeled genes have a log2 fold change greater than 1 or less than negative 1 and an Benjamini-Hochberg adjusted False Discovery Rate of < 0.01. * $p < 0.05$. ** $p < 0.01$. p-value determined using the Mann-Whitney U test for nonparametric data.

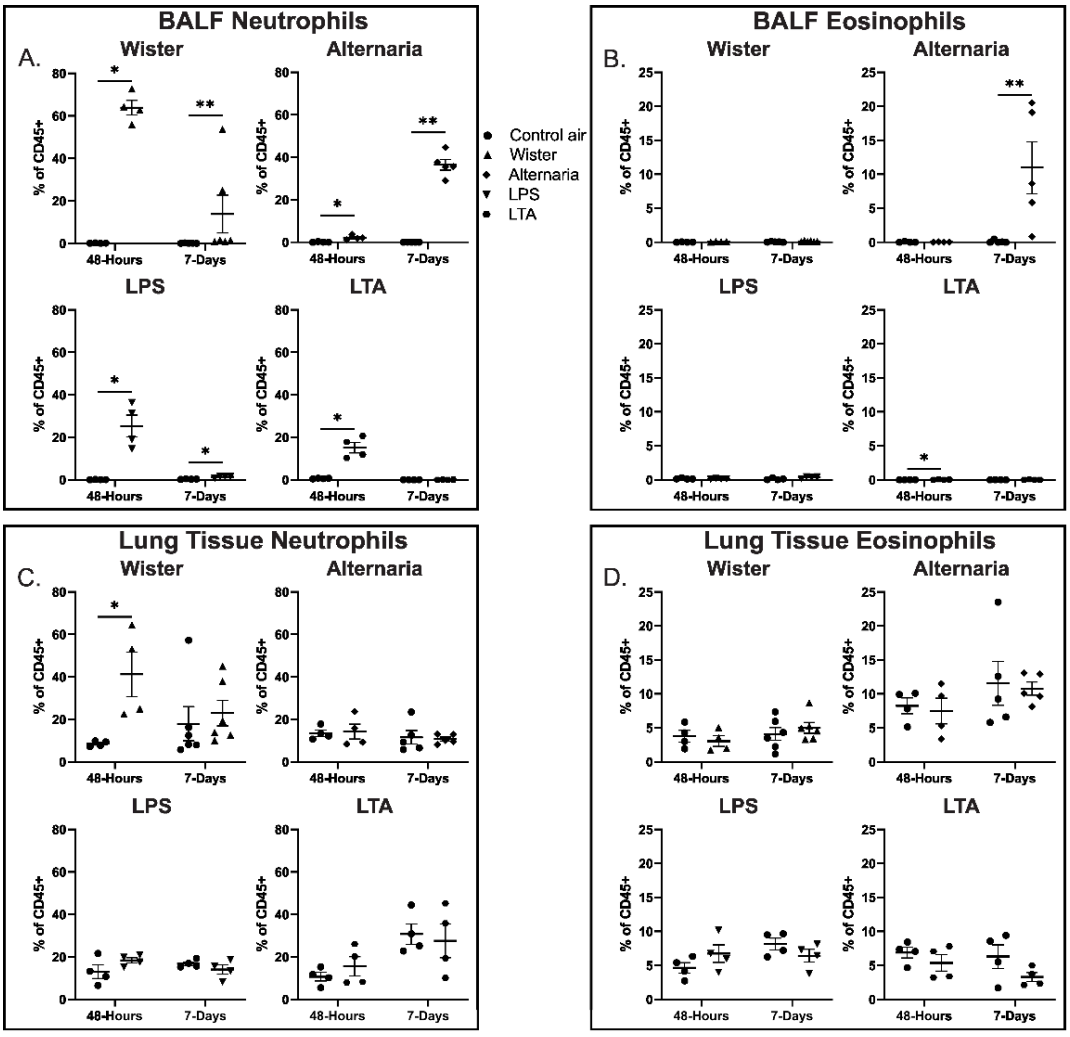
BALF Neutrophils
A.
Wister
Alternaria
LPS
LTA
% of CD45+
48-Hours
7-Days
Control air
Wister
Alternaria
LPS
LTA
BALF Eosinophils
B.
Lung Tissue Neutrophils
C.
Lung Tissue Eosinophils
D.

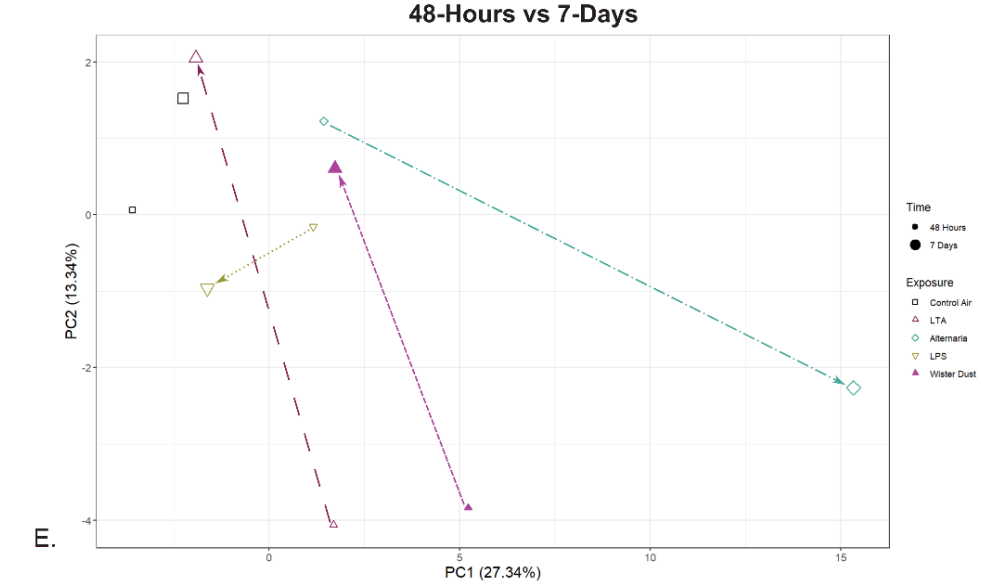
48-Hours vs 7-Days
E.
PC2 (13.34%)
PC1 (27.34%)
Time
48 Hours
7 Days
Exposure
Control Air
LTA
Alternaria
LPS
Wister Dust

Figure 4.3 - Changes from 48-hour to 7-day timepoints for Salton Sea (Wister) Dust extract, Alternaria, LTA, and LPS exposed mice

(A) Neutrophil infiltration at 48-hours and 7-days in the bronchoalveolar lavage fluid (BALF) as a percent of total immune cells (CD45+) for Wister Dust extract, *Alternaria*, LTA, and LPS exposed mice. (B) Eosinophil infiltration at 48-hours and 7-days in the bronchoalveolar lavage fluid (BALF) as a percent of total immune cells (CD45+) for Wister Dust extract, *Alternaria*, LTA, and LPS exposed mice. (C) Neutrophil infiltration at 48-hours and 7-days in the lung tissue as a percent of total immune cells (CD45+) for Wister Dust extract, *Alternaria*, LTA, and LPS exposed mice. (D) Eosinophil infiltration at 48-hours and 7-days in the lung tissue as a percent of total immune cells (CD45+) for Wister Dust extract, *Alternaria*, LTA, and LPS exposed mice. Neutrophils were defined as $CD45^{+}CD11b^{+}Ly6G^{+}SiglecF^{-}CD11c^{-}$, while eosinophils were defined as $CD45^{+}CD11b^{+}SiglecF^{+}CD11c^{-}$. All timepoint and exposure combinations were compared to contemporaneous sex- and age-matched mice exposed to filtered house air. *n = 4-6* (E) PCA plot showing the changes from the 48-hour timepoints to 7-day timepoints for Wister Dust extract, *Alternaria*, LTA, and LPS exposed mice. PCA was generated using the *prcomp* function in R and visualized using *ggplot2*. Each point represents the average location of the specific timepoint and exposure combination on PC1 and PC2. Arrows highlight trend line from 48-hour to 7-day for each exposure. *n = 6-9*. * $p < 0.05$, ** $p < 0.01$. p-value calculated using the Mann-Whitney U test for nonparametric data.

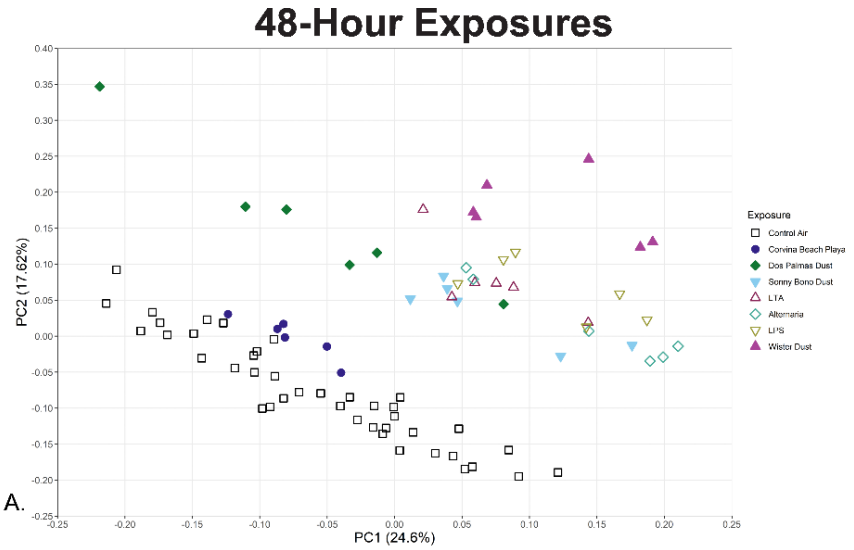
48-Hour Exposures
PC2 (17.62%)
PC1 (24.6%)
Exposure
Control Air
Corvina Beach Playa
Dos Palmas Dust
Sonny Bono Dust
LTA
Alternaria
LPS
Wister Dust

A.

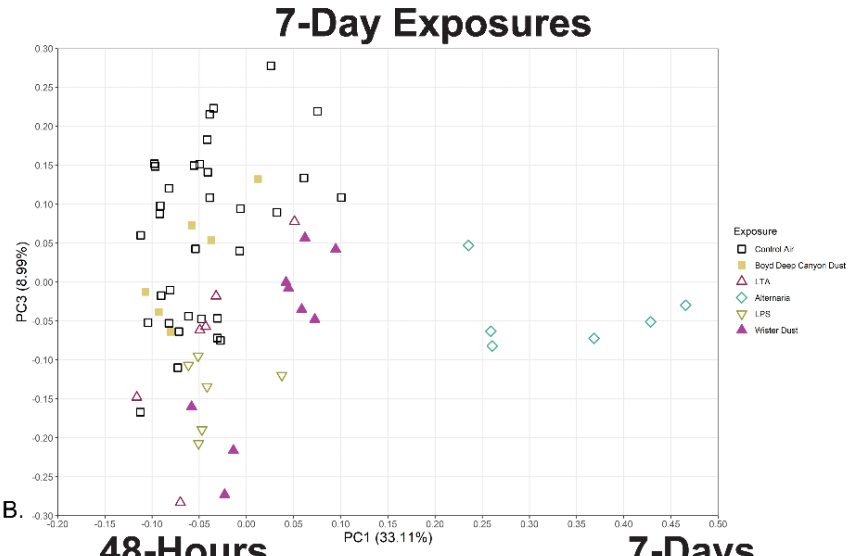
7-Day Exposures
PC3 (8.99%)
PC1 (33.11%)
Exposure
Control Air
Boyd Deep Canyon Dust
LTA
Alternaria
LPS
Wister Dust

B.

C.

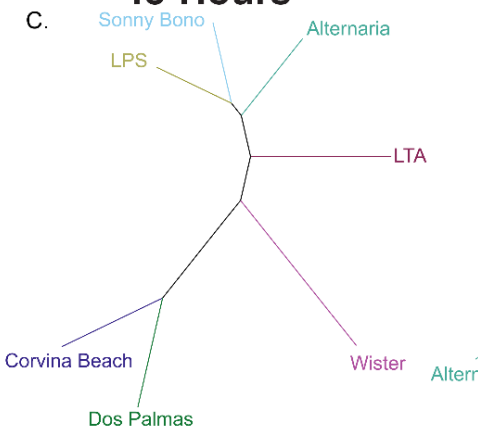
48-Hours
Sonny Bono
Alternaria
LPS
LTA
Corvina Beach
Wister
Dos Palmas

D.

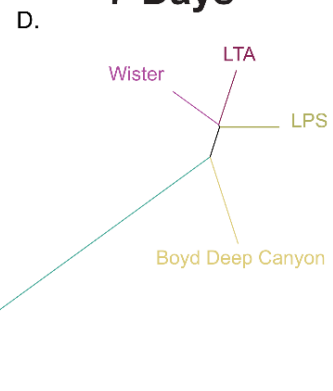
7-Days
LTA
Wister
LPS
Boyd Deep Canyon
Alternaria

Figure 4.4 - Gene expression comparisons for 48 hour and 7-day timepoints

(A) PCA plot comparing Salton Sea Dust extract (Wister, Sonny Bono, Dos Palmas), Salton Sea Playa extract (Corvina Beach), LTA, LPS and *Alternaria* exposed mice at 48-hour (*n=6)*. (B) PCA plot comparing Salton Sea Dust extract (Wister), Desert Dust extract (Boyd Deep Canyon), LTA, LPS and *Alternaria* exposed mice at 7-days (*n = 6-9)*. PCA was generated using the *prcomp* function in R and visualized using *ggplot2*. (C) Dendrogram showing the relationship between Salton Sea Dust extract (Wister, Sonny Bono, Dos Palmas), Salton Sea Playa extract (Corvina Beach), LTA, LPS and *Alternaria* exposed mice at 48-hour (*n = 6*). (D) Dendrogram showing the relationship between Salton Sea Dust extract (Wister), Desert Dust extract (Boyd Deep Canyon), LTA, LPS and *Alternaria* exposed mice at 7-days (*n = 6-9).* Dendrograms were generated using the log2 value for each gene averaged by the exposure. This average was then used with the hclust function (method = Ward.D2) and visualized using the *ape* package.

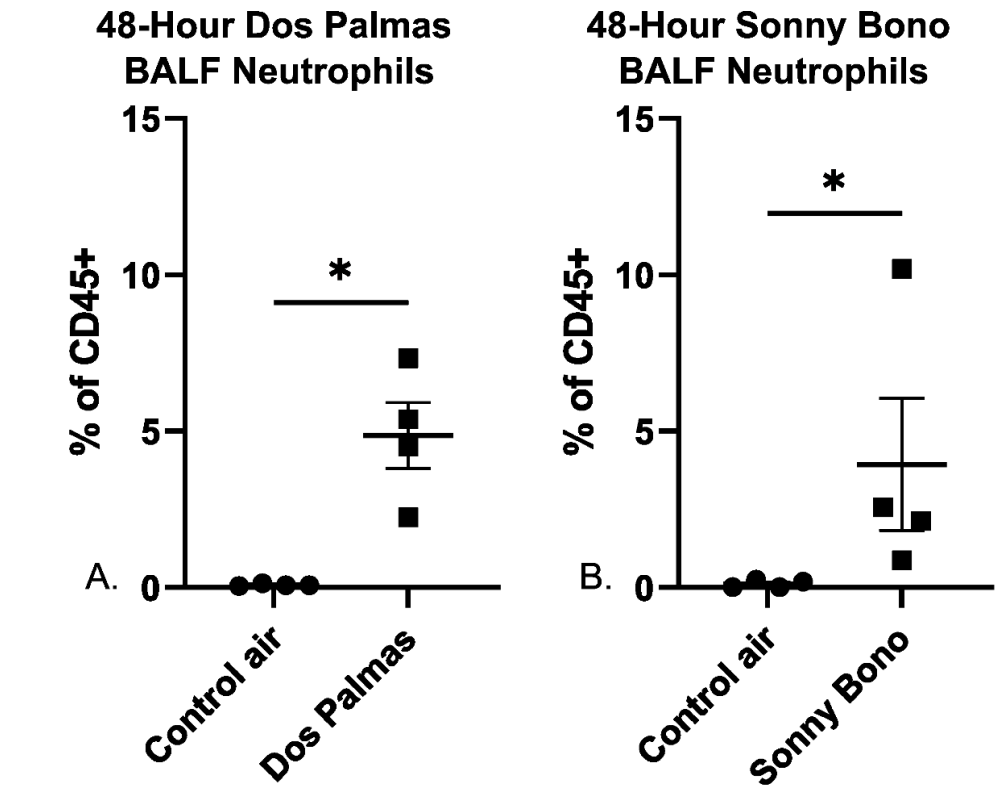
48-Hour Dos Palmas
BALF Neutrophils
% of CD45+
15
10
5
0
*
A.
Control air
Dos Palmas
48-Hour Sonny Bono
BALF Neutrophils
% of CD45+
15
10
5
0
*
B.
Control air
Sonny Bono

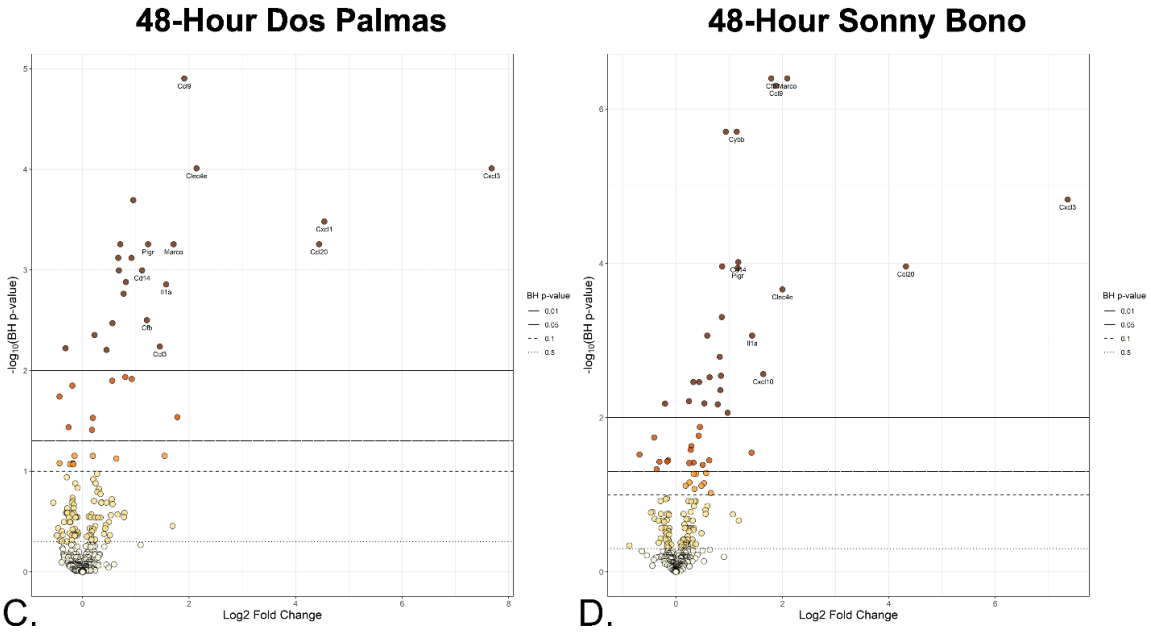
48-Hour Dos Palmas
-log10(BH p-value)
Log2 Fold Change
BH p-value
0.01
0.05
0.1
0.5
C.
48-Hour Sonny Bono
-log10(BH p-value)
Log2 Fold Change
BH p-value
0.01
0.05
0.1
0.5
D.

Figure 4.S1 - Dos Palmas and Sonny Bono Cell infiltration and Gene expression

(A) Neutrophilic infiltration into the bronchoalveolar lavage fluid in mice exposed to Dos Palmas Dust extract for 48-hours measured as a percentage of total immune cells (CD45+) as determined by flow cytometry. (B) Neutrophilic infiltration into the bronchoalveolar lavage fluid in mice exposed to Sonny Bono Dust extract for 48-hours measured as a percentage of total immune cells (CD45+) as determined by flow cytometry. Neutrophil were defined as $CD45^{+}CD11b^{+}Ly6G^{+}SiglecF^{-}CD11c^{-}$. All Dos Palmas Dust extract (*n* = *4*) and Sonny Bono Dust extract (*n* = *6*) exposed mice were compared to contemporaneous sex- and age-matched mice exposed to filtered house air. (C) Differential expression plot for Dos Palmas Dust extract exposed mice (*n* = *6*) compared to contemporaneous sex- and age-matched mice exposed to filtered house air (*n* = *6)*. (D) Differential expression plot for Sonny Bono Dust extract exposed mice (*n* = *6*) compared to contemporaneous sex- and age-matched mice exposed to filtered house air (*n* = *6*). Gene expression was measured by a Nanostring Sprint Profiler using the mouse immunology panel; analysis was done using the accompanying nSolver software and visualized using *ggplot2*. Labeled genes have a log2 fold change greater than 1 or less than negative 1 and an Benjamini-Hochberg adjusted False Discovery Rate of < 0.01. * $p < 0.05$. ** $p < 0.01$. p-value determined using the Mann-Whitney U test for nonparametric data. Average $\pm$ standard error shown.

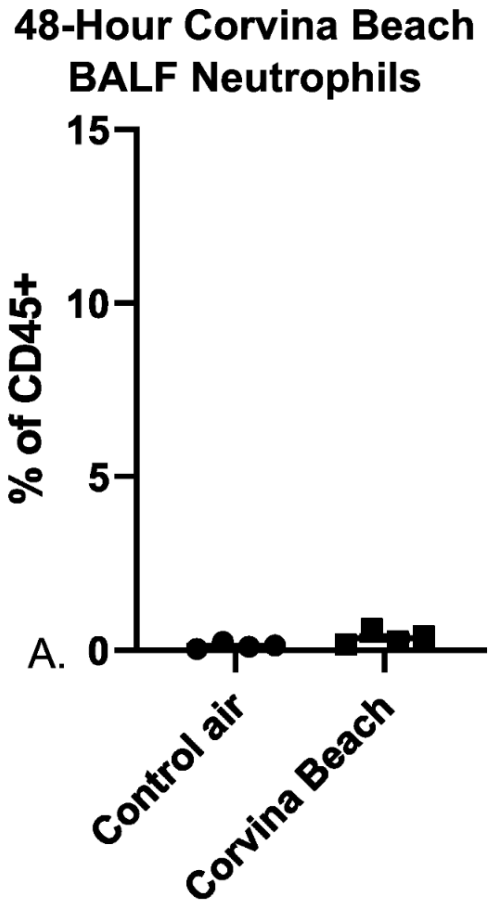
48-Hour Corvina Beach
BALF Neutrophils
% of CD45+
15
10
5
0
Control air
Corvina Beach

A.

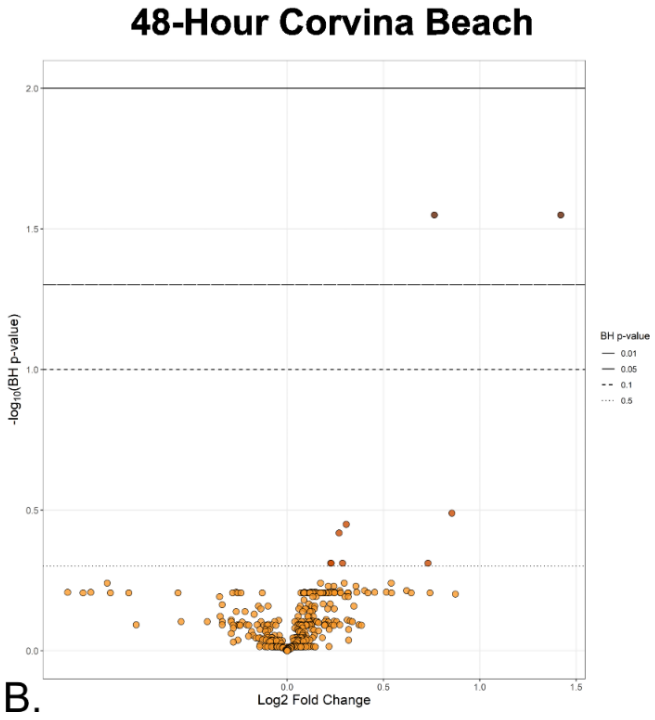
48-Hour Corvina Beach
-log10(BH p-value)
Log2 Fold Change
BH p-value
0.01
0.05
0.1
0.5

B.

Figure 4.S2 - Response to Corvina Beach Playa

(A) Neutrophilic infiltration into the bronchoalveolar lavage fluid in mice exposed to Corvina Beach Playa extract for 48-hours Neutrophil were defined as $CD45^{+}CD11b^{+}Ly6G^{+}SiglecF^{-}CD11c^{-}$. Corvina Beach Playa extract (*n = 4*) exposed mice were compared to contemporaneous sex- and age-matched mice exposed to filtered house air. (B) Differential expression plot for Corvina Beach Playa extract exposed mice (*n = 6*) compared to contemporaneous sex- and age-matched mice exposed to filtered house air (*n = 6*). Gene expression was measured by a Nanostring Sprint Profiler using the mouse immunology panel; analysis was done using the accompanying nSolver software and visualized using *ggplot2*. Labeled genes have a log2 fold change greater than 1 or less than negative 1 and an Benjamini-Hochberg adjusted False Discovery Rate of < 0.01. * $p < 0.05$. ** $p < 0.01$. p-value determined using the Mann-Whitney U test for nonparametric data. Average $\pm$ standard error shown.

Table 4.1 - Site and sampling characteristics

Coordinates and deployment dates for each of five sites Salton Sea Basin of California.

Site	Latitude (ºN)	Longitude (ºW)	Sampling dates	Deployment (days)	Sample type
Corvina Beach	33°28'36.5	115°53'31.3	08/21/21	n/a	playa
Boyd Deep	33°39'04.0	116°22'22.9	08/14/20-10/08/20	55	dust
Sonny Bono	33°11'16.0	115°35'57.3	08/30/20-10/10/20	44	dust
Wister	33°17'01.7	115°36'00.3	08/30/20-10/10/20, 09/18/21-12/08/21	44, 81	dust
Dos Palmas	33°29'22.1	115°50'06.3	08/30/20-10/10/20	44	dust

Chapter 5: Conclusion

The aerosols generated around the Salton Sea are a complex mixture of various sources and pollutants that will take many years to fully describe. However, as the Salton Sea is rapidly drying and exposing the surrounding communities to more dust, rapid action is required. In order to aid the communities, it is important to understand how these aerosols can contribute to pulmonary inflammation even if we do not fully understand the composition. The research presented in this dissertation is the first step in describing how two potential sources of pulmonary inflammation contribute to pulmonary health in the region.

Salton Sea Water was capable of triggering minor changes in lung tissue gene expression. However, there was no significant change in inflammatory cell infiltration in the airways, and the gene expression profile did not match that of the T2-like allergen *Alternaria*. The water failed to predispose mice to *Alternaria*, indicating that it likely has little effect on asthma development even in combination with a potent allergen. Based on our results, the Salton Sea Water aerosols (sea spray) are unlikely to be the primary source of pulmonary inflammation and asthma, either directly or indirectly.

Particulate matter (PM) is an ongoing concern in the Salton Sea Basin, as the region is designated a nonattainment area for PM_{10} (Particulate matter between 2.5 μm and 10 μm in aerosol diameter) and $PM_{2.5}$ (Particulate matter under 2.5 μm in aerosol diameter) (Environmental Protection Agency, 2022). As

the Salton Sea dries, the PM in the region is projected to worsen (Parajuli and Zender, 2018). This newly exposed playa (dried lakebed) likely contains a higher concentration of pollutants than the water, as levels of pollutants such as pesticides are elevated in the sediment (Xu et al., 2016).

Our results indicate that dust from around the Salton Sea is already capable of triggering neutrophilic pulmonary inflammation with high expression of acute inflammatory genes. While this response is greater at 48-hours than at 7-days, we found persistent inflammation even at the 7-day timepoint. This response is similar to those of TLR2/4 agonists lipoteichoic acid (LTA) and lipopolysaccharide (LPS). However, this response still does not explain the high levels of asthma (Farzan et al., 2019) and asthma-related ER visits in the region (California Environmental Protection Agency and Office of Environmental Health Hazard Assessment, 2021). As epidemiological data from the region is scarce, there could be multiple explanations for this discrepancy. The people in the Salton Sea Basin may not have traditional T2 asthma, instead having chronic low-level inflammation due to dust exposure that manifests as asthma-like symptoms. The dust could also be predisposing individuals to asthma by modulating the inflammatory response, similar to other sources of desert dust such as Asian Sand Dust (Ren et al., 2014; He et al., 2016; He et al., 2019; Sadakane et al., 2022). If dust is modulating asthma development, it would be critical to understand the mechanisms, as other immunomodulatory agents such as LPS have been shown to exacerbate T2 asthma or convert T2 asthma to

Th17 asthma (Li et al., 1998; Barboza et al., 2013; Yu and Chen, 2018; Sadakane et al., 2019; Thakur et al., 2019). As Th17 driven asthma has been linked to corticosteroid resistance, a shift towards Th17 asthma would help explain the high rates of severe asthma in the region.

More work remains to be done to understand the mechanisms driving Salton Sea Dust related pulmonary inflammation and its effect on community health. While we know that the immune response to Salton Sea Dust mimics the response to LTA and LPS, we do not know if these rely on the same mechanisms. We also do not know if long-term exposure to Salton Sea Dust alone is sufficient to cause airway hyperreactivity. Despite other models of dust and TLR driven inflammation demonstrating the worsening or conversion of the T2 response when combined with a potent allergen, we do not yet know if Salton Sea Dust interacts the same way. Additionally, more work needs to be done to understand if there is substantial season variation in the Salton Sea Dust. While our results show year-to-year consistency in the general profile of Salton Sea Dust driven inflammation, our samples were exclusively collected in autumn.

With a deeper understanding of how Salton Sea Dust drives pulmonary inflammation, healthcare professionals can be better informed on how to treat patients, and more targeted epidemiological studies can be performed. This information also allows for a more direct search into the causal agent(s) driving pulmonary inflammation. The results from the studies performed for this

dissertation are merely the first of many to transform our understanding of the Salton Sea basin and the health of the communities within.

References

Environmental Protection Agency. (2022, August 31). *Nonattainment Areas for Criteria Pollutants (Green Book)*. https://www.epa.gov/green-book

Parajuli, S. P., & Zender, C. S. (2018). Projected changes in dust emissions and regional air quality due to the shrinking Salton Sea. *Aeolian Research*, *33*(June), 82–92. https://doi.org/10.1016/j.aeolia.2018.05.004

Xu, E. G., Bui, C., Lamerdin, C., & Schlenk, D. (2016). Spatial and temporal assessment of environmental contaminants in water, sediments and fish of the Salton Sea and its two primary tributaries, California, USA, from 2002 to 2012. *Science of the Total Environment*, *559*, 130–140. https://doi.org/10.1016/j.scitotenv.2016.03.144

Farzan, S. F., Razafy, M., Eckel, S. P., Olmedo, L., Bejarano, E., & Johnston, J. E. (2019). Assessment of respiratory health symptoms and asthma in children near a drying saline lake. *International Journal of Environmental Research and Public Health*, *16*(20). https://doi.org/10.3390/ijerph16203828

California Environmental Protection Agency, Office of Environmental Health Hazard Assessment, 2021, October 20. CalEnviroScreen 4.0. Retrieved from. https://oehha.ca.gov/calenviroscreen/report/calenviroscreen-40

Ren Y, Ichinose T, He M, Song Y, Yoshida Y, Yoshida S, Nishikawa M, Takano H, Sun G, Shibamoto T. Enhancement of OVA-induced murine lung eosinophilia by co-exposure to contamination levels of LPS in Asian sand dust and heated dust. Allergy Asthma Clin Immunol. 2014 Jun 9;10(1):30. doi: 10.1186/1710-1492-10-30. PMID: 24982682; PMCID: PMC4058696.

He M, Ichinose T, Song Y, Yoshida Y, Bekki K, Arashidani K, Yoshida S, Nishikawa M, Takano H, Shibamoto T, Sun G. Desert dust induces TLR signaling to trigger Th2-dominant lung allergic inflammation via a MyD88-dependent signaling pathway. Toxicol Appl Pharmacol. 2016 Apr 1;296:61-72. doi: 10.1016/j.taap.2016.02.011. Epub 2016 Feb 13. PMID: 26882889.

He M, Ichinose T, Yoshida S, Nishikawa M, Sun G, Shibamoto T. Role of iron and oxidative stress in the exacerbation of allergic inflammation in murine lungs caused by urban particulate matter <2.5 μm and desert dust. J Appl Toxicol. 2019 Jun;39(6):855-867. doi: 10.1002/jat.3773. Epub 2019 Jan 30. PMID: 30698282.

Sadakane K, Ichinose T, Maki T, Nishikawa M. Co-exposure of peptidoglycan and heat-inactivated Asian sand dust exacerbates ovalbumin-induced allergic airway inflammation in mice. Inhal Toxicol. 2022;34(9-10):231-

243. doi: 10.1080/08958378.2022.2086650. Epub 2022 Jun 13. PMID: 35698289.

Li, L., Xia, Y., Nguyen, A., Feng, L., & Lo, D. (1998). Th2-induced eotaxin expression and eosinophilia coexist with Th1 responses at the effector stage of lung inflammation. *Journal of Immunology (Baltimore, Md. : 1950)*, *161*(6), 3128–3135. http://www.ncbi.nlm.nih.gov/pubmed/9743380

Barboza, R., Câmara, N. O. S., Gomes, E., Sá-Nunes, A., Florsheim, E., Mirotti, L., Labrada, A., Alcântara-Neves, N. M., & Russo, M. (2013). Endotoxin Exposure during Sensitization to Blomia tropicalis Allergens Shifts TH2 Immunity Towards a TH17-Mediated Airway Neutrophilic Inflammation: Role of TLR4 and TLR2. *PLoS ONE*, *8*(6). https://doi.org/10.1371/journal.pone.0067115

Yu, Q. L., & Chen, Z. (2018). Establishment of different experimental asthma models in mice. *Experimental and Therapeutic Medicine*, *15*(3), 2492–2498. https://doi.org/10.3892/etm.2018.5721

Sadakane, K., Ichinose, T., & Nishikawa, M. (2019). Effects of co-exposure of lipopolysaccharide and β-glucan (Zymosan A) in exacerbating murine allergic asthma associated with Asian sand dust. *Journal of Applied Toxicology*, *39*(4), 672–684. https://doi.org/10.1002/jat.3759

Thakur, V. R., Khuman, V., Beladiya, J. V., Chaudagar, K. K., & Mehta, A. A. (2019). An experimental model of asthma in rats using ovalbumin and lipopolysaccharide allergens. *Heliyon*, *5*(11), e02864. https://doi.org/10.1016/j.heliyon.2019.e02864